be heads. See Dauphin *et al.* (2014) for a review of the relevant theoretical work.

An amazing property of many random functions is that the eigenvalues of the Hessian become more likely to be positive as we reach regions of lower cost. In our coin tossing analogy, this means we are more likely to have our coin come up heads n times if we are at a critical point with low cost. This means that local minima are much more likely to have low cost than high cost. Critical points with high cost are far more likely to be saddle points. Critical points with extremely high cost are more likely to be local maxima.

This happens for many classes of random functions. Does it happen for neural networks? Baldi and Hornik (1989) showed theoretically that shallow autoencoders (feedforward networks trained to copy their input to their output, described in chapter 14) with no nonlinearities have global minima and saddle points but no local minima with higher cost than the global minimum. They observed without proof that these results extend to deeper networks without nonlinearities. The output of such networks is a linear function of their input, but they are useful to study as a model of nonlinear neural networks because their loss function is a non-convex function of their parameters. Such networks are essentially just multiple matrices composed together. Saxe *et al.* (2013) provided exact solutions to the complete learning dynamics in such networks and showed that learning in these models captures many of the qualitative features observed in the training of deep models with nonlinear activation functions. Dauphin *et al.* (2014) showed experimentally that real neural networks also have loss functions that contain very many high-cost saddle points. Choromanska *et al.* (2014) provided additional theoretical arguments, showing that another class of high-dimensional random functions related to neural networks does so as well.

What are the implications of the proliferation of saddle points for training algorithms? For first-order optimization algorithms that use only gradient information, the situation is unclear. The gradient can often become very small near a saddle point. On the other hand, gradient descent empirically seems to be able to escape saddle points in many cases. Goodfellow *et al.* (2015) provided visualizations of several learning trajectories of state-of-the-art neural networks, with an example given in figure 8.2. These visualizations show a flattening of the cost function near a prominent saddle point where the weights are all zero, but they also show the gradient descent trajectory rapidly escaping this region. Goodfellow *et al.* (2015) also argue that continuous-time gradient descent may be shown analytically to be repelled from, rather than attracted to, a nearby saddle point, but the situation may be different for more realistic uses of gradient descent.

For Newton's method, it is clear that saddle points constitute a problem.

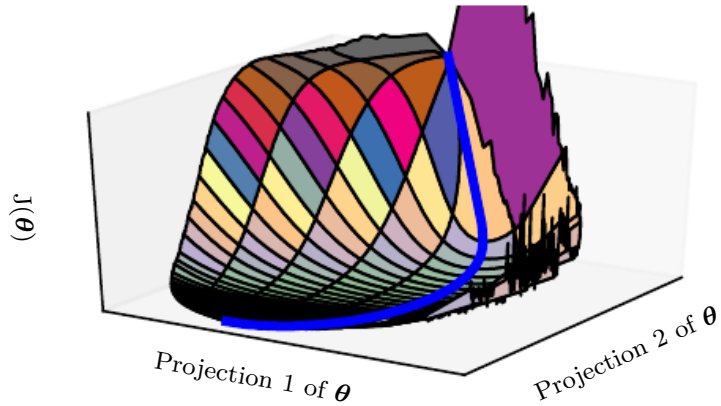

Figure 8.2: A visualization of the cost function of a neural network. Image adapted with permission from Goodfellow *et al.* (2015). These visualizations appear similar for feedforward neural networks, convolutional networks, and recurrent networks applied to real object recognition and natural language processing tasks. Surprisingly, these visualizations usually do not show many conspicuous obstacles. Prior to the success of stochastic gradient descent for training very large models beginning in roughly 2012, neural net cost function surfaces were generally believed to have much more non-convex structure than is revealed by these projections. The primary obstacle revealed by this projection is a saddle point of high cost near where the parameters are initialized, but, as indicated by the blue path, the SGD training trajectory escapes this saddle point readily. Most of training time is spent traversing the relatively flat valley of the cost function, which may be due to high noise in the gradient, poor conditioning of the Hessian matrix in this region, or simply the need to circumnavigate the tall "mountain" visible in the figure via an indirect arcing path.

Gradient descent is designed to move "downhill" and is not explicitly designed to seek a critical point. Newton's method, however, is designed to solve for a point where the gradient is zero. Without appropriate modification, it can jump to a saddle point. The proliferation of saddle points in high dimensional spaces presumably explains why second-order methods have not succeeded in replacing gradient descent for neural network training. Dauphin *et al.* (2014) introduced a **saddle-free Newton method** for second-order optimization and showed that it improves significantly over the traditional version. Second-order methods remain difficult to scale to large neural networks, but this saddle-free approach holds promise if it could be scaled.

There are other kinds of points with zero gradient besides minima and saddle points. There are also maxima, which are much like saddle points from the perspective of optimization—many algorithms are not attracted to them, but unmodified Newton's method is. Maxima of many classes of random functions become exponentially rare in high dimensional space, just like minima do.

There may also be wide, flat regions of constant value. In these locations, the gradient and also the Hessian are all zero. Such degenerate locations pose major problems for all numerical optimization algorithms. In a convex problem, a wide, flat region must consist entirely of global minima, but in a general optimization problem, such a region could correspond to a high value of the objective function.

8.2.4 Cliffs and Exploding Gradients

Neural networks with many layers often have extremely steep regions resembling cliffs, as illustrated in figure 8.3. These result from the multiplication of several large weights together. On the face of an extremely steep cliff structure, the gradient update step can move the parameters extremely far, usually jumping off of the cliff structure altogether.

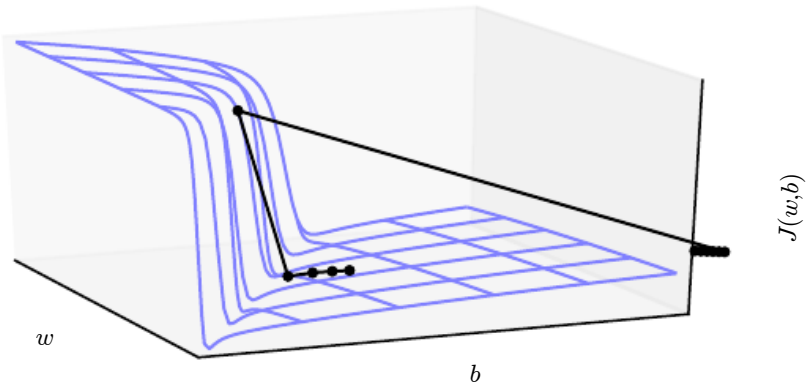

Figure 8.3: The objective function for highly nonlinear deep neural networks or for recurrent neural networks often contains sharp nonlinearities in parameter space resulting from the multiplication of several parameters. These nonlinearities give rise to very high derivatives in some places. When the parameters get close to such a cliff region, a gradient descent update can catapult the parameters very far, possibly losing most of the optimization work that had been done. Figure adapted with permission from Pascanu *et al.* (2013).

The cliff can be dangerous whether we approach it from above or from below, but fortunately its most serious consequences can be avoided using the **gradient clipping** heuristic described in section 10.11.1. The basic idea is to recall that the gradient does not specify the optimal step size, but only the optimal direction within an infinitesimal region. When the traditional gradient descent algorithm proposes to make a very large step, the gradient clipping heuristic intervenes to reduce the step size to be small enough that it is less likely to go outside the region where the gradient indicates the direction of approximately steepest descent. Cliff structures are most common in the cost functions for recurrent neural networks, because such models involve a multiplication of many factors, with one factor for each time step. Long temporal sequences thus incur an extreme amount of multiplication.

8.2.5 Long-Term Dependencies

Another difficulty that neural network optimization algorithms must overcome arises when the computational graph becomes extremely deep. Feedforward networks with many layers have such deep computational graphs. So do recurrent networks, described in chapter 10, which construct very deep computational graphs

by repeatedly applying the same operation at each time step of a long temporal sequence. Repeated application of the same parameters gives rise to especially pronounced difficulties.

For example, suppose that a computational graph contains a path that consists of repeatedly multiplying by a matrix $\boldsymbol{W}$. After t steps, this is equivalent to multiplying by $\boldsymbol{W}^t$. Suppose that $\boldsymbol{W}$ has an eigendecomposition $\boldsymbol{W} = \boldsymbol{V}\text{diag}(\boldsymbol{\lambda})\boldsymbol{V}^{-1}$. In this simple case, it is straightforward to see that

$$\boldsymbol{W}^t = \left(\boldsymbol{V}\text{diag}(\boldsymbol{\lambda})\boldsymbol{V}^{-1}\right)^t = \boldsymbol{V}\text{diag}(\boldsymbol{\lambda})^t\boldsymbol{V}^{-1}. \tag{8.11}$$

Any eigenvalues λ_i that are not near an absolute value of 1 will either explode if they are greater than 1 in magnitude or vanish if they are less than 1 in magnitude. The **vanishing and exploding gradient problem** refers to the fact that gradients through such a graph are also scaled according to $\text{diag}(\boldsymbol{\lambda})^t$. Vanishing gradients make it difficult to know which direction the parameters should move to improve the cost function, while exploding gradients can make learning unstable. The cliff structures described earlier that motivate gradient clipping are an example of the exploding gradient phenomenon.

The repeated multiplication by $\boldsymbol{W}$ at each time step described here is very similar to the **power method** algorithm used to find the largest eigenvalue of a matrix $\boldsymbol{W}$ and the corresponding eigenvector. From this point of view it is not surprising that $\boldsymbol{x}^\top\boldsymbol{W}^t$ will eventually discard all components of $\boldsymbol{x}$ that are orthogonal to the principal eigenvector of $\boldsymbol{W}$.

Recurrent networks use the same matrix $\boldsymbol{W}$ at each time step, but feedforward networks do not, so even very deep feedforward networks can largely avoid the vanishing and exploding gradient problem (Sussillo, 2014).

We defer a further discussion of the challenges of training recurrent networks until section 10.7, after recurrent networks have been described in more detail.

8.2.6 Inexact Gradients

Most optimization algorithms are designed with the assumption that we have access to the exact gradient or Hessian matrix. In practice, we usually only have a noisy or even biased estimate of these quantities. Nearly every deep learning algorithm relies on sampling-based estimates at least insofar as using a minibatch of training examples to compute the gradient.

In other cases, the objective function we want to minimize is actually intractable. When the objective function is intractable, typically its gradient is intractable as well. In such cases we can only approximate the gradient. These issues mostly arise

with the more advanced models in part III. For example, contrastive divergence gives a technique for approximating the gradient of the intractable log-likelihood of a Boltzmann machine.

Various neural network optimization algorithms are designed to account for imperfections in the gradient estimate. One can also avoid the problem by choosing a surrogate loss function that is easier to approximate than the true loss.

8.2.7 Poor Correspondence between Local and Global Structure

Many of the problems we have discussed so far correspond to properties of the loss function at a single point—it can be difficult to make a single step if $J(\boldsymbol{\theta})$ is poorly conditioned at the current point $\boldsymbol{\theta}$, or if $\boldsymbol{\theta}$ lies on a cliff, or if $\boldsymbol{\theta}$ is a saddle point hiding the opportunity to make progress downhill from the gradient.

It is possible to overcome all of these problems at a single point and still perform poorly if the direction that results in the most improvement locally does not point toward distant regions of much lower cost.

Goodfellow *et al.* (2015) argue that much of the runtime of training is due to the length of the trajectory needed to arrive at the solution. Figure 8.2 shows that the learning trajectory spends most of its time tracing out a wide arc around a mountain-shaped structure.

Much of research into the difficulties of optimization has focused on whether training arrives at a global minimum, a local minimum, or a saddle point, but in practice neural networks do not arrive at a critical point of any kind. Figure 8.1 shows that neural networks often do not arrive at a region of small gradient. Indeed, such critical points do not even necessarily exist. For example, the loss function $-\log p(y \mid \boldsymbol{x}; \boldsymbol{\theta})$ can lack a global minimum point and instead asymptotically approach some value as the model becomes more confident. For a classifier with discrete y and $p(y \mid \boldsymbol{x})$ provided by a softmax, the negative log-likelihood can become arbitrarily close to zero if the model is able to correctly classify every example in the training set, but it is impossible to actually reach the value of zero. Likewise, a model of real values $p(y \mid \boldsymbol{x}) = \mathcal{N}(y; f(\boldsymbol{\theta}), \beta^{-1})$ can have negative log-likelihood that asymptotes to negative infinity—if $f(\boldsymbol{\theta})$ is able to correctly predict the value of all training set y targets, the learning algorithm will increase β without bound. See figure 8.4 for an example of a failure of local optimization to find a good cost function value even in the absence of any local minima or saddle points.

Future research will need to develop further understanding of the factors that influence the length of the learning trajectory and better characterize the outcome

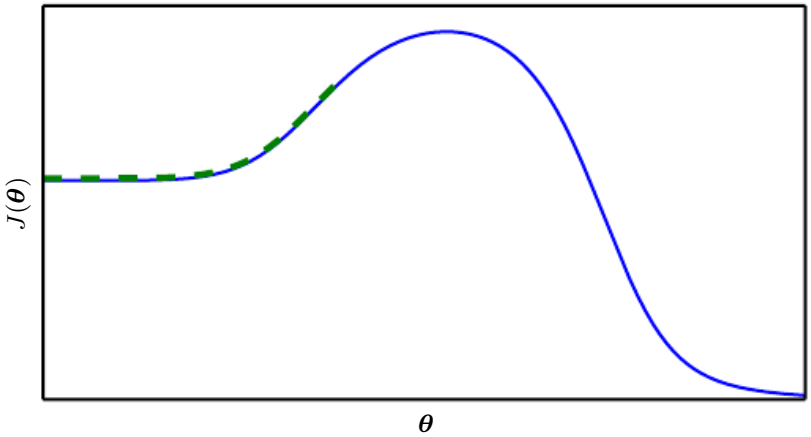

Figure 8.4: Optimization based on local downhill moves can fail if the local surface does not point toward the global solution. Here we provide an example of how this can occur, even if there are no saddle points and no local minima. This example cost function contains only asymptotes toward low values, not minima. The main cause of difficulty in this case is being initialized on the wrong side of the "mountain" and not being able to traverse it. In higher dimensional space, learning algorithms can often circumnavigate such mountains but the trajectory associated with doing so may be long and result in excessive training time, as illustrated in figure 8.2.

of the process.

Many existing research directions are aimed at finding good initial points for problems that have difficult global structure, rather than developing algorithms that use non-local moves.

Gradient descent and essentially all learning algorithms that are effective for training neural networks are based on making small, local moves. The previous sections have primarily focused on how the correct direction of these local moves can be difficult to compute. We may be able to compute some properties of the objective function, such as its gradient, only approximately, with bias or variance in our estimate of the correct direction. In these cases, local descent may or may not define a reasonably short path to a valid solution, but we are not actually able to follow the local descent path. The objective function may have issues such as poor conditioning or discontinuous gradients, causing the region where the gradient provides a good model of the objective function to be very small. In these cases, local descent with steps of size ϵ may define a reasonably short path to the solution, but we are only able to compute the local descent direction with steps of size $\delta \ll \epsilon$. In these cases, local descent may or may not define a path to the solution, but the path contains many steps, so following the path incurs a

high computational cost. Sometimes local information provides us no guide, when the function has a wide flat region, or if we manage to land exactly on a critical point (usually this latter scenario only happens to methods that solve explicitly for critical points, such as Newton's method). In these cases, local descent does not define a path to a solution at all. In other cases, local moves can be too greedy and lead us along a path that moves downhill but away from any solution, as in figure 8.4, or along an unnecessarily long trajectory to the solution, as in figure 8.2. Currently, we do not understand which of these problems are most relevant to making neural network optimization difficult, and this is an active area of research.

Regardless of which of these problems are most significant, all of them might be avoided if there exists a region of space connected reasonably directly to a solution by a path that local descent can follow, and if we are able to initialize learning within that well-behaved region. This last view suggests research into choosing good initial points for traditional optimization algorithms to use.

8.2.8 Theoretical Limits of Optimization

Several theoretical results show that there are limits on the performance of any optimization algorithm we might design for neural networks (Blum and Rivest, 1992; Judd, 1989; Wolpert and MacReady, 1997). Typically these results have little bearing on the use of neural networks in practice.

Some theoretical results apply only to the case where the units of a neural network output discrete values. However, most neural network units output smoothly increasing values that make optimization via local search feasible. Some theoretical results show that there exist problem classes that are intractable, but it can be difficult to tell whether a particular problem falls into that class. Other results show that finding a solution for a network of a given size is intractable, but in practice we can find a solution easily by using a larger network for which many more parameter settings correspond to an acceptable solution. Moreover, in the context of neural network training, we usually do not care about finding the exact minimum of a function, but seek only to reduce its value sufficiently to obtain good generalization error. Theoretical analysis of whether an optimization algorithm can accomplish this goal is extremely difficult. Developing more realistic bounds on the performance of optimization algorithms therefore remains an important goal for machine learning research.

8.3 Basic Algorithms

We have previously introduced the gradient descent (section 4.3) algorithm that follows the gradient of an entire training set downhill. This may be accelerated considerably by using stochastic gradient descent to follow the gradient of randomly selected minibatches downhill, as discussed in section 5.9 and section 8.1.3.

8.3.1 Stochastic Gradient Descent

Stochastic gradient descent (SGD) and its variants are probably the most used optimization algorithms for machine learning in general and for deep learning in particular. As discussed in section 8.1.3, it is possible to obtain an unbiased estimate of the gradient by taking the average gradient on a minibatch of m examples drawn i.i.d from the data generating distribution.

Algorithm 8.1 shows how to follow this estimate of the gradient downhill.

Algorithm 8.1 Stochastic gradient descent (SGD) update at training iteration k

Require: Learning rate ϵ_k.
Require: Initial parameter $\boldsymbol{\theta}$
  while stopping criterion not met **do**
    Sample a minibatch of m examples from the training set $\{\boldsymbol{x}^{(1)}, \ldots, \boldsymbol{x}^{(m)}\}$ with corresponding targets $\boldsymbol{y}^{(i)}$.
    Compute gradient estimate: $\hat{\boldsymbol{g}} \leftarrow +\frac{1}{m} \nabla_{\boldsymbol{\theta}} \sum_i L(f(\boldsymbol{x}^{(i)}; \boldsymbol{\theta}), \boldsymbol{y}^{(i)})$
    Apply update: $\boldsymbol{\theta} \leftarrow \boldsymbol{\theta} - \epsilon \hat{\boldsymbol{g}}$
  end while

A crucial parameter for the SGD algorithm is the learning rate. Previously, we have described SGD as using a fixed learning rate ϵ. In practice, it is necessary to gradually decrease the learning rate over time, so we now denote the learning rate at iteration k as ϵ_k.

This is because the SGD gradient estimator introduces a source of noise (the random sampling of m training examples) that does not vanish even when we arrive at a minimum. By comparison, the true gradient of the total cost function becomes small and then $\mathbf{0}$ when we approach and reach a minimum using batch gradient descent, so batch gradient descent can use a fixed learning rate. A sufficient condition to guarantee convergence of SGD is that

$$\sum_{k=1}^{\infty} \epsilon_k = \infty, \quad \text{and} \tag{8.12}$$

$$\sum_{k=1}^{\infty} \epsilon_k^2 < \infty. \tag{8.13}$$

In practice, it is common to decay the learning rate linearly until iteration τ:

$$\epsilon_k = (1 - \alpha)\epsilon_0 + \alpha\epsilon_\tau \tag{8.14}$$

with $\alpha = \frac{k}{\tau}$. After iteration τ, it is common to leave ϵ constant.

The learning rate may be chosen by trial and error, but it is usually best to choose it by monitoring learning curves that plot the objective function as a function of time. This is more of an art than a science, and most guidance on this subject should be regarded with some skepticism. When using the linear schedule, the parameters to choose are ϵ_0, ϵ_τ, and τ. Usually τ may be set to the number of iterations required to make a few hundred passes through the training set. Usually ϵ_τ should be set to roughly 1% the value of ϵ_0. The main question is how to set ϵ_0. If it is too large, the learning curve will show violent oscillations, with the cost function often increasing significantly. Gentle oscillations are fine, especially if training with a stochastic cost function such as the cost function arising from the use of dropout. If the learning rate is too low, learning proceeds slowly, and if the initial learning rate is too low, learning may become stuck with a high cost value. Typically, the optimal initial learning rate, in terms of total training time and the final cost value, is higher than the learning rate that yields the best performance after the first 100 iterations or so. Therefore, it is usually best to monitor the first several iterations and use a learning rate that is higher than the best-performing learning rate at this time, but not so high that it causes severe instability.

The most important property of SGD and related minibatch or online gradient-based optimization is that computation time per update does not grow with the number of training examples. This allows convergence even when the number of training examples becomes very large. For a large enough dataset, SGD may converge to within some fixed tolerance of its final test set error before it has processed the entire training set.

To study the convergence rate of an optimization algorithm it is common to measure the **excess error** $J(\boldsymbol{\theta}) - \min_{\boldsymbol{\theta}} J(\boldsymbol{\theta})$, which is the amount that the current cost function exceeds the minimum possible cost. When SGD is applied to a convex problem, the excess error is $O(\frac{1}{\sqrt{k}})$ after k iterations, while in the strongly convex case it is $O(\frac{1}{k})$. These bounds cannot be improved unless extra conditions are assumed. Batch gradient descent enjoys better convergence rates than stochastic gradient descent in theory. However, the Cramér-Rao bound (Cramér, 1946; Rao, 1945) states that generalization error cannot decrease faster than $O(\frac{1}{k})$. Bottou

and Bousquet (2008) argue that it therefore may not be worthwhile to pursue an optimization algorithm that converges faster than $O(\frac{1}{k})$ for machine learning tasks—faster convergence presumably corresponds to overfitting. Moreover, the asymptotic analysis obscures many advantages that stochastic gradient descent has after a small number of steps. With large datasets, the ability of SGD to make rapid initial progress while evaluating the gradient for only very few examples outweighs its slow asymptotic convergence. Most of the algorithms described in the remainder of this chapter achieve benefits that matter in practice but are lost in the constant factors obscured by the $O(\frac{1}{k})$ asymptotic analysis. One can also trade off the benefits of both batch and stochastic gradient descent by gradually increasing the minibatch size during the course of learning.

For more information on SGD, see Bottou (1998).

8.3.2 Momentum

While stochastic gradient descent remains a very popular optimization strategy, learning with it can sometimes be slow. The method of momentum (Polyak, 1964) is designed to accelerate learning, especially in the face of high curvature, small but consistent gradients, or noisy gradients. The momentum algorithm accumulates an exponentially decaying moving average of past gradients and continues to move in their direction. The effect of momentum is illustrated in figure 8.5.

Formally, the momentum algorithm introduces a variable $\boldsymbol{v}$ that plays the role of velocity—it is the direction and speed at which the parameters move through parameter space. The velocity is set to an exponentially decaying average of the negative gradient. The name **momentum** derives from a physical analogy, in which the negative gradient is a force moving a particle through parameter space, according to Newton's laws of motion. Momentum in physics is mass times velocity. In the momentum learning algorithm, we assume unit mass, so the velocity vector $\boldsymbol{v}$ may also be regarded as the momentum of the particle. A hyperparameter $\alpha \in [0, 1)$ determines how quickly the contributions of previous gradients exponentially decay. The update rule is given by:

$$\boldsymbol{v} \leftarrow \alpha \boldsymbol{v} - \epsilon \nabla_{\boldsymbol{\theta}} \left(\frac{1}{m} \sum_{i=1}^{m} L(\boldsymbol{f}(\boldsymbol{x}^{(i)}; \boldsymbol{\theta}), \boldsymbol{y}^{(i)}) \right), \tag{8.15}$$

$$\boldsymbol{\theta} \leftarrow \boldsymbol{\theta} + \boldsymbol{v}. \tag{8.16}$$

The velocity $\boldsymbol{v}$ accumulates the gradient elements $\nabla_{\boldsymbol{\theta}} \left(\frac{1}{m} \sum_{i=1}^{m} L(\boldsymbol{f}(\boldsymbol{x}^{(i)}; \boldsymbol{\theta}), \boldsymbol{y}^{(i)}) \right)$. The larger α is relative to ϵ, the more previous gradients affect the current direction. The SGD algorithm with momentum is given in algorithm 8.2.

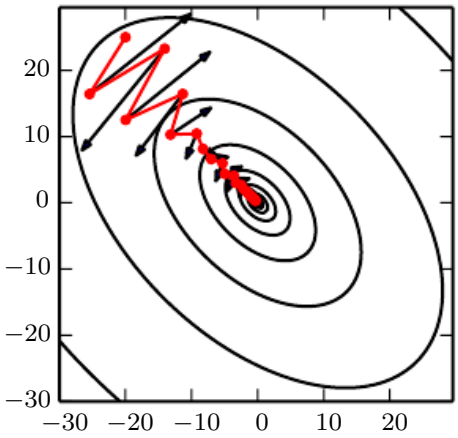

Figure 8.5: Momentum aims primarily to solve two problems: poor conditioning of the Hessian matrix and variance in the stochastic gradient. Here, we illustrate how momentum overcomes the first of these two problems. The contour lines depict a quadratic loss function with a poorly conditioned Hessian matrix. The red path cutting across the contours indicates the path followed by the momentum learning rule as it minimizes this function. At each step along the way, we draw an arrow indicating the step that gradient descent would take at that point. We can see that a poorly conditioned quadratic objective looks like a long, narrow valley or canyon with steep sides. Momentum correctly traverses the canyon lengthwise, while gradient steps waste time moving back and forth across the narrow axis of the canyon. Compare also figure 4.6, which shows the behavior of gradient descent without momentum.

Previously, the size of the step was simply the norm of the gradient multiplied by the learning rate. Now, the size of the step depends on how large and how aligned a *sequence* of gradients are. The step size is largest when many successive gradients point in exactly the same direction. If the momentum algorithm always observes gradient $\boldsymbol{g}$, then it will accelerate in the direction of $-\boldsymbol{g}$, until reaching a terminal velocity where the size of each step is

$$\frac{\epsilon||\boldsymbol{g}||}{1-\alpha}. \tag{8.17}$$

It is thus helpful to think of the momentum hyperparameter in terms of $\frac{1}{1-\alpha}$. For example, $\alpha = .9$ corresponds to multiplying the maximum speed by 10 relative to the gradient descent algorithm.

Common values of α used in practice include .5, .9, and .99. Like the learning rate, α may also be adapted over time. Typically it begins with a small value and is later raised. It is less important to adapt α over time than to shrink ϵ over time.

Algorithm 8.2 Stochastic gradient descent (SGD) with momentum

Require: Learning rate ϵ, momentum parameter α.
Require: Initial parameter $\boldsymbol{\theta}$, initial velocity $\boldsymbol{v}$.
while stopping criterion not met **do**
  Sample a minibatch of m examples from the training set $\{\boldsymbol{x}^{(1)}, \ldots, \boldsymbol{x}^{(m)}\}$ with corresponding targets $\boldsymbol{y}^{(i)}$.
  Compute gradient estimate: $\boldsymbol{g} \leftarrow \frac{1}{m}\nabla_{\boldsymbol{\theta}} \sum_i L(f(\boldsymbol{x}^{(i)}; \boldsymbol{\theta}), \boldsymbol{y}^{(i)})$
  Compute velocity update: $\boldsymbol{v} \leftarrow \alpha\boldsymbol{v} - \epsilon\boldsymbol{g}$
  Apply update: $\boldsymbol{\theta} \leftarrow \boldsymbol{\theta} + \boldsymbol{v}$
end while

We can view the momentum algorithm as simulating a particle subject to continuous-time Newtonian dynamics. The physical analogy can help to build intuition for how the momentum and gradient descent algorithms behave.

The position of the particle at any point in time is given by $\boldsymbol{\theta}(t)$. The particle experiences net force $\boldsymbol{f}(t)$. This force causes the particle to accelerate:

$$\boldsymbol{f}(t) = \frac{\partial^2}{\partial t^2}\boldsymbol{\theta}(t). \tag{8.18}$$

Rather than viewing this as a second-order differential equation of the position, we can introduce the variable $\boldsymbol{v}(t)$ representing the velocity of the particle at time t and rewrite the Newtonian dynamics as a first-order differential equation:

$$\boldsymbol{v}(t) = \frac{\partial}{\partial t}\boldsymbol{\theta}(t), \tag{8.19}$$

$$\boldsymbol{f}(t) = \frac{\partial}{\partial t}\boldsymbol{v}(t). \tag{8.20}$$

The momentum algorithm then consists of solving the differential equations via numerical simulation. A simple numerical method for solving differential equations is Euler's method, which simply consists of simulating the dynamics defined by the equation by taking small, finite steps in the direction of each gradient.

This explains the basic form of the momentum update, but what specifically are the forces? One force is proportional to the negative gradient of the cost function: $-\nabla_{\boldsymbol{\theta}} J(\boldsymbol{\theta})$. This force pushes the particle downhill along the cost function surface. The gradient descent algorithm would simply take a single step based on each gradient, but the Newtonian scenario used by the momentum algorithm instead uses this force to alter the velocity of the particle. We can think of the particle as being like a hockey puck sliding down an icy surface. Whenever it descends a steep part of the surface, it gathers speed and continues sliding in that direction until it begins to go uphill again.

One other force is necessary. If the only force is the gradient of the cost function, then the particle might never come to rest. Imagine a hockey puck sliding down one side of a valley and straight up the other side, oscillating back and forth forever, assuming the ice is perfectly frictionless. To resolve this problem, we add one other force, proportional to $-\boldsymbol{v}(t)$. In physics terminology, this force corresponds to viscous drag, as if the particle must push through a resistant medium such as syrup. This causes the particle to gradually lose energy over time and eventually converge to a local minimum.

Why do we use $-\boldsymbol{v}(t)$ and viscous drag in particular? Part of the reason to use $-\boldsymbol{v}(t)$ is mathematical convenience—an integer power of the velocity is easy to work with. However, other physical systems have other kinds of drag based on other integer powers of the velocity. For example, a particle traveling through the air experiences turbulent drag, with force proportional to the square of the velocity, while a particle moving along the ground experiences dry friction, with a force of constant magnitude. We can reject each of these options. Turbulent drag, proportional to the square of the velocity, becomes very weak when the velocity is small. It is not powerful enough to force the particle to come to rest. A particle with a non-zero initial velocity that experiences only the force of turbulent drag will move away from its initial position forever, with the distance from the starting point growing like $O(\log t)$. We must therefore use a lower power of the velocity. If we use a power of zero, representing dry friction, then the force is too strong. When the force due to the gradient of the cost function is small but non-zero, the constant force due to friction can cause the particle to come to rest before reaching a local minimum. Viscous drag avoids both of these problems—it is weak enough

that the gradient can continue to cause motion until a minimum is reached, but strong enough to prevent motion if the gradient does not justify moving.

8.3.3 Nesterov Momentum

Sutskever *et al.* (2013) introduced a variant of the momentum algorithm that was inspired by Nesterov's accelerated gradient method (Nesterov, 1983, 2004). The update rules in this case are given by:

$$\boldsymbol{v} \leftarrow \alpha \boldsymbol{v} - \epsilon \nabla_{\boldsymbol{\theta}} \left[\frac{1}{m} \sum_{i=1}^{m} L\left(\boldsymbol{f}(\boldsymbol{x}^{(i)}; \boldsymbol{\theta} + \alpha \boldsymbol{v}), \boldsymbol{y}^{(i)} \right) \right], \tag{8.21}$$

$$\boldsymbol{\theta} \leftarrow \boldsymbol{\theta} + \boldsymbol{v}, \tag{8.22}$$

where the parameters α and ϵ play a similar role as in the standard momentum method. The difference between Nesterov momentum and standard momentum is where the gradient is evaluated. With Nesterov momentum the gradient is evaluated after the current velocity is applied. Thus one can interpret Nesterov momentum as attempting to add a *correction factor* to the standard method of momentum. The complete Nesterov momentum algorithm is presented in algorithm 8.3.

In the convex batch gradient case, Nesterov momentum brings the rate of convergence of the excess error from $O(1/k)$ (after k steps) to $O(1/k^2)$ as shown by Nesterov (1983). Unfortunately, in the stochastic gradient case, Nesterov momentum does not improve the rate of convergence.

Algorithm 8.3 Stochastic gradient descent (SGD) with Nesterov momentum

Require: Learning rate ϵ, momentum parameter α.
Require: Initial parameter $\boldsymbol{\theta}$, initial velocity $\boldsymbol{v}$.
  while stopping criterion not met **do**
    Sample a minibatch of m examples from the training set $\{\boldsymbol{x}^{(1)}, \ldots, \boldsymbol{x}^{(m)}\}$ with corresponding labels $\boldsymbol{y}^{(i)}$.
    Apply interim update: $\tilde{\boldsymbol{\theta}} \leftarrow \boldsymbol{\theta} + \alpha \boldsymbol{v}$
    Compute gradient (at interim point): $\boldsymbol{g} \leftarrow \frac{1}{m} \nabla_{\tilde{\boldsymbol{\theta}}} \sum_i L(f(\boldsymbol{x}^{(i)}; \tilde{\boldsymbol{\theta}}), \boldsymbol{y}^{(i)})$
    Compute velocity update: $\boldsymbol{v} \leftarrow \alpha \boldsymbol{v} - \epsilon \boldsymbol{g}$
    Apply update: $\boldsymbol{\theta} \leftarrow \boldsymbol{\theta} + \boldsymbol{v}$
  end while

8.4 Parameter Initialization Strategies

Some optimization algorithms are not iterative by nature and simply solve for a solution point. Other optimization algorithms are iterative by nature but, when applied to the right class of optimization problems, converge to acceptable solutions in an acceptable amount of time regardless of initialization. Deep learning training algorithms usually do not have either of these luxuries. Training algorithms for deep learning models are usually iterative in nature and thus require the user to specify some initial point from which to begin the iterations. Moreover, training deep models is a sufficiently difficult task that most algorithms are strongly affected by the choice of initialization. The initial point can determine whether the algorithm converges at all, with some initial points being so unstable that the algorithm encounters numerical difficulties and fails altogether. When learning does converge, the initial point can determine how quickly learning converges and whether it converges to a point with high or low cost. Also, points of comparable cost can have wildly varying generalization error, and the initial point can affect the generalization as well.

Modern initialization strategies are simple and heuristic. Designing improved initialization strategies is a difficult task because neural network optimization is not yet well understood. Most initialization strategies are based on achieving some nice properties when the network is initialized. However, we do not have a good understanding of which of these properties are preserved under which circumstances after learning begins to proceed. A further difficulty is that some initial points may be beneficial from the viewpoint of optimization but detrimental from the viewpoint of generalization. Our understanding of how the initial point affects generalization is especially primitive, offering little to no guidance for how to select the initial point.

Perhaps the only property known with complete certainty is that the initial parameters need to "break symmetry" between different units. If two hidden units with the same activation function are connected to the same inputs, then these units must have different initial parameters. If they have the same initial parameters, then a deterministic learning algorithm applied to a deterministic cost and model will constantly update both of these units in the same way. Even if the model or training algorithm is capable of using stochasticity to compute different updates for different units (for example, if one trains with dropout), it is usually best to initialize each unit to compute a different function from all of the other units. This may help to make sure that no input patterns are lost in the null space of forward propagation and no gradient patterns are lost in the null space of back-propagation. The goal of having each unit compute a different function

motivates random initialization of the parameters. We could explicitly search for a large set of basis functions that are all mutually different from each other, but this often incurs a noticeable computational cost. For example, if we have at most as many outputs as inputs, we could use Gram-Schmidt orthogonalization on an initial weight matrix, and be guaranteed that each unit computes a very different function from each other unit. Random initialization from a high-entropy distribution over a high-dimensional space is computationally cheaper and unlikely to assign any units to compute the same function as each other.

Typically, we set the biases for each unit to heuristically chosen constants, and initialize only the weights randomly. Extra parameters, for example, parameters encoding the conditional variance of a prediction, are usually set to heuristically chosen constants much like the biases are.

We almost always initialize all the weights in the model to values drawn randomly from a Gaussian or uniform distribution. The choice of Gaussian or uniform distribution does not seem to matter very much, but has not been exhaustively studied. The scale of the initial distribution, however, does have a large effect on both the outcome of the optimization procedure and on the ability of the network to generalize.

Larger initial weights will yield a stronger symmetry breaking effect, helping to avoid redundant units. They also help to avoid losing signal during forward or back-propagation through the linear component of each layer—larger values in the matrix result in larger outputs of matrix multiplication. Initial weights that are too large may, however, result in exploding values during forward propagation or back-propagation. In recurrent networks, large weights can also result in **chaos** (such extreme sensitivity to small perturbations of the input that the behavior of the deterministic forward propagation procedure appears random). To some extent, the exploding gradient problem can be mitigated by gradient clipping (thresholding the values of the gradients before performing a gradient descent step). Large weights may also result in extreme values that cause the activation function to saturate, causing complete loss of gradient through saturated units. These competing factors determine the ideal initial scale of the weights.

The perspectives of regularization and optimization can give very different insights into how we should initialize a network. The optimization perspective suggests that the weights should be large enough to propagate information successfully, but some regularization concerns encourage making them smaller. The use of an optimization algorithm such as stochastic gradient descent that makes small incremental changes to the weights and tends to halt in areas that are nearer to the initial parameters (whether due to getting stuck in a region of low gradient, or

due to triggering some early stopping criterion based on overfitting) expresses a prior that the final parameters should be close to the initial parameters. Recall from section 7.8 that gradient descent with early stopping is equivalent to weight decay for some models. In the general case, gradient descent with early stopping is not the same as weight decay, but does provide a loose analogy for thinking about the effect of initialization. We can think of initializing the parameters $\boldsymbol{\theta}$ to $\boldsymbol{\theta}_0$ as being similar to imposing a Gaussian prior $p(\boldsymbol{\theta})$ with mean $\boldsymbol{\theta}_0$. From this point of view, it makes sense to choose $\boldsymbol{\theta}_0$ to be near 0. This prior says that it is more likely that units do not interact with each other than that they do interact. Units interact only if the likelihood term of the objective function expresses a strong preference for them to interact. On the other hand, if we initialize $\boldsymbol{\theta}_0$ to large values, then our prior specifies which units should interact with each other, and how they should interact.

Some heuristics are available for choosing the initial scale of the weights. One heuristic is to initialize the weights of a fully connected layer with m inputs and n outputs by sampling each weight from $U(-\frac{1}{\sqrt{m}}, \frac{1}{\sqrt{m}})$, while Glorot and Bengio (2010) suggest using the **normalized initialization**

$$\mathrm{W}_{i,j} \sim U\left(-\sqrt{\frac{6}{m+n}}, \sqrt{\frac{6}{m+n}}\right). \tag{8.23}$$

This latter heuristic is designed to compromise between the goal of initializing all layers to have the same activation variance and the goal of initializing all layers to have the same gradient variance. The formula is derived using the assumption that the network consists only of a chain of matrix multiplications, with no nonlinearities. Real neural networks obviously violate this assumption, but many strategies designed for the linear model perform reasonably well on its nonlinear counterparts.

Saxe *et al.* (2013) recommend initializing to random orthogonal matrices, with a carefully chosen scaling or **gain** factor g that accounts for the nonlinearity applied at each layer. They derive specific values of the scaling factor for different types of nonlinear activation functions. This initialization scheme is also motivated by a model of a deep network as a sequence of matrix multiplies without nonlinearities. Under such a model, this initialization scheme guarantees that the total number of training iterations required to reach convergence is independent of depth.

Increasing the scaling factor g pushes the network toward the regime where activations increase in norm as they propagate forward through the network and gradients increase in norm as they propagate backward. Sussillo (2014) showed that setting the gain factor correctly is sufficient to train networks as deep as

1,000 layers, without needing to use orthogonal initializations. A key insight of this approach is that in feedforward networks, activations and gradients can grow or shrink on each step of forward or back-propagation, following a random walk behavior. This is because feedforward networks use a different weight matrix at each layer. If this random walk is tuned to preserve norms, then feedforward networks can mostly avoid the vanishing and exploding gradients problem that arises when the same weight matrix is used at each step, described in section 8.2.5.

Unfortunately, these optimal criteria for initial weights often do not lead to optimal performance. This may be for three different reasons. First, we may be using the wrong criteria—it may not actually be beneficial to preserve the norm of a signal throughout the entire network. Second, the properties imposed at initialization may not persist after learning has begun to proceed. Third, the criteria might succeed at improving the speed of optimization but inadvertently increase generalization error. In practice, we usually need to treat the scale of the weights as a hyperparameter whose optimal value lies somewhere roughly near but not exactly equal to the theoretical predictions.

One drawback to scaling rules that set all of the initial weights to have the same standard deviation, such as $\frac{1}{\sqrt{m}}$, is that every individual weight becomes extremely small when the layers become large. Martens (2010) introduced an alternative initialization scheme called **sparse initialization** in which each unit is initialized to have exactly k non-zero weights. The idea is to keep the total amount of input to the unit independent from the number of inputs m without making the magnitude of individual weight elements shrink with m. Sparse initialization helps to achieve more diversity among the units at initialization time. However, it also imposes a very strong prior on the weights that are chosen to have large Gaussian values. Because it takes a long time for gradient descent to shrink "incorrect" large values, this initialization scheme can cause problems for units such as maxout units that have several filters that must be carefully coordinated with each other.

When computational resources allow it, it is usually a good idea to treat the initial scale of the weights for each layer as a hyperparameter, and to choose these scales using a hyperparameter search algorithm described in section 11.4.2, such as random search. The choice of whether to use dense or sparse initialization can also be made a hyperparameter. Alternately, one can manually search for the best initial scales. A good rule of thumb for choosing the initial scales is to look at the range or standard deviation of activations or gradients on a single minibatch of data. If the weights are too small, the range of activations across the minibatch will shrink as the activations propagate forward through the network. By repeatedly identifying the first layer with unacceptably small activations and

increasing its weights, it is possible to eventually obtain a network with reasonable initial activations throughout. If learning is still too slow at this point, it can be useful to look at the range or standard deviation of the gradients as well as the activations. This procedure can in principle be automated and is generally less computationally costly than hyperparameter optimization based on validation set error because it is based on feedback from the behavior of the initial model on a single batch of data, rather than on feedback from a trained model on the validation set. While long used heuristically, this protocol has recently been specified more formally and studied by Mishkin and Matas (2015).

So far we have focused on the initialization of the weights. Fortunately, initialization of other parameters is typically easier.

The approach for setting the biases must be coordinated with the approach for settings the weights. Setting the biases to zero is compatible with most weight initialization schemes. There are a few situations where we may set some biases to non-zero values:

- If a bias is for an output unit, then it is often beneficial to initialize the bias to obtain the right marginal statistics of the output. To do this, we assume that the initial weights are small enough that the output of the unit is determined only by the bias. This justifies setting the bias to the inverse of the activation function applied to the marginal statistics of the output in the training set. For example, if the output is a distribution over classes and this distribution is a highly skewed distribution with the marginal probability of class i given by element c_i of some vector $\boldsymbol{c}$, then we can set the bias vector $\boldsymbol{b}$ by solving the equation $\text{softmax}(\boldsymbol{b}) = \boldsymbol{c}$. This applies not only to classifiers but also to models we will encounter in Part III, such as autoencoders and Boltzmann machines. These models have layers whose output should resemble the input data $\boldsymbol{x}$, and it can be very helpful to initialize the biases of such layers to match the marginal distribution over $\boldsymbol{x}$.

- Sometimes we may want to choose the bias to avoid causing too much saturation at initialization. For example, we may set the bias of a ReLU hidden unit to 0.1 rather than 0 to avoid saturating the ReLU at initialization. This approach is not compatible with weight initialization schemes that do not expect strong input from the biases though. For example, it is not recommended for use with random walk initialization (Sussillo, 2014).

- Sometimes a unit controls whether other units are able to participate in a function. In such situations, we have a unit with output u and another unit $h \in [0, 1]$, and they are multiplied together to produce an output uh. We

can view h as a gate that determines whether $uh \approx u$ or $uh \approx 0$. In these situations, we want to set the bias for h so that $h \approx 1$ most of the time at initialization. Otherwise u does not have a chance to learn. For example, Jozefowicz *et al.* (2015) advocate setting the bias to 1 for the forget gate of the LSTM model, described in section 10.10.

Another common type of parameter is a variance or precision parameter. For example, we can perform linear regression with a conditional variance estimate using the model

$$p(y \mid \boldsymbol{x}) = \mathcal{N}(y \mid \boldsymbol{w}^T \boldsymbol{x} + b, 1/\beta) \tag{8.24}$$

where β is a precision parameter. We can usually initialize variance or precision parameters to 1 safely. Another approach is to assume the initial weights are close enough to zero that the biases may be set while ignoring the effect of the weights, then set the biases to produce the correct marginal mean of the output, and set the variance parameters to the marginal variance of the output in the training set.

Besides these simple constant or random methods of initializing model parameters, it is possible to initialize model parameters using machine learning. A common strategy discussed in part III of this book is to initialize a supervised model with the parameters learned by an unsupervised model trained on the same inputs. One can also perform supervised training on a related task. Even performing supervised training on an unrelated task can sometimes yield an initialization that offers faster convergence than a random initialization. Some of these initialization strategies may yield faster convergence and better generalization because they encode information about the distribution in the initial parameters of the model. Others apparently perform well primarily because they set the parameters to have the right scale or set different units to compute different functions from each other.

8.5 Algorithms with Adaptive Learning Rates

Neural network researchers have long realized that the learning rate was reliably one of the hyperparameters that is the most difficult to set because it has a significant impact on model performance. As we have discussed in sections 4.3 and 8.2, the cost is often highly sensitive to some directions in parameter space and insensitive to others. The momentum algorithm can mitigate these issues somewhat, but does so at the expense of introducing another hyperparameter. In the face of this, it is natural to ask if there is another way. If we believe that the directions of sensitivity are somewhat axis-aligned, it can make sense to use a separate learning

rate for each parameter, and automatically adapt these learning rates throughout the course of learning.

The **delta-bar-delta** algorithm (Jacobs, 1988) is an early heuristic approach to adapting individual learning rates for model parameters during training. The approach is based on a simple idea: if the partial derivative of the loss, with respect to a given model parameter, remains the same sign, then the learning rate should increase. If the partial derivative with respect to that parameter changes sign, then the learning rate should decrease. Of course, this kind of rule can only be applied to full batch optimization.

More recently, a number of incremental (or mini-batch-based) methods have been introduced that adapt the learning rates of model parameters. This section will briefly review a few of these algorithms.

8.5.1 AdaGrad

The **AdaGrad** algorithm, shown in algorithm 8.4, individually adapts the learning rates of all model parameters by scaling them inversely proportional to the square root of the sum of all of their historical squared values (Duchi *et al.*, 2011). The parameters with the largest partial derivative of the loss have a correspondingly rapid decrease in their learning rate, while parameters with small partial derivatives have a relatively small decrease in their learning rate. The net effect is greater progress in the more gently sloped directions of parameter space.

In the context of convex optimization, the AdaGrad algorithm enjoys some desirable theoretical properties. However, empirically it has been found that—for training deep neural network models—the accumulation of squared gradients *from the beginning of training* can result in a premature and excessive decrease in the effective learning rate. AdaGrad performs well for some but not all deep learning models.

8.5.2 RMSProp

The **RMSProp** algorithm (Hinton, 2012) modifies AdaGrad to perform better in the non-convex setting by changing the gradient accumulation into an exponentially weighted moving average. AdaGrad is designed to converge rapidly when applied to a convex function. When applied to a non-convex function to train a neural network, the learning trajectory may pass through many different structures and eventually arrive at a region that is a locally convex bowl. AdaGrad shrinks the learning rate according to the entire history of the squared gradient and may

Algorithm 8.4 The AdaGrad algorithm

Require: Global learning rate ϵ
Require: Initial parameter $\boldsymbol{\theta}$
Require: Small constant δ, perhaps 10^{-7}, for numerical stability
Initialize gradient accumulation variable $\boldsymbol{r} = \boldsymbol{0}$
while stopping criterion not met **do**
Sample a minibatch of m examples from the training set $\{\boldsymbol{x}^{(1)}, \ldots, \boldsymbol{x}^{(m)}\}$ with corresponding targets $\boldsymbol{y}^{(i)}$.
Compute gradient: $\boldsymbol{g} \leftarrow \frac{1}{m} \nabla_{\boldsymbol{\theta}} \sum_i L(f(\boldsymbol{x}^{(i)}; \boldsymbol{\theta}), \boldsymbol{y}^{(i)})$
Accumulate squared gradient: $\boldsymbol{r} \leftarrow \boldsymbol{r} + \boldsymbol{g} \odot \boldsymbol{g}$
Compute update: $\Delta\boldsymbol{\theta} \leftarrow -\frac{\epsilon}{\delta + \sqrt{\boldsymbol{r}}} \odot \boldsymbol{g}$. (Division and square root applied element-wise)
Apply update: $\boldsymbol{\theta} \leftarrow \boldsymbol{\theta} + \Delta\boldsymbol{\theta}$
end while

have made the learning rate too small before arriving at such a convex structure. RMSProp uses an exponentially decaying average to discard history from the extreme past so that it can converge rapidly after finding a convex bowl, as if it were an instance of the AdaGrad algorithm initialized within that bowl.

RMSProp is shown in its standard form in algorithm 8.5 and combined with Nesterov momentum in algorithm 8.6. Compared to AdaGrad, the use of the moving average introduces a new hyperparameter, ρ, that controls the length scale of the moving average.

Empirically, RMSProp has been shown to be an effective and practical optimization algorithm for deep neural networks. It is currently one of the go-to optimization methods being employed routinely by deep learning practitioners.

8.5.3 Adam

Adam (Kingma and Ba, 2014) is yet another adaptive learning rate optimization algorithm and is presented in algorithm 8.7. The name "Adam" derives from the phrase "adaptive moments." In the context of the earlier algorithms, it is perhaps best seen as a variant on the combination of RMSProp and momentum with a few important distinctions. First, in Adam, momentum is incorporated directly as an estimate of the first order moment (with exponential weighting) of the gradient. The most straightforward way to add momentum to RMSProp is to apply momentum to the rescaled gradients. The use of momentum in combination with rescaling does not have a clear theoretical motivation. Second, Adam includes

Algorithm 8.5 The RMSProp algorithm

Require: Global learning rate ϵ, decay rate ρ.
Require: Initial parameter $\boldsymbol{\theta}$
Require: Small constant δ, usually 10^{-6}, used to stabilize division by small numbers.
Initialize accumulation variables $\boldsymbol{r} = 0$
while stopping criterion not met **do**
Sample a minibatch of m examples from the training set $\{\boldsymbol{x}^{(1)}, \ldots, \boldsymbol{x}^{(m)}\}$ with corresponding targets $\boldsymbol{y}^{(i)}$.
Compute gradient: $\boldsymbol{g} \leftarrow \frac{1}{m} \nabla_{\boldsymbol{\theta}} \sum_i L(f(\boldsymbol{x}^{(i)}; \boldsymbol{\theta}), \boldsymbol{y}^{(i)})$
Accumulate squared gradient: $\boldsymbol{r} \leftarrow \rho \boldsymbol{r} + (1 - \rho) \boldsymbol{g} \odot \boldsymbol{g}$
Compute parameter update: $\Delta \boldsymbol{\theta} = -\frac{\epsilon}{\sqrt{\delta + \boldsymbol{r}}} \odot \boldsymbol{g}$. ($\frac{1}{\sqrt{\delta + \boldsymbol{r}}}$ applied element-wise)
Apply update: $\boldsymbol{\theta} \leftarrow \boldsymbol{\theta} + \Delta \boldsymbol{\theta}$
end while

bias corrections to the estimates of both the first-order moments (the momentum term) and the (uncentered) second-order moments to account for their initialization at the origin (see algorithm 8.7). RMSProp also incorporates an estimate of the (uncentered) second-order moment, however it lacks the correction factor. Thus, unlike in Adam, the RMSProp second-order moment estimate may have high bias early in training. Adam is generally regarded as being fairly robust to the choice of hyperparameters, though the learning rate sometimes needs to be changed from the suggested default.

8.5.4 Choosing the Right Optimization Algorithm

In this section, we discussed a series of related algorithms that each seek to address the challenge of optimizing deep models by adapting the learning rate for each model parameter. At this point, a natural question is: which algorithm should one choose?

Unfortunately, there is currently no consensus on this point. Schaul *et al.* (2014) presented a valuable comparison of a large number of optimization algorithms across a wide range of learning tasks. While the results suggest that the family of algorithms with adaptive learning rates (represented by RMSProp and AdaDelta) performed fairly robustly, no single best algorithm has emerged.

Currently, the most popular optimization algorithms actively in use include SGD, SGD with momentum, RMSProp, RMSProp with momentum, AdaDelta and Adam. The choice of which algorithm to use, at this point, seems to depend

Algorithm 8.6 RMSProp algorithm with Nesterov momentum

Require: Global learning rate ϵ, decay rate ρ, momentum coefficient α.
Require: Initial parameter $\boldsymbol{\theta}$, initial velocity $\boldsymbol{v}$.
  Initialize accumulation variable $\boldsymbol{r} = \boldsymbol{0}$
  while stopping criterion not met **do**
    Sample a minibatch of m examples from the training set $\{\boldsymbol{x}^{(1)}, \ldots, \boldsymbol{x}^{(m)}\}$ with corresponding targets $\boldsymbol{y}^{(i)}$.
    Compute interim update: $\tilde{\boldsymbol{\theta}} \leftarrow \boldsymbol{\theta} + \alpha \boldsymbol{v}$
    Compute gradient: $\boldsymbol{g} \leftarrow \frac{1}{m} \nabla_{\tilde{\boldsymbol{\theta}}} \sum_i L(f(\boldsymbol{x}^{(i)}; \tilde{\boldsymbol{\theta}}), \boldsymbol{y}^{(i)})$
    Accumulate gradient: $\boldsymbol{r} \leftarrow \rho \boldsymbol{r} + (1 - \rho) \boldsymbol{g} \odot \boldsymbol{g}$
    Compute velocity update: $\boldsymbol{v} \leftarrow \alpha \boldsymbol{v} - \frac{\epsilon}{\sqrt{\boldsymbol{r}}} \odot \boldsymbol{g}$. ($\frac{1}{\sqrt{\boldsymbol{r}}}$ applied element-wise)
    Apply update: $\boldsymbol{\theta} \leftarrow \boldsymbol{\theta} + \boldsymbol{v}$
  end while

largely on the user's familiarity with the algorithm (for ease of hyperparameter tuning).

8.6 Approximate Second-Order Methods

In this section we discuss the application of second-order methods to the training of deep networks. See LeCun *et al.* (1998a) for an earlier treatment of this subject. For simplicity of exposition, the only objective function we examine is the empirical risk:

$$J(\boldsymbol{\theta}) = \mathbb{E}_{\mathbf{x},\mathrm{y} \sim \hat{p}_{\mathrm{data}}(\boldsymbol{x},y)}[L(f(\boldsymbol{x}; \boldsymbol{\theta}), y)] = \frac{1}{m} \sum_{i=1}^{m} L(f(\boldsymbol{x}^{(i)}; \boldsymbol{\theta}), y^{(i)}). \tag{8.25}$$

However the methods we discuss here extend readily to more general objective functions that, for instance, include parameter regularization terms such as those discussed in chapter 7.

8.6.1 Newton's Method

In section 4.3, we introduced second-order gradient methods. In contrast to first-order methods, second-order methods make use of second derivatives to improve optimization. The most widely used second-order method is Newton's method. We now describe Newton's method in more detail, with emphasis on its application to neural network training.

Algorithm 8.7 The Adam algorithm

Require: Step size ϵ (Suggested default: 0.001)
Require: Exponential decay rates for moment estimates, ρ_1 and ρ_2 in $[0, 1)$. (Suggested defaults: 0.9 and 0.999 respectively)
Require: Small constant δ used for numerical stabilization. (Suggested default: 10^{-8})
Require: Initial parameters $\boldsymbol{\theta}$
  Initialize 1st and 2nd moment variables $\boldsymbol{s} = \boldsymbol{0}$, $\boldsymbol{r} = \boldsymbol{0}$
  Initialize time step $t = 0$
  while stopping criterion not met **do**
    Sample a minibatch of m examples from the training set $\{\boldsymbol{x}^{(1)}, \ldots, \boldsymbol{x}^{(m)}\}$ with corresponding targets $\boldsymbol{y}^{(i)}$.
    Compute gradient: $\boldsymbol{g} \leftarrow \frac{1}{m} \nabla_{\boldsymbol{\theta}} \sum_i L(f(\boldsymbol{x}^{(i)}; \boldsymbol{\theta}), \boldsymbol{y}^{(i)})$
    $t \leftarrow t + 1$
    Update biased first moment estimate: $\boldsymbol{s} \leftarrow \rho_1 \boldsymbol{s} + (1 - \rho_1)\boldsymbol{g}$
    Update biased second moment estimate: $\boldsymbol{r} \leftarrow \rho_2 \boldsymbol{r} + (1 - \rho_2)\boldsymbol{g} \odot \boldsymbol{g}$
    Correct bias in first moment: $\hat{\boldsymbol{s}} \leftarrow \frac{\boldsymbol{s}}{1 - \rho_1^t}$
    Correct bias in second moment: $\hat{\boldsymbol{r}} \leftarrow \frac{\boldsymbol{r}}{1 - \rho_2^t}$
    Compute update: $\Delta\boldsymbol{\theta} = -\epsilon \frac{\hat{\boldsymbol{s}}}{\sqrt{\hat{\boldsymbol{r}}} + \delta}$ (operations applied element-wise)
    Apply update: $\boldsymbol{\theta} \leftarrow \boldsymbol{\theta} + \Delta\boldsymbol{\theta}$
  end while

Newton's method is an optimization scheme based on using a second-order Taylor series expansion to approximate $J(\boldsymbol{\theta})$ near some point $\boldsymbol{\theta}_0$, ignoring derivatives of higher order:

$$J(\boldsymbol{\theta}) \approx J(\boldsymbol{\theta}_0) + (\boldsymbol{\theta} - \boldsymbol{\theta}_0)^\top \nabla_{\boldsymbol{\theta}} J(\boldsymbol{\theta}_0) + \frac{1}{2}(\boldsymbol{\theta} - \boldsymbol{\theta}_0)^\top \boldsymbol{H}(\boldsymbol{\theta} - \boldsymbol{\theta}_0), \tag{8.26}$$

where $\boldsymbol{H}$ is the Hessian of J with respect to $\boldsymbol{\theta}$ evaluated at $\boldsymbol{\theta}_0$. If we then solve for the critical point of this function, we obtain the Newton parameter update rule:

$$\boldsymbol{\theta}^* = \boldsymbol{\theta}_0 - \boldsymbol{H}^{-1} \nabla_{\boldsymbol{\theta}} J(\boldsymbol{\theta}_0) \tag{8.27}$$

Thus for a locally quadratic function (with positive definite $\boldsymbol{H}$), by rescaling the gradient by $\boldsymbol{H}^{-1}$, Newton's method jumps directly to the minimum. If the objective function is convex but not quadratic (there are higher-order terms), this update can be iterated, yielding the training algorithm associated with Newton's method, given in algorithm 8.8.

Algorithm 8.8 Newton's method with objective $J(\boldsymbol{\theta}) = \frac{1}{m}\sum_{i=1}^{m} L(f(\boldsymbol{x}^{(i)}; \boldsymbol{\theta}), y^{(i)})$.

Require: Initial parameter $\boldsymbol{\theta}_0$
Require: Training set of m examples
  while stopping criterion not met **do**
    Compute gradient: $\boldsymbol{g} \leftarrow \frac{1}{m}\nabla_{\boldsymbol{\theta}} \sum_i L(f(\boldsymbol{x}^{(i)}; \boldsymbol{\theta}), \boldsymbol{y}^{(i)})$
    Compute Hessian: $\boldsymbol{H} \leftarrow \frac{1}{m}\nabla^2_{\boldsymbol{\theta}} \sum_i L(f(\boldsymbol{x}^{(i)}; \boldsymbol{\theta}), \boldsymbol{y}^{(i)})$
    Compute Hessian inverse: $\boldsymbol{H}^{-1}$
    Compute update: $\Delta\boldsymbol{\theta} = -\boldsymbol{H}^{-1}\boldsymbol{g}$
    Apply update: $\boldsymbol{\theta} = \boldsymbol{\theta} + \Delta\boldsymbol{\theta}$
  end while

For surfaces that are not quadratic, as long as the Hessian remains positive definite, Newton's method can be applied iteratively. This implies a two-step iterative procedure. First, update or compute the inverse Hessian (i.e. by updating the quadratic approximation). Second, update the parameters according to equation 8.27.

In section 8.2.3, we discussed how Newton's method is appropriate only when the Hessian is positive definite. In deep learning, the surface of the objective function is typically non-convex with many features, such as saddle points, that are problematic for Newton's method. If the eigenvalues of the Hessian are not all positive, for example, near a saddle point, then Newton's method can actually cause updates to move in the wrong direction. This situation can be avoided by regularizing the Hessian. Common regularization strategies include adding a constant, α, along the diagonal of the Hessian. The regularized update becomes

$$\boldsymbol{\theta}^* = \boldsymbol{\theta}_0 - \left[H\left(f(\boldsymbol{\theta}_0)\right) + \alpha \boldsymbol{I}\right]^{-1} \nabla_{\boldsymbol{\theta}} f(\boldsymbol{\theta}_0). \tag{8.28}$$

This regularization strategy is used in approximations to Newton's method, such as the Levenberg–Marquardt algorithm (Levenberg, 1944; Marquardt, 1963), and works fairly well as long as the negative eigenvalues of the Hessian are still relatively close to zero. In cases where there are more extreme directions of curvature, the value of α would have to be sufficiently large to offset the negative eigenvalues. However, as α increases in size, the Hessian becomes dominated by the $\alpha\boldsymbol{I}$ diagonal and the direction chosen by Newton's method converges to the standard gradient divided by α. When strong negative curvature is present, α may need to be so large that Newton's method would make smaller steps than gradient descent with a properly chosen learning rate.

Beyond the challenges created by certain features of the objective function,

such as saddle points, the application of Newton's method for training large neural networks is limited by the significant computational burden it imposes. The number of elements in the Hessian is squared in the number of parameters, so with k parameters (and for even very small neural networks the number of parameters k can be in the millions), Newton's method would require the inversion of a $k \times k$ matrix—with computational complexity of $O(k^3)$. Also, since the parameters will change with every update, the inverse Hessian has to be computed *at every training iteration*. As a consequence, only networks with a very small number of parameters can be practically trained via Newton's method. In the remainder of this section, we will discuss alternatives that attempt to gain some of the advantages of Newton's method while side-stepping the computational hurdles.

8.6.2 Conjugate Gradients

Conjugate gradients is a method to efficiently avoid the calculation of the inverse Hessian by iteratively descending **conjugate directions**. The inspiration for this approach follows from a careful study of the weakness of the method of steepest descent (see section 4.3 for details), where line searches are applied iteratively in the direction associated with the gradient. Figure 8.6 illustrates how the method of steepest descent, when applied in a quadratic bowl, progresses in a rather ineffective back-and-forth, zig-zag pattern. This happens because each line search direction, when given by the gradient, is guaranteed to be orthogonal to the previous line search direction.

Let the previous search direction be $\boldsymbol{d}_{t-1}$. At the minimum, where the line search terminates, the directional derivative is zero in direction $\boldsymbol{d}_{t-1}$: $\nabla_{\boldsymbol{\theta}} J(\boldsymbol{\theta}) \cdot \boldsymbol{d}_{t-1} = 0$. Since the gradient at this point defines the current search direction, $\boldsymbol{d}_t = \nabla_{\boldsymbol{\theta}} J(\boldsymbol{\theta})$ will have no contribution in the direction $\boldsymbol{d}_{t-1}$. Thus $\boldsymbol{d}_t$ is orthogonal to $\boldsymbol{d}_{t-1}$. This relationship between $\boldsymbol{d}_{t-1}$ and $\boldsymbol{d}_t$ is illustrated in figure 8.6 for multiple iterations of steepest descent. As demonstrated in the figure, the choice of orthogonal directions of descent do not preserve the minimum along the previous search directions. This gives rise to the zig-zag pattern of progress, where by descending to the minimum in the current gradient direction, we must re-minimize the objective in the previous gradient direction. Thus, by following the gradient at the end of each line search we are, in a sense, undoing progress we have already made in the direction of the previous line search. The method of conjugate gradients seeks to address this problem.

In the method of conjugate gradients, we seek to find a search direction that is **conjugate** to the previous line search direction, i.e. it will not undo progress made in that direction. At training iteration t, the next search direction $\boldsymbol{d}_t$ takes

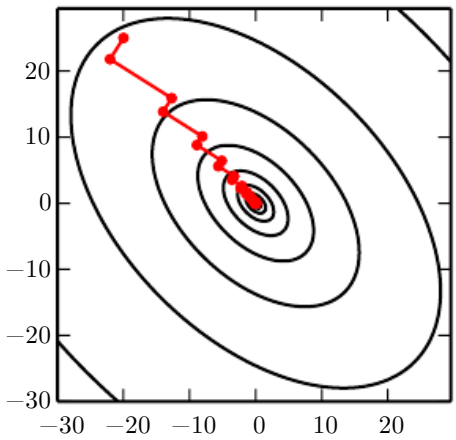

Figure 8.6: The method of steepest descent applied to a quadratic cost surface. The method of steepest descent involves jumping to the point of lowest cost along the line defined by the gradient at the initial point on each step. This resolves some of the problems seen with using a fixed learning rate in figure 4.6, but even with the optimal step size the algorithm still makes back-and-forth progress toward the optimum. By definition, at the minimum of the objective along a given direction, the gradient at the final point is orthogonal to that direction.

the form:

$$\boldsymbol{d}_t = \nabla_{\boldsymbol{\theta}} J(\boldsymbol{\theta}) + \beta_t \boldsymbol{d}_{t-1} \tag{8.29}$$

where β_t is a coefficient whose magnitude controls how much of the direction, $\boldsymbol{d}_{t-1}$, we should add back to the current search direction.

Two directions, $\boldsymbol{d}_t$ and $\boldsymbol{d}_{t-1}$, are defined as conjugate if $\boldsymbol{d}_t^\top \boldsymbol{H} \boldsymbol{d}_{t-1} = 0$, where $\boldsymbol{H}$ is the Hessian matrix.

The straightforward way to impose conjugacy would involve calculation of the eigenvectors of $\boldsymbol{H}$ to choose β_t, which would not satisfy our goal of developing a method that is more computationally viable than Newton's method for large problems. Can we calculate the conjugate directions without resorting to these calculations? Fortunately the answer to that is yes.

Two popular methods for computing the β_t are:

1. Fletcher-Reeves:

$$\beta_t = \frac{\nabla_{\boldsymbol{\theta}} J(\boldsymbol{\theta}_t)^\top \nabla_{\boldsymbol{\theta}} J(\boldsymbol{\theta}_t)}{\nabla_{\boldsymbol{\theta}} J(\boldsymbol{\theta}_{t-1})^\top \nabla_{\boldsymbol{\theta}} J(\boldsymbol{\theta}_{t-1})} \tag{8.30}$$

2. Polak-Ribière:

$$\beta_t = \frac{(\nabla_{\boldsymbol{\theta}} J(\boldsymbol{\theta}_t) - \nabla_{\boldsymbol{\theta}} J(\boldsymbol{\theta}_{t-1}))^\top \nabla_{\boldsymbol{\theta}} J(\boldsymbol{\theta}_t)}{\nabla_{\boldsymbol{\theta}} J(\boldsymbol{\theta}_{t-1})^\top \nabla_{\boldsymbol{\theta}} J(\boldsymbol{\theta}_{t-1})} \tag{8.31}$$

For a quadratic surface, the conjugate directions ensure that the gradient along the previous direction does not increase in magnitude. We therefore stay at the minimum along the previous directions. As a consequence, in a k-dimensional parameter space, the conjugate gradient method requires at most k line searches to achieve the minimum. The conjugate gradient algorithm is given in algorithm 8.9.

Algorithm 8.9 The conjugate gradient method

Require: Initial parameters $\boldsymbol{\theta}_0$
Require: Training set of m examples
  Initialize $\boldsymbol{\rho}_0 = \mathbf{0}$
  Initialize $g_0 = 0$
  Initialize $t = 1$
  while stopping criterion not met **do**
    Initialize the gradient $\boldsymbol{g}_t = \mathbf{0}$
    Compute gradient: $\boldsymbol{g}_t \leftarrow \frac{1}{m} \nabla_{\boldsymbol{\theta}} \sum_i L(f(\boldsymbol{x}^{(i)}; \boldsymbol{\theta}), \boldsymbol{y}^{(i)})$
    Compute $\beta_t = \frac{(\boldsymbol{g}_t - \boldsymbol{g}_{t-1})^\top \boldsymbol{g}_t}{\boldsymbol{g}_{t-1}^\top \boldsymbol{g}_{t-1}}$ (Polak-Ribière)
    (Nonlinear conjugate gradient: optionally reset β_t to zero, for example if t is a multiple of some constant k, such as $k = 5$)
    Compute search direction: $\boldsymbol{\rho}_t = -\boldsymbol{g}_t + \beta_t \boldsymbol{\rho}_{t-1}$
    Perform line search to find: $\epsilon^* = \text{argmin}_\epsilon \frac{1}{m} \sum_{i=1}^{m} L(f(\boldsymbol{x}^{(i)}; \boldsymbol{\theta}_t + \epsilon \boldsymbol{\rho}_t), \boldsymbol{y}^{(i)})$
    (On a truly quadratic cost function, analytically solve for ϵ^* rather than explicitly searching for it)
    Apply update: $\boldsymbol{\theta}_{t+1} = \boldsymbol{\theta}_t + \epsilon^* \boldsymbol{\rho}_t$
    $t \leftarrow t + 1$
  end while

Nonlinear Conjugate Gradients: So far we have discussed the method of conjugate gradients as it is applied to quadratic objective functions. Of course, our primary interest in this chapter is to explore optimization methods for training neural networks and other related deep learning models where the corresponding objective function is far from quadratic. Perhaps surprisingly, the method of conjugate gradients is still applicable in this setting, though with some modification. Without any assurance that the objective is quadratic, the conjugate directions

are no longer assured to remain at the minimum of the objective for previous directions. As a result, the **nonlinear conjugate gradients** algorithm includes occasional resets where the method of conjugate gradients is restarted with line search along the unaltered gradient.

Practitioners report reasonable results in applications of the nonlinear conjugate gradients algorithm to training neural networks, though it is often beneficial to initialize the optimization with a few iterations of stochastic gradient descent before commencing nonlinear conjugate gradients. Also, while the (nonlinear) conjugate gradients algorithm has traditionally been cast as a batch method, minibatch versions have been used successfully for the training of neural networks (Le *et al.*, 2011). Adaptations of conjugate gradients specifically for neural networks have been proposed earlier, such as the scaled conjugate gradients algorithm (Moller, 1993).

8.6.3 BFGS

The **Broyden–Fletcher–Goldfarb–Shanno (BFGS) algorithm** attempts to bring some of the advantages of Newton's method without the computational burden. In that respect, BFGS is similar to the conjugate gradient method. However, BFGS takes a more direct approach to the approximation of Newton's update. Recall that Newton's update is given by

$$\boldsymbol{\theta}^* = \boldsymbol{\theta}_0 - \boldsymbol{H}^{-1}\nabla_{\boldsymbol{\theta}} J(\boldsymbol{\theta}_0), \tag{8.32}$$

where $\boldsymbol{H}$ is the Hessian of J with respect to $\boldsymbol{\theta}$ evaluated at $\boldsymbol{\theta}_0$. The primary computational difficulty in applying Newton's update is the calculation of the inverse Hessian $\boldsymbol{H}^{-1}$. The approach adopted by quasi-Newton methods (of which the BFGS algorithm is the most prominent) is to approximate the inverse with a matrix $\boldsymbol{M}_t$ that is iteratively refined by low rank updates to become a better approximation of $\boldsymbol{H}^{-1}$.

The specification and derivation of the BFGS approximation is given in many textbooks on optimization, including Luenberger (1984).

Once the inverse Hessian approximation $\boldsymbol{M}_t$ is updated, the direction of descent $\boldsymbol{\rho}_t$ is determined by $\boldsymbol{\rho}_t = \boldsymbol{M}_t \boldsymbol{g}_t$. A line search is performed in this direction to determine the size of the step, ϵ^*, taken in this direction. The final update to the parameters is given by:

$$\boldsymbol{\theta}_{t+1} = \boldsymbol{\theta}_t + \epsilon^* \boldsymbol{\rho}_t . \tag{8.33}$$

Like the method of conjugate gradients, the BFGS algorithm iterates a series of line searches with the direction incorporating second-order information. However

unlike conjugate gradients, the success of the approach is not heavily dependent on the line search finding a point very close to the true minimum along the line. Thus, relative to conjugate gradients, BFGS has the advantage that it can spend less time refining each line search. On the other hand, the BFGS algorithm must store the inverse Hessian matrix, $\boldsymbol{M}$, that requires $O(n^2)$ memory, making BFGS impractical for most modern deep learning models that typically have millions of parameters.

Limited Memory BFGS (or L-BFGS) The memory costs of the BFGS algorithm can be significantly decreased by avoiding storing the complete inverse Hessian approximation $\boldsymbol{M}$. The L-BFGS algorithm computes the approximation $\boldsymbol{M}$ using the same method as the BFGS algorithm, but beginning with the assumption that $\boldsymbol{M}^{(t-1)}$ is the identity matrix, rather than storing the approximation from one step to the next. If used with exact line searches, the directions defined by L-BFGS are mutually conjugate. However, unlike the method of conjugate gradients, this procedure remains well behaved when the minimum of the line search is reached only approximately. The L-BFGS strategy with no storage described here can be generalized to include more information about the Hessian by storing some of the vectors used to update $\boldsymbol{M}$ at each time step, which costs only $O(n)$ per step.

8.7 Optimization Strategies and Meta-Algorithms

Many optimization techniques are not exactly algorithms, but rather general templates that can be specialized to yield algorithms, or subroutines that can be incorporated into many different algorithms.

8.7.1 Batch Normalization

Batch normalization (Ioffe and Szegedy, 2015) is one of the most exciting recent innovations in optimizing deep neural networks and it is actually not an optimization algorithm at all. Instead, it is a method of adaptive reparametrization, motivated by the difficulty of training very deep models.

Very deep models involve the composition of several functions or layers. The gradient tells how to update each parameter, under the assumption that the other layers do not change. In practice, we update all of the layers simultaneously. When we make the update, unexpected results can happen because many functions composed together are changed simultaneously, using updates that were computed under the assumption that the other functions remain constant. As a simple

example, suppose we have a deep neural network that has only one unit per layer and does not use an activation function at each hidden layer: $\hat{y} = xw_1 w_2 w_3 \dots w_l$. Here, w_i provides the weight used by layer i. The output of layer i is $h_i = h_{i-1} w_i$. The output $\hat{y}$ is a linear function of the input x, but a nonlinear function of the weights w_i. Suppose our cost function has put a gradient of 1 on $\hat{y}$, so we wish to decrease $\hat{y}$ slightly. The back-propagation algorithm can then compute a gradient $\boldsymbol{g} = \nabla_{\boldsymbol{w}} \hat{y}$. Consider what happens when we make an update $\boldsymbol{w} \leftarrow \boldsymbol{w} - \epsilon \boldsymbol{g}$. The first-order Taylor series approximation of $\hat{y}$ predicts that the value of $\hat{y}$ will decrease by $\epsilon \boldsymbol{g}^\top \boldsymbol{g}$. If we wanted to decrease $\hat{y}$ by .1, this first-order information available in the gradient suggests we could set the learning rate ϵ to $\frac{.1}{\boldsymbol{g}^\top \boldsymbol{g}}$. However, the actual update will include second-order and third-order effects, on up to effects of order l. The new value of $\hat{y}$ is given by

$$x(w_1 - \epsilon g_1)(w_2 - \epsilon g_2) \dots (w_l - \epsilon g_l). \tag{8.34}$$

An example of one second-order term arising from this update is $\epsilon^2 g_1 g_2 \prod_{i=3}^{l} w_i$. This term might be negligible if $\prod_{i=3}^{l} w_i$ is small, or might be exponentially large if the weights on layers 3 through l are greater than 1. This makes it very hard to choose an appropriate learning rate, because the effects of an update to the parameters for one layer depends so strongly on all of the other layers. Second-order optimization algorithms address this issue by computing an update that takes these second-order interactions into account, but we can see that in very deep networks, even higher-order interactions can be significant. Even second-order optimization algorithms are expensive and usually require numerous approximations that prevent them from truly accounting for all significant second-order interactions. Building an n-th order optimization algorithm for $n > 2$ thus seems hopeless. What can we do instead?

Batch normalization provides an elegant way of reparametrizing almost any deep network. The reparametrization significantly reduces the problem of coordinating updates across many layers. Batch normalization can be applied to any input or hidden layer in a network. Let $\boldsymbol{H}$ be a minibatch of activations of the layer to normalize, arranged as a design matrix, with the activations for each example appearing in a row of the matrix. To normalize $\boldsymbol{H}$, we replace it with

$$\boldsymbol{H}' = \frac{\boldsymbol{H} - \boldsymbol{\mu}}{\boldsymbol{\sigma}}, \tag{8.35}$$

where $\boldsymbol{\mu}$ is a vector containing the mean of each unit and $\boldsymbol{\sigma}$ is a vector containing the standard deviation of each unit. The arithmetic here is based on broadcasting the vector $\boldsymbol{\mu}$ and the vector $\boldsymbol{\sigma}$ to be applied to every row of the matrix $\boldsymbol{H}$. Within each row, the arithmetic is element-wise, so $H_{i,j}$ is normalized by subtracting μ_j

and dividing by σ_j. The rest of the network then operates on $\boldsymbol{H}'$ in exactly the same way that the original network operated on $\boldsymbol{H}$.

At training time,

$$\boldsymbol{\mu} = \frac{1}{m} \sum_i \boldsymbol{H}_{i,:} \tag{8.36}$$

and

$$\boldsymbol{\sigma} = \sqrt{\delta + \frac{1}{m} \sum_i (\boldsymbol{H} - \boldsymbol{\mu})_i^2}, \tag{8.37}$$

where δ is a small positive value such as 10^{-8} imposed to avoid encountering the undefined gradient of $\sqrt{z}$ at $z = 0$. Crucially, *we back-propagate through these operations* for computing the mean and the standard deviation, and for applying them to normalize $\boldsymbol{H}$. This means that the gradient will never propose an operation that acts simply to increase the standard deviation or mean of h_i; the normalization operations remove the effect of such an action and zero out its component in the gradient. This was a major innovation of the batch normalization approach. Previous approaches had involved adding penalties to the cost function to encourage units to have normalized activation statistics or involved intervening to renormalize unit statistics after each gradient descent step. The former approach usually resulted in imperfect normalization and the latter usually resulted in significant wasted time as the learning algorithm repeatedly proposed changing the mean and variance and the normalization step repeatedly undid this change. Batch normalization reparametrizes the model to make some units always be standardized by definition, deftly sidestepping both problems.

At test time, $\boldsymbol{\mu}$ and $\boldsymbol{\sigma}$ may be replaced by running averages that were collected during training time. This allows the model to be evaluated on a single example, without needing to use definitions of $\boldsymbol{\mu}$ and $\boldsymbol{\sigma}$ that depend on an entire minibatch.

Revisiting the $\hat{y} = xw_1w_2 \dots w_l$ example, we see that we can mostly resolve the difficulties in learning this model by normalizing h_{l-1}. Suppose that x is drawn from a unit Gaussian. Then h_{l-1} will also come from a Gaussian, because the transformation from x to h_l is linear. However, h_{l-1} will no longer have zero mean and unit variance. After applying batch normalization, we obtain the normalized $\hat{h}_{l-1}$ that restores the zero mean and unit variance properties. For almost any update to the lower layers, $\hat{h}_{l-1}$ will remain a unit Gaussian. The output $\hat{y}$ may then be learned as a simple linear function $\hat{y} = w_l\hat{h}_{l-1}$. Learning in this model is now very simple because the parameters at the lower layers simply do not have an effect in most cases; their output is always renormalized to a unit Gaussian. In some corner cases, the lower layers can have an effect. Changing one of the lower layer weights to 0 can make the output become degenerate, and changing the sign

of one of the lower weights can flip the relationship between $\hat{h}_{l-1}$ and y. These situations are very rare. Without normalization, nearly every update would have an extreme effect on the statistics of h_{l-1}. Batch normalization has thus made this model significantly easier to learn. In this example, the ease of learning of course came at the cost of making the lower layers useless. In our linear example, the lower layers no longer have any harmful effect, but they also no longer have any beneficial effect. This is because we have normalized out the first and second order statistics, which is all that a linear network can influence. In a deep neural network with nonlinear activation functions, the lower layers can perform nonlinear transformations of the data, so they remain useful. Batch normalization acts to standardize only the mean and variance of each unit in order to stabilize learning, but allows the relationships between units and the nonlinear statistics of a single unit to change.

Because the final layer of the network is able to learn a linear transformation, we may actually wish to remove all linear relationships between units within a layer. Indeed, this is the approach taken by Desjardins *et al.* (2015), who provided the inspiration for batch normalization. Unfortunately, eliminating all linear interactions is much more expensive than standardizing the mean and standard deviation of each individual unit, and so far batch normalization remains the most practical approach.

Normalizing the mean and standard deviation of a unit can reduce the expressive power of the neural network containing that unit. In order to maintain the expressive power of the network, it is common to replace the batch of hidden unit activations $\boldsymbol{H}$ with $\boldsymbol{\gamma H'} + \boldsymbol{\beta}$ rather than simply the normalized $\boldsymbol{H'}$. The variables $\boldsymbol{\gamma}$ and $\boldsymbol{\beta}$ are learned parameters that allow the new variable to have any mean and standard deviation. At first glance, this may seem useless—why did we set the mean to $\mathbf{0}$, and then introduce a parameter that allows it to be set back to any arbitrary value $\boldsymbol{\beta}$? The answer is that the new parametrization can represent the same family of functions of the input as the old parametrization, but the new parametrization has different learning dynamics. In the old parametrization, the mean of $\boldsymbol{H}$ was determined by a complicated interaction between the parameters in the layers below $\boldsymbol{H}$. In the new parametrization, the mean of $\boldsymbol{\gamma H'} + \boldsymbol{\beta}$ is determined solely by $\boldsymbol{\beta}$. The new parametrization is much easier to learn with gradient descent.

Most neural network layers take the form of $\phi(\boldsymbol{XW} + \boldsymbol{b})$ where ϕ is some fixed nonlinear activation function such as the rectified linear transformation. It is natural to wonder whether we should apply batch normalization to the input $\boldsymbol{X}$, or to the transformed value $\boldsymbol{XW} + \boldsymbol{b}$. Ioffe and Szegedy (2015) recommend

the latter. More specifically, $\boldsymbol{XW} + \boldsymbol{b}$ should be replaced by a normalized version of $\boldsymbol{XW}$. The bias term should be omitted because it becomes redundant with the β parameter applied by the batch normalization reparametrization. The input to a layer is usually the output of a nonlinear activation function such as the rectified linear function in a previous layer. The statistics of the input are thus more non-Gaussian and less amenable to standardization by linear operations.

In convolutional networks, described in chapter 9, it is important to apply the same normalizing μ and σ at every spatial location within a feature map, so that the statistics of the feature map remain the same regardless of spatial location.

8.7.2 Coordinate Descent

In some cases, it may be possible to solve an optimization problem quickly by breaking it into separate pieces. If we minimize $f(\boldsymbol{x})$ with respect to a single variable x_i, then minimize it with respect to another variable x_j and so on, repeatedly cycling through all variables, we are guaranteed to arrive at a (local) minimum. This practice is known as **coordinate descent**, because we optimize one coordinate at a time. More generally, **block coordinate descent** refers to minimizing with respect to a subset of the variables simultaneously. The term "coordinate descent" is often used to refer to block coordinate descent as well as the strictly individual coordinate descent.

Coordinate descent makes the most sense when the different variables in the optimization problem can be clearly separated into groups that play relatively isolated roles, or when optimization with respect to one group of variables is significantly more efficient than optimization with respect to all of the variables. For example, consider the cost function

$$J(\boldsymbol{H}, \boldsymbol{W}) = \sum_{i,j} |H_{i,j}| + \sum_{i,j} \left(\boldsymbol{X} - \boldsymbol{W}^\top \boldsymbol{H} \right)^2_{i,j}. \tag{8.38}$$

This function describes a learning problem called sparse coding, where the goal is to find a weight matrix $\boldsymbol{W}$ that can linearly decode a matrix of activation values $\boldsymbol{H}$ to reconstruct the training set $\boldsymbol{X}$. Most applications of sparse coding also involve weight decay or a constraint on the norms of the columns of $\boldsymbol{W}$, in order to prevent the pathological solution with extremely small $\boldsymbol{H}$ and large $\boldsymbol{W}$.

The function J is not convex. However, we can divide the inputs to the training algorithm into two sets: the dictionary parameters $\boldsymbol{W}$ and the code representations $\boldsymbol{H}$. Minimizing the objective function with respect to either one of these sets of variables is a convex problem. Block coordinate descent thus gives

us an optimization strategy that allows us to use efficient convex optimization algorithms, by alternating between optimizing $\boldsymbol{W}$ with $\boldsymbol{H}$ fixed, then optimizing $\boldsymbol{H}$ with $\boldsymbol{W}$ fixed.

Coordinate descent is not a very good strategy when the value of one variable strongly influences the optimal value of another variable, as in the function $f(\boldsymbol{x}) = (x_1 - x_2)^2 + \alpha\left(x_1^2 + x_2^2\right)$ where α is a positive constant. The first term encourages the two variables to have similar value, while the second term encourages them to be near zero. The solution is to set both to zero. Newton's method can solve the problem in a single step because it is a positive definite quadratic problem. However, for small α, coordinate descent will make very slow progress because the first term does not allow a single variable to be changed to a value that differs significantly from the current value of the other variable.

8.7.3 Polyak Averaging

Polyak averaging (Polyak and Juditsky, 1992) consists of averaging together several points in the trajectory through parameter space visited by an optimization algorithm. If t iterations of gradient descent visit points $\boldsymbol{\theta}^{(1)}, \ldots, \boldsymbol{\theta}^{(t)}$, then the output of the Polyak averaging algorithm is $\hat{\boldsymbol{\theta}}^{(t)} = \frac{1}{t}\sum_i \boldsymbol{\theta}^{(i)}$. On some problem classes, such as gradient descent applied to convex problems, this approach has strong convergence guarantees. When applied to neural networks, its justification is more heuristic, but it performs well in practice. The basic idea is that the optimization algorithm may leap back and forth across a valley several times without ever visiting a point near the bottom of the valley. The average of all of the locations on either side should be close to the bottom of the valley though.

In non-convex problems, the path taken by the optimization trajectory can be very complicated and visit many different regions. Including points in parameter space from the distant past that may be separated from the current point by large barriers in the cost function does not seem like a useful behavior. As a result, when applying Polyak averaging to non-convex problems, it is typical to use an exponentially decaying running average:

$$\hat{\boldsymbol{\theta}}^{(t)} = \alpha\hat{\boldsymbol{\theta}}^{(t-1)} + (1-\alpha)\boldsymbol{\theta}^{(t)}. \tag{8.39}$$

The running average approach is used in numerous applications. See Szegedy *et al.* (2015) for a recent example.

8.7.4 Supervised Pretraining

Sometimes, directly training a model to solve a specific task can be too ambitious if the model is complex and hard to optimize or if the task is very difficult. It is sometimes more effective to train a simpler model to solve the task, then make the model more complex. It can also be more effective to train the model to solve a simpler task, then move on to confront the final task. These strategies that involve training simple models on simple tasks before confronting the challenge of training the desired model to perform the desired task are collectively known as **pretraining**.

Greedy algorithms break a problem into many components, then solve for the optimal version of each component in isolation. Unfortunately, combining the individually optimal components is not guaranteed to yield an optimal complete solution. However, greedy algorithms can be computationally much cheaper than algorithms that solve for the best joint solution, and the quality of a greedy solution is often acceptable if not optimal. Greedy algorithms may also be followed by a **fine-tuning** stage in which a joint optimization algorithm searches for an optimal solution to the full problem. Initializing the joint optimization algorithm with a greedy solution can greatly speed it up and improve the quality of the solution it finds.

Pretraining, and especially greedy pretraining, algorithms are ubiquitous in deep learning. In this section, we describe specifically those pretraining algorithms that break supervised learning problems into other simpler supervised learning problems. This approach is known as **greedy supervised pretraining**.

In the original (Bengio *et al.*, 2007) version of greedy supervised pretraining, each stage consists of a supervised learning training task involving only a subset of the layers in the final neural network. An example of greedy supervised pretraining is illustrated in figure 8.7, in which each added hidden layer is pretrained as part of a shallow supervised MLP, taking as input the output of the previously trained hidden layer. Instead of pretraining one layer at a time, Simonyan and Zisserman (2015) pretrain a deep convolutional network (eleven weight layers) and then use the first four and last three layers from this network to initialize even deeper networks (with up to nineteen layers of weights). The middle layers of the new, very deep network are initialized randomly. The new network is then jointly trained. Another option, explored by Yu *et al.* (2010) is to use the *outputs* of the previously trained MLPs, as well as the raw input, as inputs for each added stage.

Why would greedy supervised pretraining help? The hypothesis initially discussed by Bengio *et al.* (2007) is that it helps to provide better guidance to the

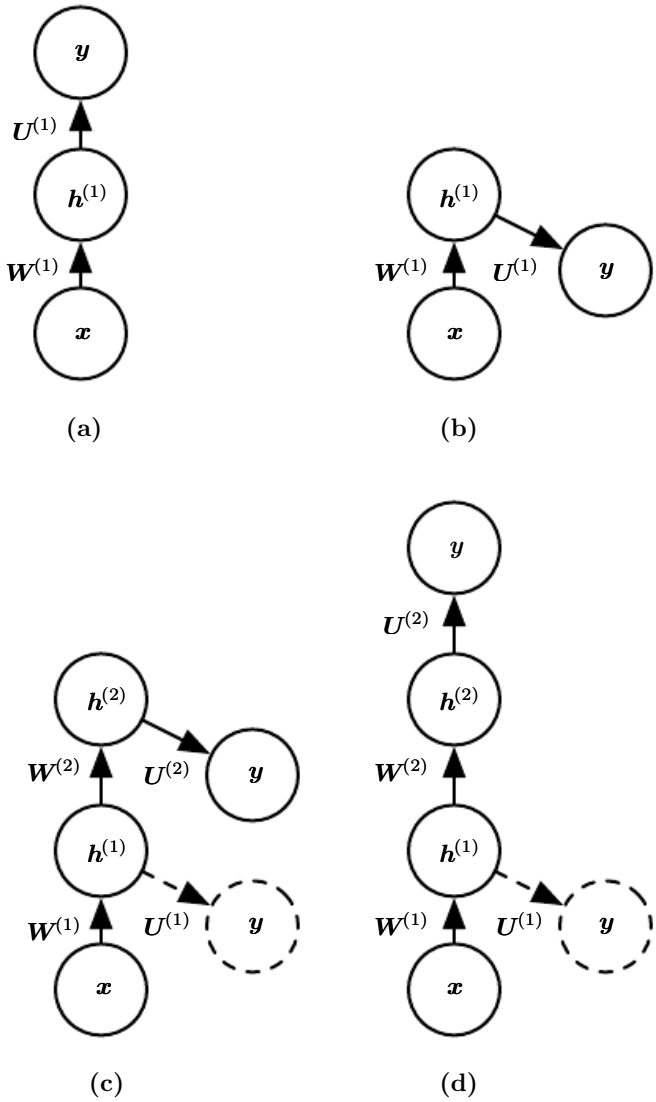

Figure 8.7: Illustration of one form of greedy supervised pretraining (Bengio *et al.*, 2007). *(a)*We start by training a sufficiently shallow architecture. *(b)*Another drawing of the same architecture. *(c)*We keep only the input-to-hidden layer of the original network and discard the hidden-to-output layer. We send the output of the first hidden layer as input to another supervised single hidden layer MLP that is trained with the same objective as the first network was, thus adding a second hidden layer. This can be repeated for as many layers as desired. *(d)*Another drawing of the result, viewed as a feedforward network. To further improve the optimization, we can jointly fine-tune all the layers, either only at the end or at each stage of this process.

intermediate levels of a deep hierarchy. In general, pretraining may help both in terms of optimization and in terms of generalization.

An approach related to supervised pretraining extends the idea to the context of transfer learning: Yosinski *et al.* (2014) pretrain a deep convolutional net with 8 layers of weights on a set of tasks (a subset of the 1000 ImageNet object categories) and then initialize a same-size network with the first k layers of the first net. All the layers of the second network (with the upper layers initialized randomly) are then jointly trained to perform a different set of tasks (another subset of the 1000 ImageNet object categories), with fewer training examples than for the first set of tasks. Other approaches to transfer learning with neural networks are discussed in section 15.2.

Another related line of work is the **FitNets** (Romero *et al.*, 2015) approach. This approach begins by training a network that has low enough depth and great enough width (number of units per layer) to be easy to train. This network then becomes a **teacher** for a second network, designated the **student**. The student network is much deeper and thinner (eleven to nineteen layers) and would be difficult to train with SGD under normal circumstances. The training of the student network is made easier by training the student network not only to predict the output for the original task, but also to predict the value of the middle layer of the teacher network. This extra task provides a set of hints about how the hidden layers should be used and can simplify the optimization problem. Additional parameters are introduced to regress the middle layer of the 5-layer teacher network from the middle layer of the deeper student network. However, instead of predicting the final classification target, the objective is to predict the middle hidden layer of the teacher network. The lower layers of the student networks thus have two objectives: to help the outputs of the student network accomplish their task, as well as to predict the intermediate layer of the teacher network. Although a thin and deep network appears to be more difficult to train than a wide and shallow network, the thin and deep network may generalize better and certainly has lower computational cost if it is thin enough to have far fewer parameters. Without the hints on the hidden layer, the student network performs very poorly in the experiments, both on the training and test set. Hints on middle layers may thus be one of the tools to help train neural networks that otherwise seem difficult to train, but other optimization techniques or changes in the architecture may also solve the problem.

8.7.5 Designing Models to Aid Optimization

To improve optimization, the best strategy is not always to improve the optimization algorithm. Instead, many improvements in the optimization of deep models have come from designing the models to be easier to optimize.

In principle, we could use activation functions that increase and decrease in jagged non-monotonic patterns. However, this would make optimization extremely difficult. In practice, *it is more important to choose a model family that is easy to optimize than to use a powerful optimization algorithm.* Most of the advances in neural network learning over the past 30 years have been obtained by changing the model family rather than changing the optimization procedure. Stochastic gradient descent with momentum, which was used to train neural networks in the 1980s, remains in use in modern state of the art neural network applications.

Specifically, modern neural networks reflect a *design choice* to use linear transformations between layers and activation functions that are differentiable almost everywhere and have significant slope in large portions of their domain. In particular, model innovations like the LSTM, rectified linear units and maxout units have all moved toward using more linear functions than previous models like deep networks based on sigmoidal units. These models have nice properties that make optimization easier. The gradient flows through many layers provided that the Jacobian of the linear transformation has reasonable singular values. Moreover, linear functions consistently increase in a single direction, so even if the model's output is very far from correct, it is clear simply from computing the gradient which direction its output should move to reduce the loss function. In other words, modern neural nets have been designed so that their *local* gradient information corresponds reasonably well to moving toward a distant solution.

Other model design strategies can help to make optimization easier. For example, linear paths or skip connections between layers reduce the length of the shortest path from the lower layer's parameters to the output, and thus mitigate the vanishing gradient problem (Srivastava *et al.*, 2015). A related idea to skip connections is adding extra copies of the output that are attached to the intermediate hidden layers of the network, as in GoogLeNet (Szegedy *et al.*, 2014a) and deeply-supervised nets (Lee *et al.*, 2014). These "auxiliary heads" are trained to perform the same task as the primary output at the top of the network in order to ensure that the lower layers receive a large gradient. When training is complete the auxiliary heads may be discarded. This is an alternative to the pretraining strategies, which were introduced in the previous section. In this way, one can train jointly all the layers in a single phase but change the architecture, so that intermediate layers (especially the lower ones) can get some hints about what they

should do, via a shorter path. These hints provide an error signal to lower layers.

8.7.6 Continuation Methods and Curriculum Learning

As argued in section 8.2.7, many of the challenges in optimization arise from the global structure of the cost function and cannot be resolved merely by making better estimates of local update directions. The predominant strategy for overcoming this problem is to attempt to initialize the parameters in a region that is connected to the solution by a short path through parameter space that local descent can discover.

Continuation methods are a family of strategies that can make optimization easier by choosing initial points to ensure that local optimization spends most of its time in well-behaved regions of space. The idea behind continuation methods is to construct a series of objective functions over the same parameters. In order to minimize a cost function $J(\boldsymbol{\theta})$, we will construct new cost functions $\{J^{(0)}, \ldots, J^{(n)}\}$. These cost functions are designed to be increasingly difficult, with $J^{(0)}$ being fairly easy to minimize, and $J^{(n)}$, the most difficult, being $J(\boldsymbol{\theta})$, the true cost function motivating the entire process. When we say that $J^{(i)}$ is easier than $J^{(i+1)}$, we mean that it is well behaved over more of $\boldsymbol{\theta}$ space. A random initialization is more likely to land in the region where local descent can minimize the cost function successfully because this region is larger. The series of cost functions are designed so that a solution to one is a good initial point of the next. We thus begin by solving an easy problem then refine the solution to solve incrementally harder problems until we arrive at a solution to the true underlying problem.

Traditional continuation methods (predating the use of continuation methods for neural network training) are usually based on smoothing the objective function. See Wu (1997) for an example of such a method and a review of some related methods. Continuation methods are also closely related to simulated annealing, which adds noise to the parameters (Kirkpatrick *et al.*, 1983). Continuation methods have been extremely successful in recent years. See Mobahi and Fisher (2015) for an overview of recent literature, especially for AI applications.

Continuation methods traditionally were mostly designed with the goal of overcoming the challenge of local minima. Specifically, they were designed to reach a global minimum despite the presence of many local minima. To do so, these continuation methods would construct easier cost functions by "blurring" the original cost function. This blurring operation can be done by approximating

$$J^{(i)}(\boldsymbol{\theta}) = \mathbb{E}_{\theta' \sim \mathcal{N}(\boldsymbol{\theta}'; \boldsymbol{\theta}, \sigma^{(i)2})} J(\boldsymbol{\theta}') \tag{8.40}$$

via sampling. The intuition for this approach is that some non-convex functions

become approximately convex when blurred. In many cases, this blurring preserves enough information about the location of a global minimum that we can find the global minimum by solving progressively less blurred versions of the problem. This approach can break down in three different ways. First, it might successfully define a series of cost functions where the first is convex and the optimum tracks from one function to the next arriving at the global minimum, but it might require so many incremental cost functions that the cost of the entire procedure remains high. NP-hard optimization problems remain NP-hard, even when continuation methods are applicable. The other two ways that continuation methods fail both correspond to the method not being applicable. First, the function might not become convex, no matter how much it is blurred. Consider for example the function $J(\boldsymbol{\theta}) = -\boldsymbol{\theta}^\top \boldsymbol{\theta}$. Second, the function may become convex as a result of blurring, but the minimum of this blurred function may track to a local rather than a global minimum of the original cost function.

Though continuation methods were mostly originally designed to deal with the problem of local minima, local minima are no longer believed to be the primary problem for neural network optimization. Fortunately, continuation methods can still help. The easier objective functions introduced by the continuation method can eliminate flat regions, decrease variance in gradient estimates, improve conditioning of the Hessian matrix, or do anything else that will either make local updates easier to compute or improve the correspondence between local update directions and progress toward a global solution.

Bengio *et al.* (2009) observed that an approach called **curriculum learning** or **shaping** can be interpreted as a continuation method. Curriculum learning is based on the idea of planning a learning process to begin by learning simple concepts and progress to learning more complex concepts that depend on these simpler concepts. This basic strategy was previously known to accelerate progress in animal training (Skinner, 1958; Peterson, 2004; Krueger and Dayan, 2009) and machine learning (Solomonoff, 1989; Elman, 1993; Sanger, 1994). Bengio *et al.* (2009) justified this strategy as a continuation method, where earlier $J^{(i)}$ are made easier by increasing the influence of simpler examples (either by assigning their contributions to the cost function larger coefficients, or by sampling them more frequently), and experimentally demonstrated that better results could be obtained by following a curriculum on a large-scale neural language modeling task. Curriculum learning has been successful on a wide range of natural language (Spitkovsky *et al.*, 2010; Collobert *et al.*, 2011a; Mikolov *et al.*, 2011b; Tu and Honavar, 2011) and computer vision (Kumar *et al.*, 2010; Lee and Grauman, 2011; Supancic and Ramanan, 2013) tasks. Curriculum learning was also verified as being consistent with the way in which humans *teach* (Khan *et al.*, 2011): teachers start by showing easier and

more prototypical examples and then help the learner refine the decision surface with the less obvious cases. Curriculum-based strategies are *more effective* for teaching humans than strategies based on uniform sampling of examples, and can also increase the effectiveness of other teaching strategies (Basu and Christensen, 2013).

Another important contribution to research on curriculum learning arose in the context of training recurrent neural networks to capture long-term dependencies: Zaremba and Sutskever (2014) found that much better results were obtained with a *stochastic curriculum*, in which a random mix of easy and difficult examples is always presented to the learner, but where the average proportion of the more difficult examples (here, those with longer-term dependencies) is gradually increased. With a deterministic curriculum, no improvement over the baseline (ordinary training from the full training set) was observed.

We have now described the basic family of neural network models and how to regularize and optimize them. In the chapters ahead, we turn to specializations of the neural network family, that allow neural networks to scale to very large sizes and process input data that has special structure. The optimization methods discussed in this chapter are often directly applicable to these specialized architectures with little or no modification.

Chapter 9

Convolutional Networks

Convolutional networks (LeCun, 1989), also known as **convolutional neural networks** or CNNs, are a specialized kind of neural network for processing data that has a known, grid-like topology. Examples include time-series data, which can be thought of as a 1D grid taking samples at regular time intervals, and image data, which can be thought of as a 2D grid of pixels. Convolutional networks have been tremendously successful in practical applications. The name "convolutional neural network" indicates that the network employs a mathematical operation called **convolution**. Convolution is a specialized kind of linear operation. *Convolutional networks are simply neural networks that use convolution in place of general matrix multiplication in at least one of their layers.*

In this chapter, we will first describe what convolution is. Next, we will explain the motivation behind using convolution in a neural network. We will then describe an operation called **pooling**, which almost all convolutional networks employ. Usually, the operation used in a convolutional neural network does not correspond precisely to the definition of convolution as used in other fields such as engineering or pure mathematics. We will describe several variants on the convolution function that are widely used in practice for neural networks. We will also show how convolution may be applied to many kinds of data, with different numbers of dimensions. We then discuss means of making convolution more efficient. Convolutional networks stand out as an example of neuroscientific principles influencing deep learning. We will discuss these neuroscientific principles, then conclude with comments about the role convolutional networks have played in the history of deep learning. One topic this chapter does not address is how to choose the architecture of your convolutional network. The goal of this chapter is to describe the kinds of tools that convolutional networks provide, while chapter 11

describes general guidelines for choosing which tools to use in which circumstances. Research into convolutional network architectures proceeds so rapidly that a new best architecture for a given benchmark is announced every few weeks to months, rendering it impractical to describe the best architecture in print. However, the best architectures have consistently been composed of the building blocks described here.

9.1 The Convolution Operation

In its most general form, convolution is an operation on two functions of a real-valued argument. To motivate the definition of convolution, we start with examples of two functions we might use.

Suppose we are tracking the location of a spaceship with a laser sensor. Our laser sensor provides a single output $x(t)$, the position of the spaceship at time t. Both x and t are real-valued, i.e., we can get a different reading from the laser sensor at any instant in time.

Now suppose that our laser sensor is somewhat noisy. To obtain a less noisy estimate of the spaceship's position, we would like to average together several measurements. Of course, more recent measurements are more relevant, so we will want this to be a weighted average that gives more weight to recent measurements. We can do this with a weighting function $w(a)$, where a is the age of a measurement. If we apply such a weighted average operation at every moment, we obtain a new function s providing a smoothed estimate of the position of the spaceship:

$$s(t) = \int x(a)w(t-a)da \tag{9.1}$$

This operation is called **convolution**. The convolution operation is typically denoted with an asterisk:

$$s(t) = (x * w)(t) \tag{9.2}$$

In our example, w needs to be a valid probability density function, or the output is not a weighted average. Also, w needs to be 0 for all negative arguments, or it will look into the future, which is presumably beyond our capabilities. These limitations are particular to our example though. In general, convolution is defined for any functions for which the above integral is defined, and may be used for other purposes besides taking weighted averages.

In convolutional network terminology, the first argument (in this example, the function x) to the convolution is often referred to as the **input** and the second

argument (in this example, the function w) as the **kernel**. The output is sometimes referred to as the **feature map**.

In our example, the idea of a laser sensor that can provide measurements at every instant in time is not realistic. Usually, when we work with data on a computer, time will be discretized, and our sensor will provide data at regular intervals. In our example, it might be more realistic to assume that our laser provides a measurement once per second. The time index t can then take on only integer values. If we now assume that x and w are defined only on integer t, we can define the discrete convolution:

$$s(t) = (x * w)(t) = \sum_{a=-\infty}^{\infty} x(a)w(t-a) \tag{9.3}$$

In machine learning applications, the input is usually a multidimensional array of data and the kernel is usually a multidimensional array of parameters that are adapted by the learning algorithm. We will refer to these multidimensional arrays as tensors. Because each element of the input and kernel must be explicitly stored separately, we usually assume that these functions are zero everywhere but the finite set of points for which we store the values. This means that in practice we can implement the infinite summation as a summation over a finite number of array elements.

Finally, we often use convolutions over more than one axis at a time. For example, if we use a two-dimensional image I as our input, we probably also want to use a two-dimensional kernel K:

$$S(i,j) = (I * K)(i,j) = \sum_m \sum_n I(m,n)K(i-m, j-n). \tag{9.4}$$

Convolution is commutative, meaning we can equivalently write:

$$S(i,j) = (K * I)(i,j) = \sum_m \sum_n I(i-m, j-n)K(m,n). \tag{9.5}$$

Usually the latter formula is more straightforward to implement in a machine learning library, because there is less variation in the range of valid values of m and n.

The commutative property of convolution arises because we have **flipped** the kernel relative to the input, in the sense that as m increases, the index into the input increases, but the index into the kernel decreases. The only reason to flip the kernel is to obtain the commutative property. While the commutative property

is useful for writing proofs, it is not usually an important property of a neural network implementation. Instead, many neural network libraries implement a related function called the **cross-correlation**, which is the same as convolution but without flipping the kernel:

$$S(i,j) = (I * K)(i,j) = \sum_m \sum_n I(i+m, j+n) K(m,n). \tag{9.6}$$

Many machine learning libraries implement cross-correlation but call it convolution. In this text we will follow this convention of calling both operations convolution, and specify whether we mean to flip the kernel or not in contexts where kernel flipping is relevant. In the context of machine learning, the learning algorithm will learn the appropriate values of the kernel in the appropriate place, so an algorithm based on convolution with kernel flipping will learn a kernel that is flipped relative to the kernel learned by an algorithm without the flipping. It is also rare for convolution to be used alone in machine learning; instead convolution is used simultaneously with other functions, and the combination of these functions does not commute regardless of whether the convolution operation flips its kernel or not.

See figure 9.1 for an example of convolution (without kernel flipping) applied to a 2-D tensor.

Discrete convolution can be viewed as multiplication by a matrix. However, the matrix has several entries constrained to be equal to other entries. For example, for univariate discrete convolution, each row of the matrix is constrained to be equal to the row above shifted by one element. This is known as a **Toeplitz matrix**. In two dimensions, a **doubly block circulant matrix** corresponds to convolution. In addition to these constraints that several elements be equal to each other, convolution usually corresponds to a very sparse matrix (a matrix whose entries are mostly equal to zero). This is because the kernel is usually much smaller than the input image. Any neural network algorithm that works with matrix multiplication and does not depend on specific properties of the matrix structure should work with convolution, without requiring any further changes to the neural network. Typical convolutional neural networks do make use of further specializations in order to deal with large inputs efficiently, but these are not strictly necessary from a theoretical perspective.

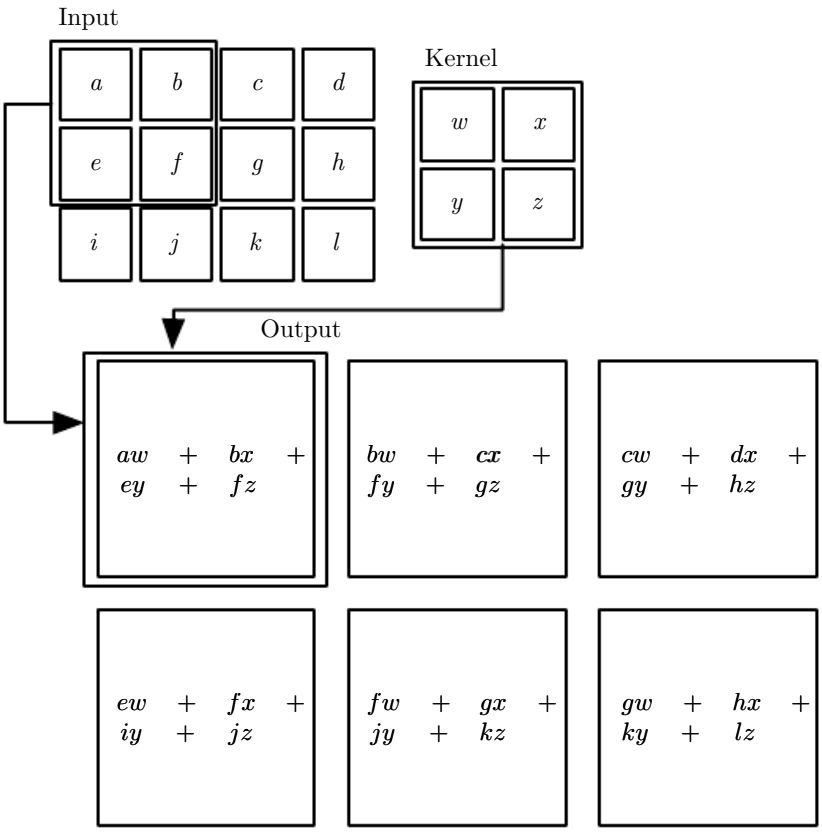

Figure 9.1: An example of 2-D convolution without kernel-flipping. In this case we restrict the output to only positions where the kernel lies entirely within the image, called "valid" convolution in some contexts. We draw boxes with arrows to indicate how the upper-left element of the output tensor is formed by applying the kernel to the corresponding upper-left region of the input tensor.

9.2 Motivation

Convolution leverages three important ideas that can help improve a machine learning system: **sparse interactions**, **parameter sharing** and **equivariant representations**. Moreover, convolution provides a means for working with inputs of variable size. We now describe each of these ideas in turn.

Traditional neural network layers use matrix multiplication by a matrix of parameters with a separate parameter describing the interaction between each input unit and each output unit. This means every output unit interacts with every input unit. Convolutional networks, however, typically have **sparse interactions** (also referred to as **sparse connectivity** or **sparse weights**). This is accomplished by making the kernel smaller than the input. For example, when processing an image, the input image might have thousands or millions of pixels, but we can detect small, meaningful features such as edges with kernels that occupy only tens or hundreds of pixels. This means that we need to store fewer parameters, which both reduces the memory requirements of the model and improves its statistical efficiency. It also means that computing the output requires fewer operations. These improvements in efficiency are usually quite large. If there are m inputs and n outputs, then matrix multiplication requires $m \times n$ parameters and the algorithms used in practice have $O(m \times n)$ runtime (per example). If we limit the number of connections each output may have to k, then the sparsely connected approach requires only $k \times n$ parameters and $O(k \times n)$ runtime. For many practical applications, it is possible to obtain good performance on the machine learning task while keeping k several orders of magnitude smaller than m. For graphical demonstrations of sparse connectivity, see figure 9.2 and figure 9.3. In a deep convolutional network, units in the deeper layers may *indirectly* interact with a larger portion of the input, as shown in figure 9.4. This allows the network to efficiently describe complicated interactions between many variables by constructing such interactions from simple building blocks that each describe only sparse interactions.

Parameter sharing refers to using the same parameter for more than one function in a model. In a traditional neural net, each element of the weight matrix is used exactly once when computing the output of a layer. It is multiplied by one element of the input and then never revisited. As a synonym for parameter sharing, one can say that a network has **tied weights**, because the value of the weight applied to one input is tied to the value of a weight applied elsewhere. In a convolutional neural net, each member of the kernel is used at every position of the input (except perhaps some of the boundary pixels, depending on the design decisions regarding the boundary). The parameter sharing used by the convolution operation means that rather than learning a separate set of parameters

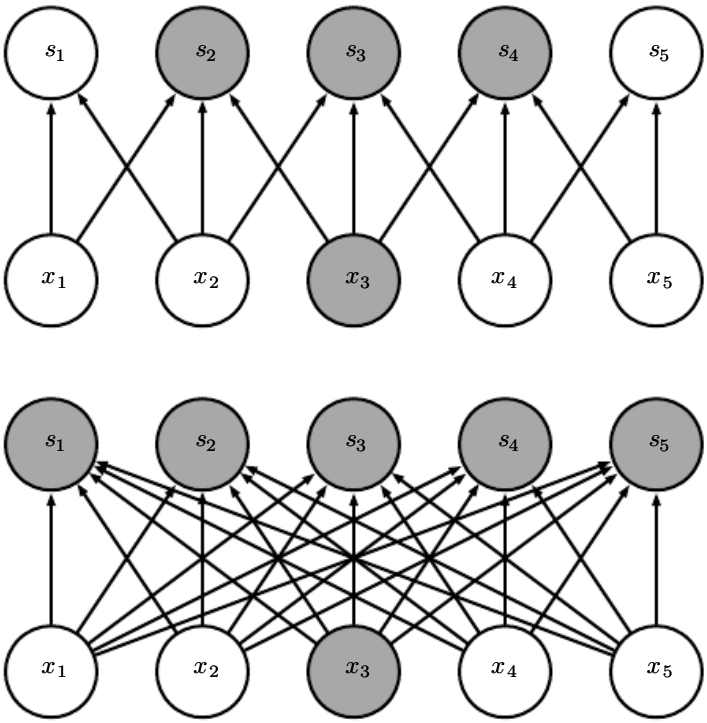

Figure 9.2: *Sparse connectivity, viewed from below:* We highlight one input unit, x_3, and also highlight the output units in $\boldsymbol{s}$ that are affected by this unit. *(Top)*When $\boldsymbol{s}$ is formed by convolution with a kernel of width 3, only three outputs are affected by $\boldsymbol{x}$. *(Bottom)*When $\boldsymbol{s}$ is formed by matrix multiplication, connectivity is no longer sparse, so all of the outputs are affected by x_3.

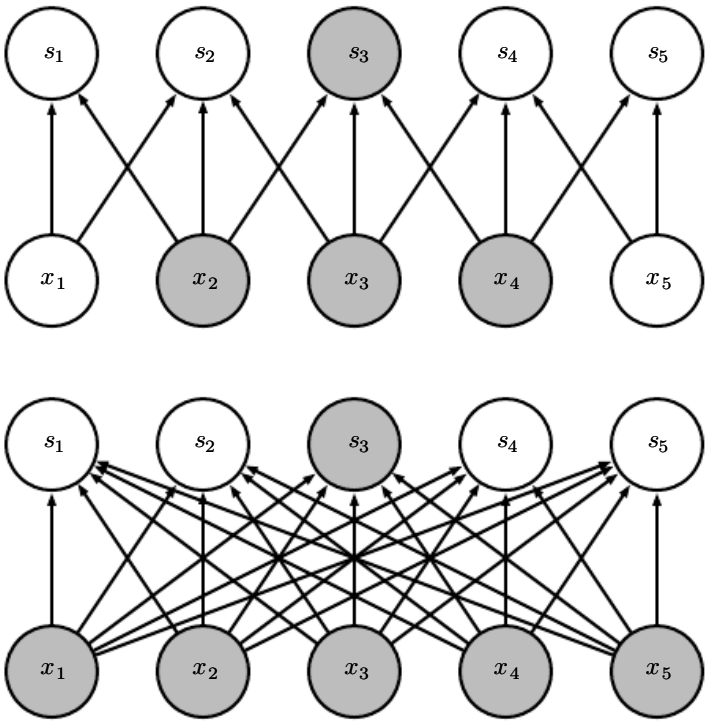

Figure 9.3: *Sparse connectivity, viewed from above:* We highlight one output unit, s_3, and also highlight the input units in $\boldsymbol{x}$ that affect this unit. These units are known as the **receptive field** of s_3. *(Top)*When $\boldsymbol{s}$ is formed by convolution with a kernel of width 3, only three inputs affect s_3. *(Bottom)*When $\boldsymbol{s}$ is formed by matrix multiplication, connectivity is no longer sparse, so all of the inputs affect s_3.

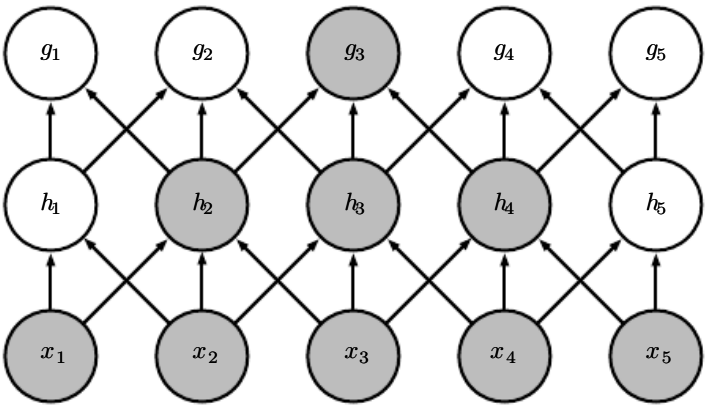

Figure 9.4: The receptive field of the units in the deeper layers of a convolutional network is larger than the receptive field of the units in the shallow layers. This effect increases if the network includes architectural features like strided convolution (figure 9.12) or pooling (section 9.3). This means that even though *direct* connections in a convolutional net are very sparse, units in the deeper layers can be *indirectly* connected to all or most of the input image.

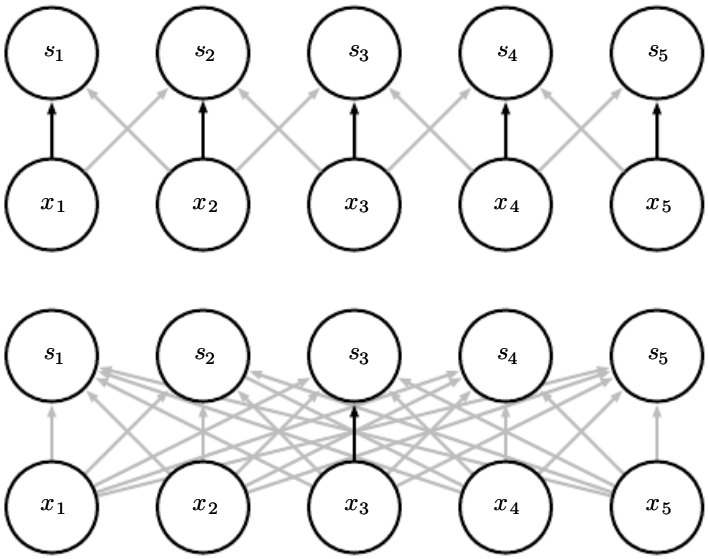

Figure 9.5: Parameter sharing: Black arrows indicate the connections that use a particular parameter in two different models. *(Top)*The black arrows indicate uses of the central element of a 3-element kernel in a convolutional model. Due to parameter sharing, this single parameter is used at all input locations. *(Bottom)*The single black arrow indicates the use of the central element of the weight matrix in a fully connected model. This model has no parameter sharing so the parameter is used only once.

for every location, we learn only one set. This does not affect the runtime of forward propagation—it is still $O(k \times n)$—but it does further reduce the storage requirements of the model to k parameters. Recall that k is usually several orders of magnitude less than m. Since m and n are usually roughly the same size, k is practically insignificant compared to $m \times n$. Convolution is thus dramatically more efficient than dense matrix multiplication in terms of the memory requirements and statistical efficiency. For a graphical depiction of how parameter sharing works, see figure 9.5.

As an example of both of these first two principles in action, figure 9.6 shows how sparse connectivity and parameter sharing can dramatically improve the efficiency of a linear function for detecting edges in an image.

In the case of convolution, the particular form of parameter sharing causes the layer to have a property called **equivariance** to translation. To say a function is equivariant means that if the input changes, the output changes in the same way. Specifically, a function $f(x)$ is equivariant to a function g if $f(g(x)) = g(f(x))$. In the case of convolution, if we let g be any function that translates the input, i.e., shifts it, then the convolution function is equivariant to g. For example, let I be a function giving image brightness at integer coordinates. Let g be a function

mapping one image function to another image function, such that $I' = g(I)$ is the image function with $I'(x, y) = I(x - 1, y)$. This shifts every pixel of I one unit to the right. If we apply this transformation to I, then apply convolution, the result will be the same as if we applied convolution to I', then applied the transformation g to the output. When processing time series data, this means that convolution produces a sort of timeline that shows when different features appear in the input. If we move an event later in time in the input, the exact same representation of it will appear in the output, just later in time. Similarly with images, convolution creates a 2-D map of where certain features appear in the input. If we move the object in the input, its representation will move the same amount in the output. This is useful for when we know that some function of a small number of neighboring pixels is useful when applied to multiple input locations. For example, when processing images, it is useful to detect edges in the first layer of a convolutional network. The same edges appear more or less everywhere in the image, so it is practical to share parameters across the entire image. In some cases, we may not wish to share parameters across the entire image. For example, if we are processing images that are cropped to be centered on an individual's face, we probably want to extract different features at different locations—the part of the network processing the top of the face needs to look for eyebrows, while the part of the network processing the bottom of the face needs to look for a chin.

Convolution is not naturally equivariant to some other transformations, such as changes in the scale or rotation of an image. Other mechanisms are necessary for handling these kinds of transformations.

Finally, some kinds of data cannot be processed by neural networks defined by matrix multiplication with a fixed-shape matrix. Convolution enables processing of some of these kinds of data. We discuss this further in section 9.7.

9.3 Pooling

A typical layer of a convolutional network consists of three stages (see figure 9.7). In the first stage, the layer performs several convolutions in parallel to produce a set of linear activations. In the second stage, each linear activation is run through a nonlinear activation function, such as the rectified linear activation function. This stage is sometimes called the **detector** stage. In the third stage, we use a **pooling function** to modify the output of the layer further.

A pooling function replaces the output of the net at a certain location with a summary statistic of the nearby outputs. For example, the **max pooling** (Zhou

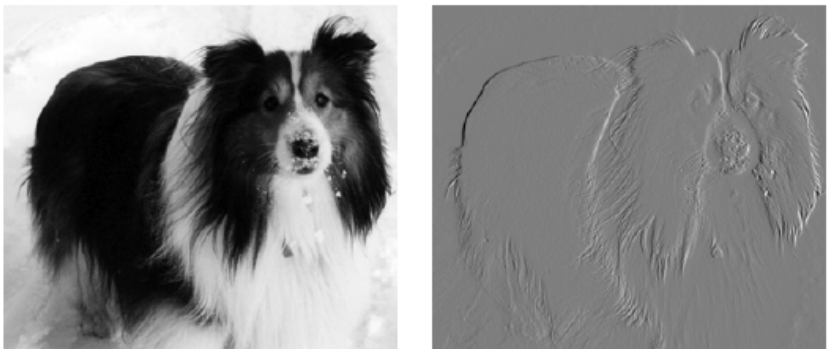

Figure 9.6: *Efficiency of edge detection.* The image on the right was formed by taking each pixel in the original image and subtracting the value of its neighboring pixel on the left. This shows the strength of all of the vertically oriented edges in the input image, which can be a useful operation for object detection. Both images are 280 pixels tall. The input image is 320 pixels wide while the output image is 319 pixels wide. This transformation can be described by a convolution kernel containing two elements, and requires $319 \times 280 \times 3 = 267,960$ floating point operations (two multiplications and one addition per output pixel) to compute using convolution. To describe the same transformation with a matrix multiplication would take $320 \times 280 \times 319 \times 280$, or over eight billion, entries in the matrix, making convolution four billion times more efficient for representing this transformation. The straightforward matrix multiplication algorithm performs over sixteen billion floating point operations, making convolution roughly 60,000 times more efficient computationally. Of course, most of the entries of the matrix would be zero. If we stored only the nonzero entries of the matrix, then both matrix multiplication and convolution would require the same number of floating point operations to compute. The matrix would still need to contain $2 \times 319 \times 280 = 178,640$ entries. Convolution is an extremely efficient way of describing transformations that apply the same linear transformation of a small, local region across the entire input. (Photo credit: Paula Goodfellow)

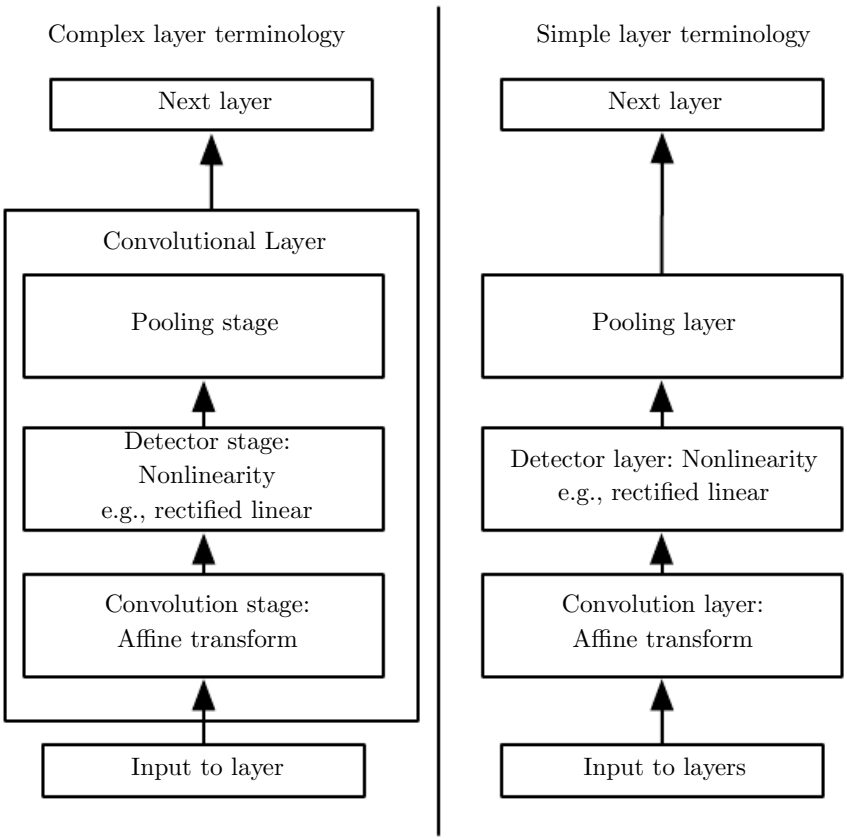

Figure 9.7: The components of a typical convolutional neural network layer. There are two commonly used sets of terminology for describing these layers. *(Left)*In this terminology, the convolutional net is viewed as a small number of relatively complex layers, with each layer having many "stages." In this terminology, there is a one-to-one mapping between kernel tensors and network layers. In this book we generally use this terminology. *(Right)*In this terminology, the convolutional net is viewed as a larger number of simple layers; every step of processing is regarded as a layer in its own right. This means that not every "layer" has parameters.

and Chellappa, 1988) operation reports the maximum output within a rectangular neighborhood. Other popular pooling functions include the average of a rectangular neighborhood, the L^2 norm of a rectangular neighborhood, or a weighted average based on the distance from the central pixel.

In all cases, pooling helps to make the representation become approximately **invariant** to small translations of the input. Invariance to translation means that if we translate the input by a small amount, the values of most of the pooled outputs do not change. See figure 9.8 for an example of how this works. *Invariance to local translation can be a very useful property if we care more about whether some feature is present than exactly where it is.* For example, when determining whether an image contains a face, we need not know the location of the eyes with pixel-perfect accuracy, we just need to know that there is an eye on the left side of the face and an eye on the right side of the face. In other contexts, it is more important to preserve the location of a feature. For example, if we want to find a corner defined by two edges meeting at a specific orientation, we need to preserve the location of the edges well enough to test whether they meet.

The use of pooling can be viewed as adding an infinitely strong prior that the function the layer learns must be invariant to small translations. When this assumption is correct, it can greatly improve the statistical efficiency of the network.

Pooling over spatial regions produces invariance to translation, but if we pool over the outputs of separately parametrized convolutions, the features can learn which transformations to become invariant to (see figure 9.9).

Because pooling summarizes the responses over a whole neighborhood, it is possible to use fewer pooling units than detector units, by reporting summary statistics for pooling regions spaced k pixels apart rather than 1 pixel apart. See figure 9.10 for an example. This improves the computational efficiency of the network because the next layer has roughly k times fewer inputs to process. When the number of parameters in the next layer is a function of its input size (such as when the next layer is fully connected and based on matrix multiplication) this reduction in the input size can also result in improved statistical efficiency and reduced memory requirements for storing the parameters.

For many tasks, pooling is essential for handling inputs of varying size. For example, if we want to classify images of variable size, the input to the classification layer must have a fixed size. This is usually accomplished by varying the size of an offset between pooling regions so that the classification layer always receives the same number of summary statistics regardless of the input size. For example, the final pooling layer of the network may be defined to output four sets of summary statistics, one for each quadrant of an image, regardless of the image size.

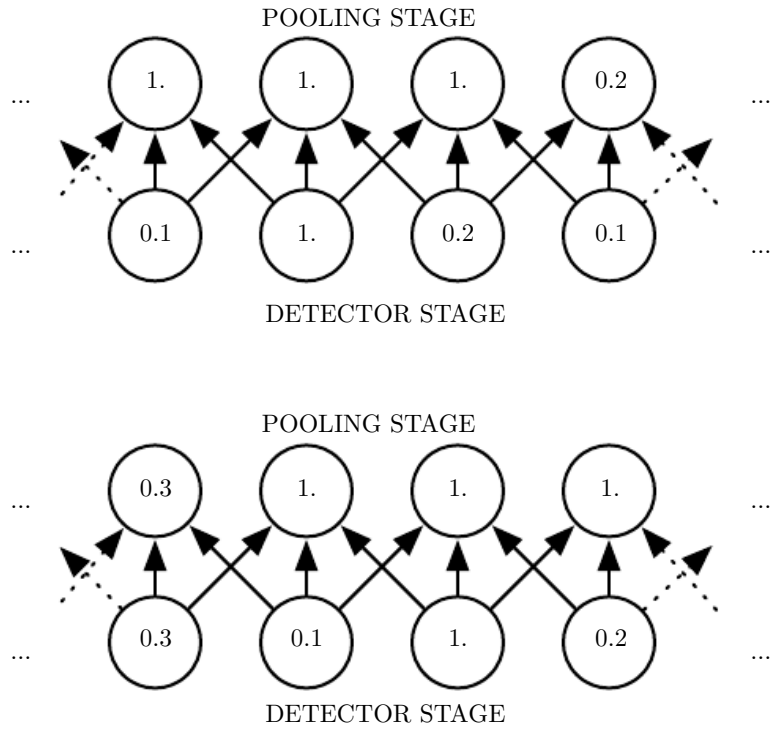

Figure 9.8: Max pooling introduces invariance. *(Top)*A view of the middle of the output of a convolutional layer. The bottom row shows outputs of the nonlinearity. The top row shows the outputs of max pooling, with a stride of one pixel between pooling regions and a pooling region width of three pixels. *(Bottom)*A view of the same network, after the input has been shifted to the right by one pixel. Every value in the bottom row has changed, but only half of the values in the top row have changed, because the max pooling units are only sensitive to the maximum value in the neighborhood, not its exact location.

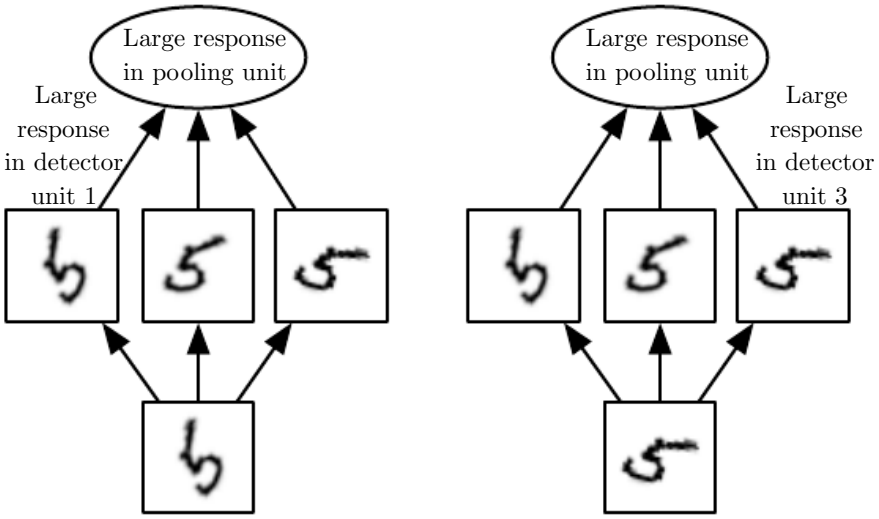

Figure 9.9: *Example of learned invariances:* A pooling unit that pools over multiple features that are learned with separate parameters can learn to be invariant to transformations of the input. Here we show how a set of three learned filters and a max pooling unit can learn to become invariant to rotation. All three filters are intended to detect a hand-written 5. Each filter attempts to match a slightly different orientation of the 5. When a 5 appears in the input, the corresponding filter will match it and cause a large activation in a detector unit. The max pooling unit then has a large activation regardless of which detector unit was activated. We show here how the network processes two different inputs, resulting in two different detector units being activated. The effect on the pooling unit is roughly the same either way. This principle is leveraged by maxout networks (Goodfellow *et al.*, 2013a) and other convolutional networks. Max pooling over spatial positions is naturally invariant to translation; this multi-channel approach is only necessary for learning other transformations.

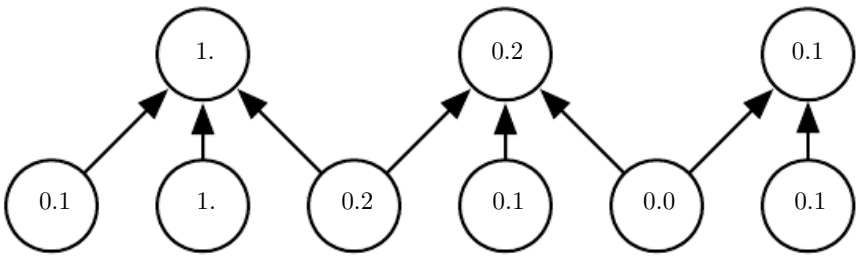

Figure 9.10: *Pooling with downsampling.* Here we use max-pooling with a pool width of three and a stride between pools of two. This reduces the representation size by a factor of two, which reduces the computational and statistical burden on the next layer. Note that the rightmost pooling region has a smaller size, but must be included if we do not want to ignore some of the detector units.

Some theoretical work gives guidance as to which kinds of pooling one should use in various situations (Boureau *et al.*, 2010). It is also possible to dynamically pool features together, for example, by running a clustering algorithm on the locations of interesting features (Boureau *et al.*, 2011). This approach yields a different set of pooling regions for each image. Another approach is to *learn* a single pooling structure that is then applied to all images (Jia *et al.*, 2012).

Pooling can complicate some kinds of neural network architectures that use top-down information, such as Boltzmann machines and autoencoders. These issues will be discussed further when we present these types of networks in part III. Pooling in convolutional Boltzmann machines is presented in section 20.6. The inverse-like operations on pooling units needed in some differentiable networks will be covered in section 20.10.6.

Some examples of complete convolutional network architectures for classification using convolution and pooling are shown in figure 9.11.

9.4 Convolution and Pooling as an Infinitely Strong Prior

Recall the concept of a **prior probability distribution** from section 5.2. This is a probability distribution over the parameters of a model that encodes our beliefs about what models are reasonable, before we have seen any data.

Priors can be considered weak or strong depending on how concentrated the probability density in the prior is. A weak prior is a prior distribution with high entropy, such as a Gaussian distribution with high variance. Such a prior allows the data to move the parameters more or less freely. A strong prior has very low entropy, such as a Gaussian distribution with low variance. Such a prior plays a more active role in determining where the parameters end up.

An infinitely strong prior places zero probability on some parameters and says that these parameter values are completely forbidden, regardless of how much support the data gives to those values.

We can imagine a convolutional net as being similar to a fully connected net, but with an infinitely strong prior over its weights. This infinitely strong prior says that the weights for one hidden unit must be identical to the weights of its neighbor, but shifted in space. The prior also says that the weights must be zero, except for in the small, spatially contiguous receptive field assigned to that hidden unit. Overall, we can think of the use of convolution as introducing an infinitely strong prior probability distribution over the parameters of a layer. This prior

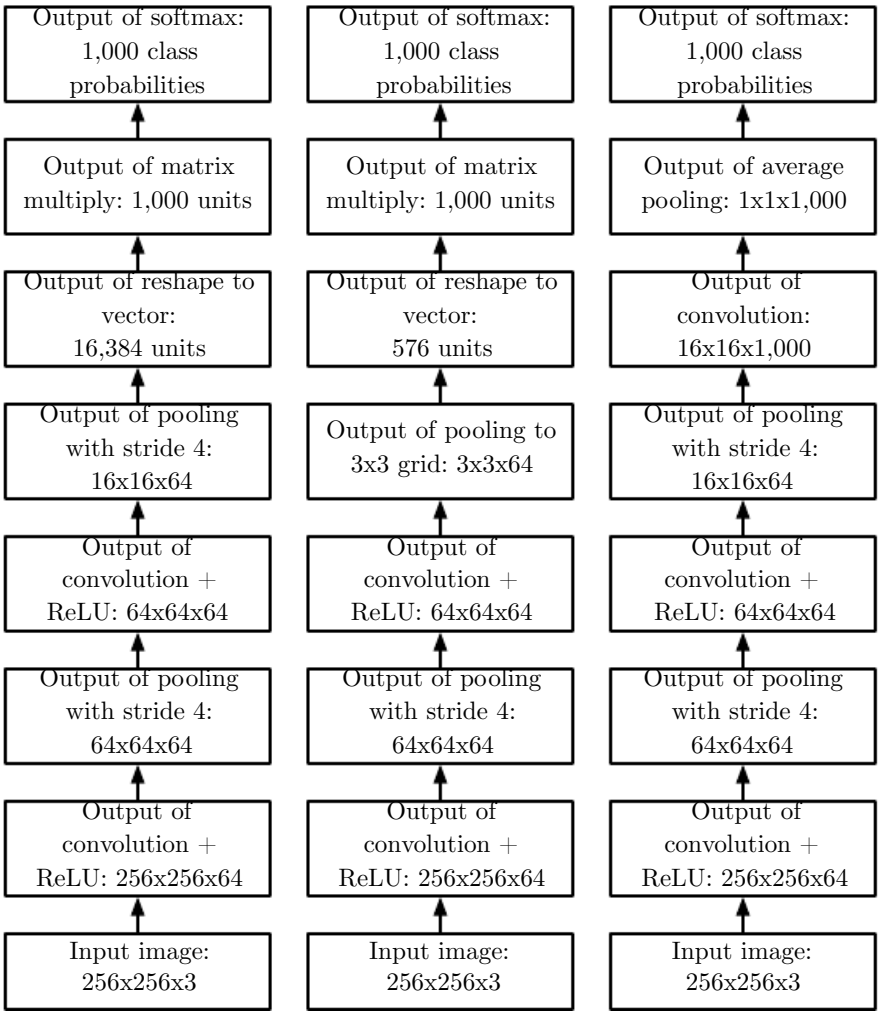

Figure 9.11: Examples of architectures for classification with convolutional networks. The specific strides and depths used in this figure are not advisable for real use; they are designed to be very shallow in order to fit onto the page. Real convolutional networks also often involve significant amounts of branching, unlike the chain structures used here for simplicity. *(Left)*A convolutional network that processes a fixed image size. After alternating between convolution and pooling for a few layers, the tensor for the convolutional feature map is reshaped to flatten out the spatial dimensions. The rest of the network is an ordinary feedforward network classifier, as described in chapter 6. *(Center)*A convolutional network that processes a variable-sized image, but still maintains a fully connected section. This network uses a pooling operation with variably-sized pools but a fixed number of pools, in order to provide a fixed-size vector of 576 units to the fully connected portion of the network. *(Right)*A convolutional network that does not have any fully connected weight layer. Instead, the last convolutional layer outputs one feature map per class. The model presumably learns a map of how likely each class is to occur at each spatial location. Averaging a feature map down to a single value provides the argument to the softmax classifier at the top.

says that the function the layer should learn contains only local interactions and is equivariant to translation. Likewise, the use of pooling is an infinitely strong prior that each unit should be invariant to small translations.

Of course, implementing a convolutional net as a fully connected net with an infinitely strong prior would be extremely computationally wasteful. But thinking of a convolutional net as a fully connected net with an infinitely strong prior can give us some insights into how convolutional nets work.

One key insight is that convolution and pooling can cause underfitting. Like any prior, convolution and pooling are only useful when the assumptions made by the prior are reasonably accurate. If a task relies on preserving precise spatial information, then using pooling on all features can increase the training error. Some convolutional network architectures (Szegedy *et al.*, 2014a) are designed to use pooling on some channels but not on other channels, in order to get both highly invariant features and features that will not underfit when the translation invariance prior is incorrect. When a task involves incorporating information from very distant locations in the input, then the prior imposed by convolution may be inappropriate.

Another key insight from this view is that we should only compare convolutional models to other convolutional models in benchmarks of statistical learning performance. Models that do not use convolution would be able to learn even if we permuted all of the pixels in the image. For many image datasets, there are separate benchmarks for models that are **permutation invariant** and must discover the concept of topology via learning, and models that have the knowledge of spatial relationships hard-coded into them by their designer.

9.5 Variants of the Basic Convolution Function

When discussing convolution in the context of neural networks, we usually do not refer exactly to the standard discrete convolution operation as it is usually understood in the mathematical literature. The functions used in practice differ slightly. Here we describe these differences in detail, and highlight some useful properties of the functions used in neural networks.

First, when we refer to convolution in the context of neural networks, we usually actually mean an operation that consists of many applications of convolution in parallel. This is because convolution with a single kernel can only extract one kind of feature, albeit at many spatial locations. Usually we want each layer of our network to extract many kinds of features, at many locations.

Additionally, the input is usually not just a grid of real values. Rather, it is a grid of vector-valued observations. For example, a color image has a red, green and blue intensity at each pixel. In a multilayer convolutional network, the input to the second layer is the output of the first layer, which usually has the output of many different convolutions at each position. When working with images, we usually think of the input and output of the convolution as being 3-D tensors, with one index into the different channels and two indices into the spatial coordinates of each channel. Software implementations usually work in batch mode, so they will actually use 4-D tensors, with the fourth axis indexing different examples in the batch, but we will omit the batch axis in our description here for simplicity.

Because convolutional networks usually use multi-channel convolution, the linear operations they are based on are not guaranteed to be commutative, even if kernel-flipping is used. These multi-channel operations are only commutative if each operation has the same number of output channels as input channels.

Assume we have a 4-D kernel tensor K with element $K_{i,j,k,l}$ giving the connection strength between a unit in channel i of the output and a unit in channel j of the input, with an offset of k rows and l columns between the output unit and the input unit. Assume our input consists of observed data V with element $V_{i,j,k}$ giving the value of the input unit within channel i at row j and column k. Assume our output consists of Z with the same format as V. If Z is produced by convolving K across V without flipping K, then

$$Z_{i,j,k} = \sum_{l,m,n} V_{l,j+m-1,k+n-1} K_{i,l,m,n} \tag{9.7}$$

where the summation over l, m and n is over all values for which the tensor indexing operations inside the summation is valid. In linear algebra notation, we index into arrays using a 1 for the first entry. This necessitates the -1 in the above formula. Programming languages such as C and Python index starting from 0, rendering the above expression even simpler.

We may want to skip over some positions of the kernel in order to reduce the computational cost (at the expense of not extracting our features as finely). We can think of this as downsampling the output of the full convolution function. If we want to sample only every s pixels in each direction in the output, then we can define a downsampled convolution function c such that

$$Z_{i,j,k} = c(\mathsf{K}, \mathsf{V}, s)_{i,j,k} = \sum_{l,m,n} \left[V_{l,(j-1)\times s+m,(k-1)\times s+n} K_{i,l,m,n} \right]. \tag{9.8}$$

We refer to s as the **stride** of this downsampled convolution. It is also possible

to define a separate stride for each direction of motion. See figure 9.12 for an illustration.

One essential feature of any convolutional network implementation is the ability to implicitly zero-pad the input $\mathbf{V}$ in order to make it wider. Without this feature, the width of the representation shrinks by one pixel less than the kernel width at each layer. Zero padding the input allows us to control the kernel width and the size of the output independently. Without zero padding, we are forced to choose between shrinking the spatial extent of the network rapidly and using small kernels—both scenarios that significantly limit the expressive power of the network. See figure 9.13 for an example.

Three special cases of the zero-padding setting are worth mentioning. One is the extreme case in which no zero-padding is used whatsoever, and the convolution kernel is only allowed to visit positions where the entire kernel is contained entirely within the image. In MATLAB terminology, this is called **valid** convolution. In this case, all pixels in the output are a function of the same number of pixels in the input, so the behavior of an output pixel is somewhat more regular. However, the size of the output shrinks at each layer. If the input image has width m and the kernel has width k, the output will be of width $m - k + 1$. The rate of this shrinkage can be dramatic if the kernels used are large. Since the shrinkage is greater than 0, it limits the number of convolutional layers that can be included in the network. As layers are added, the spatial dimension of the network will eventually drop to 1×1, at which point additional layers cannot meaningfully be considered convolutional. Another special case of the zero-padding setting is when just enough zero-padding is added to keep the size of the output equal to the size of the input. MATLAB calls this **same** convolution. In this case, the network can contain as many convolutional layers as the available hardware can support, since the operation of convolution does not modify the architectural possibilities available to the next layer. However, the input pixels near the border influence fewer output pixels than the input pixels near the center. This can make the border pixels somewhat underrepresented in the model. This motivates the other extreme case, which MATLAB refers to as **full** convolution, in which enough zeroes are added for every pixel to be visited k times in each direction, resulting in an output image of width $m + k - 1$. In this case, the output pixels near the border are a function of fewer pixels than the output pixels near the center. This can make it difficult to learn a single kernel that performs well at all positions in the convolutional feature map. Usually the optimal amount of zero padding (in terms of test set classification accuracy) lies somewhere between "valid" and "same" convolution.

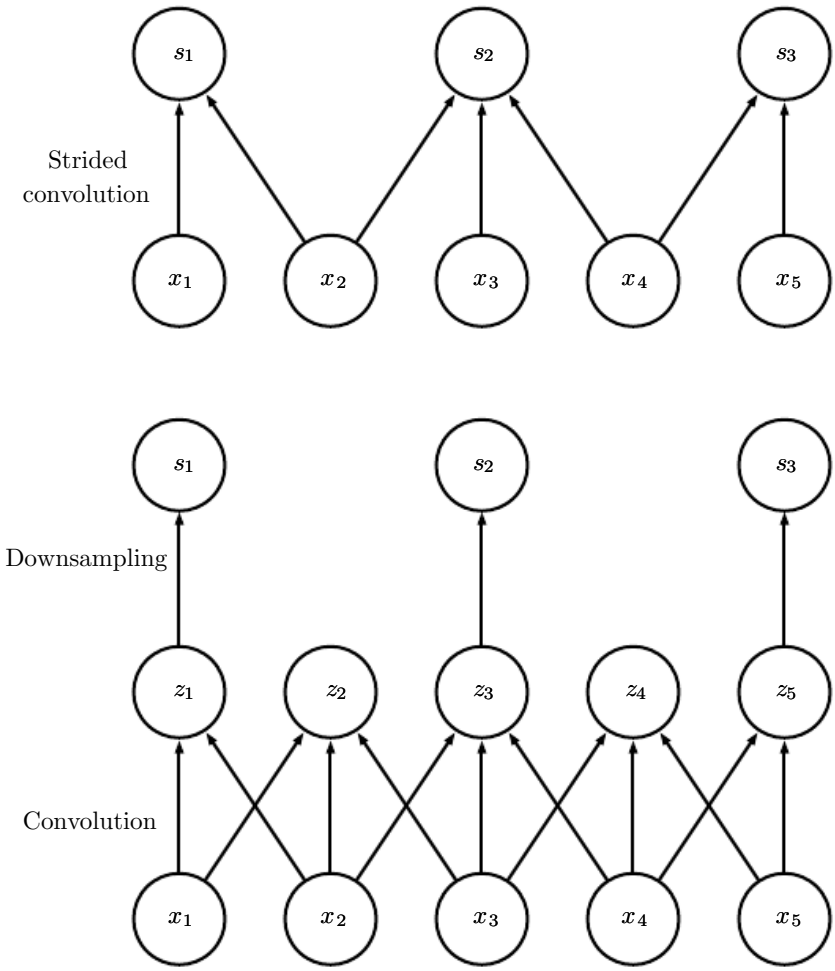

Figure 9.12: Convolution with a stride. In this example, we use a stride of two. *(Top)*Convolution with a stride length of two implemented in a single operation. *(Bottom)*Convolution with a stride greater than one pixel is mathematically equivalent to convolution with unit stride followed by downsampling. Obviously, the two-step approach involving downsampling is computationally wasteful, because it computes many values that are then discarded.

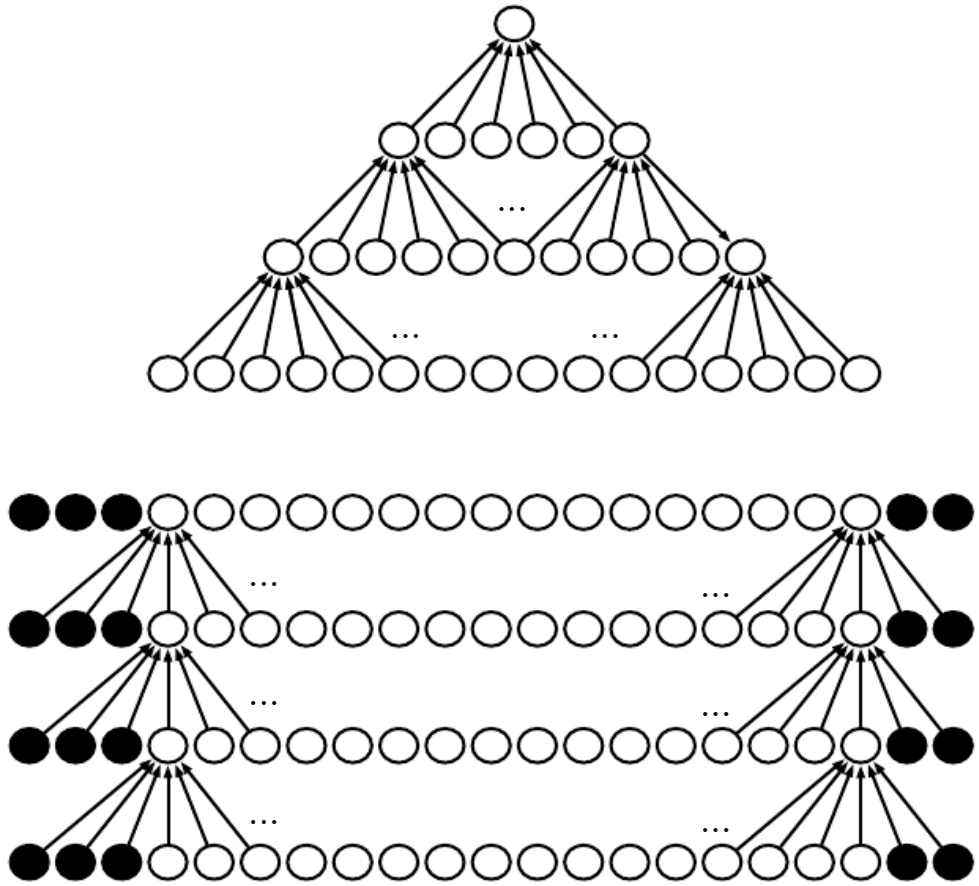

Figure 9.13: *The effect of zero padding on network size*: Consider a convolutional network with a kernel of width six at every layer. In this example, we do not use any pooling, so only the convolution operation itself shrinks the network size. *(Top)*In this convolutional network, we do not use any implicit zero padding. This causes the representation to shrink by five pixels at each layer. Starting from an input of sixteen pixels, we are only able to have three convolutional layers, and the last layer does not ever move the kernel, so arguably only two of the layers are truly convolutional. The rate of shrinking can be mitigated by using smaller kernels, but smaller kernels are less expressive and some shrinking is inevitable in this kind of architecture. *(Bottom)*By adding five implicit zeroes to each layer, we prevent the representation from shrinking with depth. This allows us to make an arbitrarily deep convolutional network.

In some cases, we do not actually want to use convolution, but rather locally connected layers (LeCun, 1986, 1989). In this case, the adjacency matrix in the graph of our MLP is the same, but every connection has its own weight, specified by a 6-D tensor $\mathbf{W}$. The indices into $\mathbf{W}$ are respectively: i, the output channel, j, the output row, k, the output column, l, the input channel, m, the row offset within the input, and n, the column offset within the input. The linear part of a locally connected layer is then given by

$$Z_{i,j,k} = \sum_{l,m,n} \left[V_{l,j+m-1,k+n-1} w_{i,j,k,l,m,n} \right]. \tag{9.9}$$

This is sometimes also called **unshared convolution**, because it is a similar operation to discrete convolution with a small kernel, but without sharing parameters across locations. Figure 9.14 compares local connections, convolution, and full connections.

Locally connected layers are useful when we know that each feature should be a function of a small part of space, but there is no reason to think that the same feature should occur across all of space. For example, if we want to tell if an image is a picture of a face, we only need to look for the mouth in the bottom half of the image.

It can also be useful to make versions of convolution or locally connected layers in which the connectivity is further restricted, for example to constrain each output channel i to be a function of only a subset of the input channels l. A common way to do this is to make the first m output channels connect to only the first n input channels, the second m output channels connect to only the second n input channels, and so on. See figure 9.15 for an example. Modeling interactions between few channels allows the network to have fewer parameters in order to reduce memory consumption and increase statistical efficiency, and also reduces the amount of computation needed to perform forward and back-propagation. It accomplishes these goals without reducing the number of hidden units.

Tiled convolution (Gregor and LeCun, 2010a; Le *et al.*, 2010) offers a compromise between a convolutional layer and a locally connected layer. Rather than learning a separate set of weights at *every* spatial location, we learn a set of kernels that we rotate through as we move through space. This means that immediately neighboring locations will have different filters, like in a locally connected layer, but the memory requirements for storing the parameters will increase only by a factor of the size of this set of kernels, rather than the size of the entire output feature map. See figure 9.16 for a comparison of locally connected layers, tiled convolution, and standard convolution.

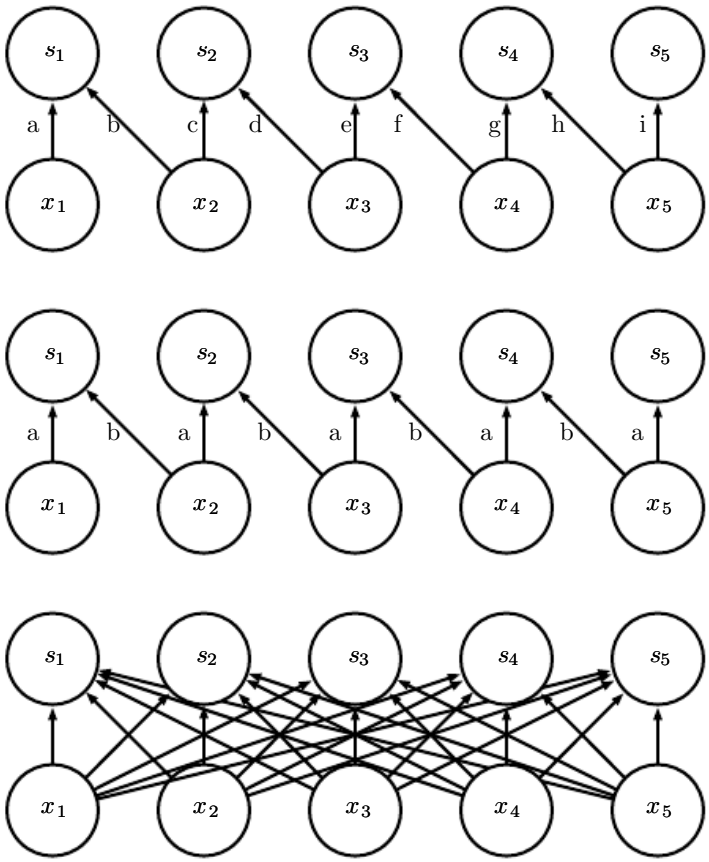

Figure 9.14: Comparison of local connections, convolution, and full connections. *(Top)*A locally connected layer with a patch size of two pixels. Each edge is labeled with a unique letter to show that each edge is associated with its own weight parameter. *(Center)*A convolutional layer with a kernel width of two pixels. This model has exactly the same connectivity as the locally connected layer. The difference lies not in which units interact with each other, but in how the parameters are shared. The locally connected layer has no parameter sharing. The convolutional layer uses the same two weights repeatedly across the entire input, as indicated by the repetition of the letters labeling each edge. *(Bottom)*A fully connected layer resembles a locally connected layer in the sense that each edge has its own parameter (there are too many to label explicitly with letters in this diagram). However, it does not have the restricted connectivity of the locally connected layer.

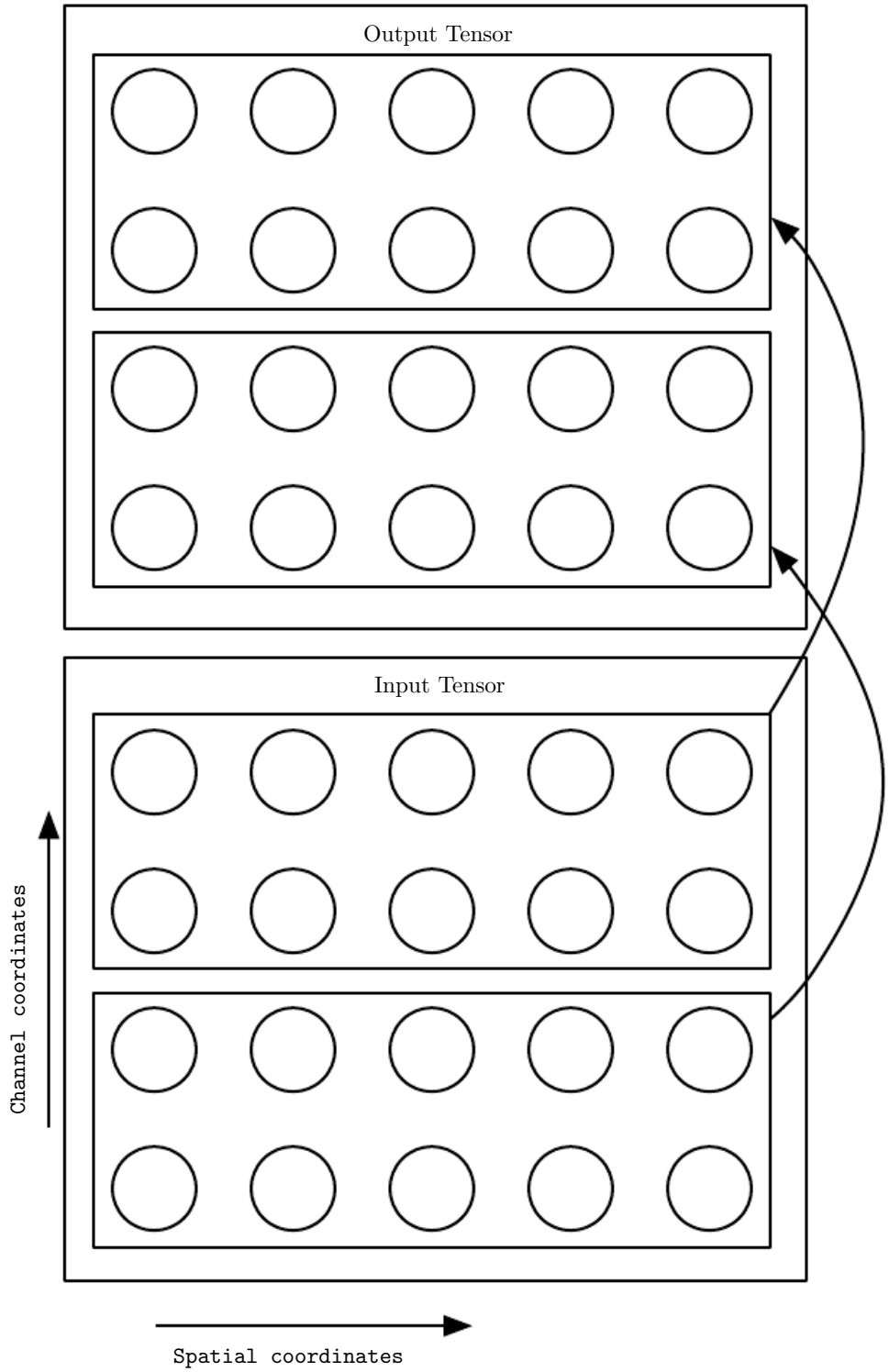

Figure 9.15: A convolutional network with the first two output channels connected to only the first two input channels, and the second two output channels connected to only the second two input channels.

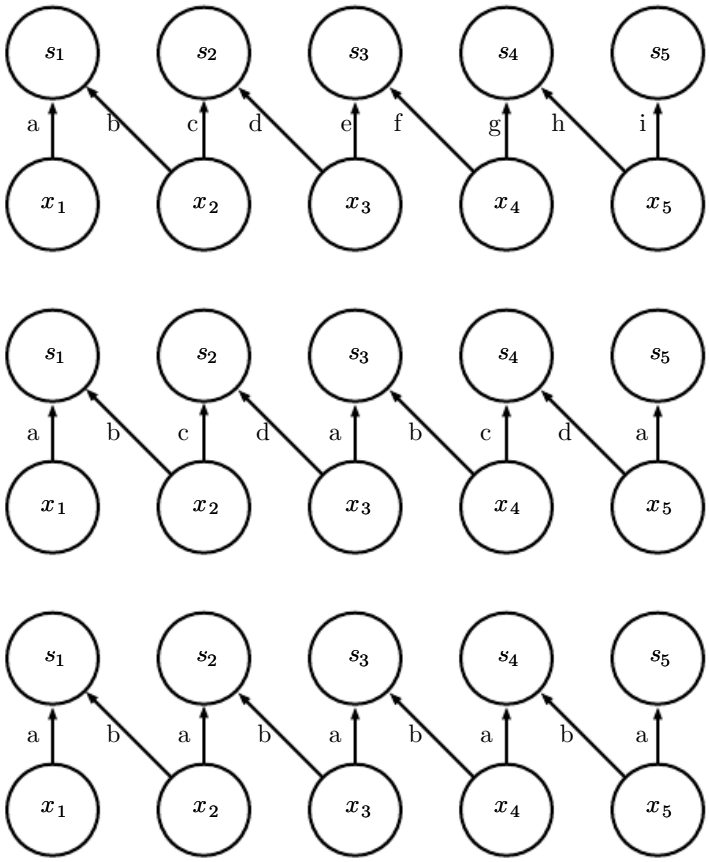

Figure 9.16: A comparison of locally connected layers, tiled convolution, and standard convolution. All three have the same sets of connections between units, when the same size of kernel is used. This diagram illustrates the use of a kernel that is two pixels wide. The differences between the methods lies in how they share parameters. *(Top)*A locally connected layer has no sharing at all. We indicate that each connection has its own weight by labeling each connection with a unique letter. *(Center)*Tiled convolution has a set of t different kernels. Here we illustrate the case of $t = 2$. One of these kernels has edges labeled "a" and "b," while the other has edges labeled "c" and "d." Each time we move one pixel to the right in the output, we move on to using a different kernel. This means that, like the locally connected layer, neighboring units in the output have different parameters. Unlike the locally connected layer, after we have gone through all t available kernels, we cycle back to the first kernel. If two output units are separated by a multiple of t steps, then they share parameters. *(Bottom)*Traditional convolution is equivalent to tiled convolution with $t = 1$. There is only one kernel and it is applied everywhere, as indicated in the diagram by using the kernel with weights labeled "a" and "b" everywhere.

To define tiled convolution algebraically, let k be a 6-D tensor, where two of the dimensions correspond to different locations in the output map. Rather than having a separate index for each location in the output map, output locations cycle through a set of t different choices of kernel stack in each direction. If t is equal to the output width, this is the same as a locally connected layer.

$$Z_{i,j,k} = \sum_{l,m,n} V_{l,j+m-1,k+n-1} K_{i,l,m,n,j\%t+1,k\%t+1}\,, \tag{9.10}$$

where $\%$ is the modulo operation, with $t\%t = 0$, $(t+1)\%t = 1$, etc. It is straightforward to generalize this equation to use a different tiling range for each dimension.

Both locally connected layers and tiled convolutional layers have an interesting interaction with max-pooling: the detector units of these layers are driven by different filters. If these filters learn to detect different transformed versions of the same underlying features, then the max-pooled units become invariant to the learned transformation (see figure 9.9). Convolutional layers are hard-coded to be invariant specifically to translation.

Other operations besides convolution are usually necessary to implement a convolutional network. To perform learning, one must be able to compute the gradient with respect to the kernel, given the gradient with respect to the outputs. In some simple cases, this operation can be performed using the convolution operation, but many cases of interest, including the case of stride greater than 1, do not have this property.

Recall that convolution is a linear operation and can thus be described as a matrix multiplication (if we first reshape the input tensor into a flat vector). The matrix involved is a function of the convolution kernel. The matrix is sparse and each element of the kernel is copied to several elements of the matrix. This view helps us to derive some of the other operations needed to implement a convolutional network.

Multiplication by the transpose of the matrix defined by convolution is one such operation. This is the operation needed to back-propagate error derivatives through a convolutional layer, so it is needed to train convolutional networks that have more than one hidden layer. This same operation is also needed if we wish to reconstruct the visible units from the hidden units (Simard *et al.*, 1992). Reconstructing the visible units is an operation commonly used in the models described in part III of this book, such as autoencoders, RBMs, and sparse coding. Transpose convolution is necessary to construct convolutional versions of those models. Like the kernel gradient operation, this input gradient operation can be

implemented using a convolution in some cases, but in the general case requires a third operation to be implemented. Care must be taken to coordinate this transpose operation with the forward propagation. The size of the output that the transpose operation should return depends on the zero padding policy and stride of the forward propagation operation, as well as the size of the forward propagation's output map. In some cases, multiple sizes of input to forward propagation can result in the same size of output map, so the transpose operation must be explicitly told what the size of the original input was.

These three operations—convolution, backprop from output to weights, and backprop from output to inputs—are sufficient to compute all of the gradients needed to train any depth of feedforward convolutional network, as well as to train convolutional networks with reconstruction functions based on the transpose of convolution. See Goodfellow (2010) for a full derivation of the equations in the fully general multi-dimensional, multi-example case. To give a sense of how these equations work, we present the two dimensional, single example version here.

Suppose we want to train a convolutional network that incorporates strided convolution of kernel stack $\mathbf{K}$ applied to multi-channel image $\mathbf{V}$ with stride s as defined by $c(\mathbf{K}, \mathbf{V}, s)$ as in equation 9.8. Suppose we want to minimize some loss function $J(\mathbf{V}, \mathbf{K})$. During forward propagation, we will need to use c itself to output $\mathbf{Z}$, which is then propagated through the rest of the network and used to compute the cost function J. During back-propagation, we will receive a tensor $\mathbf{G}$ such that $G_{i,j,k} = \frac{\partial}{\partial Z_{i,j,k}} J(\mathbf{V}, \mathbf{K})$.

To train the network, we need to compute the derivatives with respect to the weights in the kernel. To do so, we can use a function

$$g(\mathbf{G}, \mathbf{V}, s)_{i,j,k,l} = \frac{\partial}{\partial K_{i,j,k,l}} J(\mathbf{V}, \mathbf{K}) = \sum_{m,n} G_{i,m,n} V_{j,(m-1)\times s+k,(n-1)\times s+l}. \tag{9.11}$$

If this layer is not the bottom layer of the network, we will need to compute the gradient with respect to $\mathbf{V}$ in order to back-propagate the error farther down. To do so, we can use a function

$$h(\mathbf{K}, \mathbf{G}, s)_{i,j,k} = \frac{\partial}{\partial V_{i,j,k}} J(\mathbf{V}, \mathbf{K}) \tag{9.12}$$

$$= \sum_{\substack{l,m \\ \text{s.t.} \\ (l-1)\times s+m=j}} \sum_{\substack{n,p \\ \text{s.t.} \\ (n-1)\times s+p=k}} \sum_{q} K_{q,i,m,p} G_{q,l,n}. \tag{9.13}$$

Autoencoder networks, described in chapter 14, are feedforward networks trained to copy their input to their output. A simple example is the PCA algorithm,

that copies its input $\boldsymbol{x}$ to an approximate reconstruction $\boldsymbol{r}$ using the function $\boldsymbol{W}^\top \boldsymbol{W}\boldsymbol{x}$. It is common for more general autoencoders to use multiplication by the transpose of the weight matrix just as PCA does. To make such models convolutional, we can use the function h to perform the transpose of the convolution operation. Suppose we have hidden units H in the same format as Z and we define a reconstruction

$$\mathsf{R} = h(\mathsf{K}, \mathsf{H}, s). \tag{9.14}$$

In order to train the autoencoder, we will receive the gradient with respect to R as a tensor E. To train the decoder, we need to obtain the gradient with respect to K. This is given by $g(\mathsf{H}, \mathsf{E}, s)$. To train the encoder, we need to obtain the gradient with respect to H. This is given by $c(\mathsf{K}, \mathsf{E}, s)$. It is also possible to differentiate through g using c and h, but these operations are not needed for the back-propagation algorithm on any standard network architectures.

Generally, we do not use only a linear operation in order to transform from the inputs to the outputs in a convolutional layer. We generally also add some bias term to each output before applying the nonlinearity. This raises the question of how to share parameters among the biases. For locally connected layers it is natural to give each unit its own bias, and for tiled convolution, it is natural to share the biases with the same tiling pattern as the kernels. For convolutional layers, it is typical to have one bias per channel of the output and share it across all locations within each convolution map. However, if the input is of known, fixed size, it is also possible to learn a separate bias at each location of the output map. Separating the biases may slightly reduce the statistical efficiency of the model, but also allows the model to correct for differences in the image statistics at different locations. For example, when using implicit zero padding, detector units at the edge of the image receive less total input and may need larger biases.

9.6 Structured Outputs

Convolutional networks can be used to output a high-dimensional, structured object, rather than just predicting a class label for a classification task or a real value for a regression task. Typically this object is just a tensor, emitted by a standard convolutional layer. For example, the model might emit a tensor S, where $\mathsf{S}_{i,j,k}$ is the probability that pixel (j, k) of the input to the network belongs to class i. This allows the model to label every pixel in an image and draw precise masks that follow the outlines of individual objects.

One issue that often comes up is that the output plane can be smaller than the

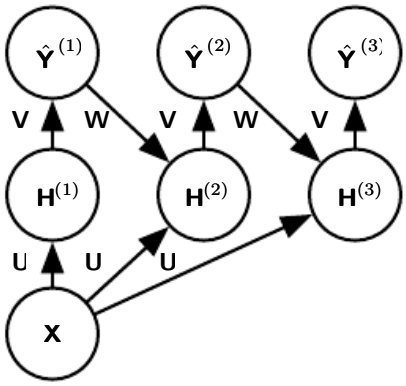

Figure 9.17: An example of a recurrent convolutional network for pixel labeling. The input is an image tensor $\mathbf{X}$, with axes corresponding to image rows, image columns, and channels (red, green, blue). The goal is to output a tensor of labels $\hat{Y}$, with a probability distribution over labels for each pixel. This tensor has axes corresponding to image rows, image columns, and the different classes. Rather than outputting $\hat{Y}$ in a single shot, the recurrent network iteratively refines its estimate $\hat{Y}$ by using a previous estimate of $\hat{Y}$ as input for creating a new estimate. The same parameters are used for each updated estimate, and the estimate can be refined as many times as we wish. The tensor of convolution kernels $\mathbf{U}$ is used on each step to compute the hidden representation given the input image. The kernel tensor $\mathbf{V}$ is used to produce an estimate of the labels given the hidden values. On all but the first step, the kernels $\mathbf{W}$ are convolved over $\hat{Y}$ to provide input to the hidden layer. On the first time step, this term is replaced by zero. Because the same parameters are used on each step, this is an example of a recurrent network, as described in chapter 10.

input plane, as shown in figure 9.13. In the kinds of architectures typically used for classification of a single object in an image, the greatest reduction in the spatial dimensions of the network comes from using pooling layers with large stride. In order to produce an output map of similar size as the input, one can avoid pooling altogether (Jain *et al.*, 2007). Another strategy is to simply emit a lower-resolution grid of labels (Pinheiro and Collobert, 2014, 2015). Finally, in principle, one could use a pooling operator with unit stride.

One strategy for pixel-wise labeling of images is to produce an initial guess of the image labels, then refine this initial guess using the interactions between neighboring pixels. Repeating this refinement step several times corresponds to using the same convolutions at each stage, sharing weights between the last layers of the deep net (Jain *et al.*, 2007). This makes the sequence of computations performed by the successive convolutional layers with weights shared across layers a particular kind of recurrent network (Pinheiro and Collobert, 2014, 2015). Figure 9.17 shows the architecture of such a recurrent convolutional network.

Once a prediction for each pixel is made, various methods can be used to further process these predictions in order to obtain a segmentation of the image into regions (Briggman *et al.*, 2009; Turaga *et al.*, 2010; Farabet *et al.*, 2013). The general idea is to assume that large groups of contiguous pixels tend to be associated with the same label. Graphical models can describe the probabilistic relationships between neighboring pixels. Alternatively, the convolutional network can be trained to maximize an approximation of the graphical model training objective (Ning *et al.*, 2005; Thompson *et al.*, 2014).

9.7 Data Types

The data used with a convolutional network usually consists of several channels, each channel being the observation of a different quantity at some point in space or time. See table 9.1 for examples of data types with different dimensionalities and number of channels.

For an example of convolutional networks applied to video, see Chen *et al.* (2010).

So far we have discussed only the case where every example in the train and test data has the same spatial dimensions. One advantage to convolutional networks is that they can also process inputs with varying spatial extents. These kinds of input simply cannot be represented by traditional, matrix multiplication-based neural networks. This provides a compelling reason to use convolutional networks even when computational cost and overfitting are not significant issues.

For example, consider a collection of images, where each image has a different width and height. It is unclear how to model such inputs with a weight matrix of fixed size. Convolution is straightforward to apply; the kernel is simply applied a different number of times depending on the size of the input, and the output of the convolution operation scales accordingly. Convolution may be viewed as matrix multiplication; the same convolution kernel induces a different size of doubly block circulant matrix for each size of input. Sometimes the output of the network is allowed to have variable size as well as the input, for example if we want to assign a class label to each pixel of the input. In this case, no further design work is necessary. In other cases, the network must produce some fixed-size output, for example if we want to assign a single class label to the entire image. In this case we must make some additional design steps, like inserting a pooling layer whose pooling regions scale in size proportional to the size of the input, in order to maintain a fixed number of pooled outputs. Some examples of this kind of strategy are shown in figure 9.11.

	Single channel	Multi-channel
1-D	Audio waveform: The axis we convolve over corresponds to time. We discretize time and measure the amplitude of the waveform once per time step.	Skeleton animation data: Animations of 3-D computer-rendered characters are generated by altering the pose of a "skeleton" over time. At each point in time, the pose of the character is described by a specification of the angles of each of the joints in the character's skeleton. Each channel in the data we feed to the convolutional model represents the angle about one axis of one joint.
2-D	Audio data that has been preprocessed with a Fourier transform: We can transform the audio waveform into a 2D tensor with different rows corresponding to different frequencies and different columns corresponding to different points in time. Using convolution in the time makes the model equivariant to shifts in time. Using convolution across the frequency axis makes the model equivariant to frequency, so that the same melody played in a different octave produces the same representation but at a different height in the network's output.	Color image data: One channel contains the red pixels, one the green pixels, and one the blue pixels. The convolution kernel moves over both the horizontal and vertical axes of the image, conferring translation equivariance in both directions.
3-D	Volumetric data: A common source of this kind of data is medical imaging technology, such as CT scans.	Color video data: One axis corresponds to time, one to the height of the video frame, and one to the width of the video frame.

Table 9.1: Examples of different formats of data that can be used with convolutional networks.

Note that the use of convolution for processing variable sized inputs only makes sense for inputs that have variable size because they contain varying amounts of observation of the same kind of thing—different lengths of recordings over time, different widths of observations over space, etc. Convolution does not make sense if the input has variable size because it can optionally include different kinds of observations. For example, if we are processing college applications, and our features consist of both grades and standardized test scores, but not every applicant took the standardized test, then it does not make sense to convolve the same weights over both the features corresponding to the grades and the features corresponding to the test scores.

9.8 Efficient Convolution Algorithms

Modern convolutional network applications often involve networks containing more than one million units. Powerful implementations exploiting parallel computation resources, as discussed in section 12.1, are essential. However, in many cases it is also possible to speed up convolution by selecting an appropriate convolution algorithm.

Convolution is equivalent to converting both the input and the kernel to the frequency domain using a Fourier transform, performing point-wise multiplication of the two signals, and converting back to the time domain using an inverse Fourier transform. For some problem sizes, this can be faster than the naive implementation of discrete convolution.

When a d-dimensional kernel can be expressed as the outer product of d vectors, one vector per dimension, the kernel is called **separable**. When the kernel is separable, naive convolution is inefficient. It is equivalent to compose d one-dimensional convolutions with each of these vectors. The composed approach is significantly faster than performing one d-dimensional convolution with their outer product. The kernel also takes fewer parameters to represent as vectors. If the kernel is w elements wide in each dimension, then naive multidimensional convolution requires $O(w^d)$ runtime and parameter storage space, while separable convolution requires $O(w \times d)$ runtime and parameter storage space. Of course, not every convolution can be represented in this way.

Devising faster ways of performing convolution or approximate convolution without harming the accuracy of the model is an active area of research. Even techniques that improve the efficiency of only forward propagation are useful because in the commercial setting, it is typical to devote more resources to deployment of a network than to its training.

9.9 Random or Unsupervised Features

Typically, the most expensive part of convolutional network training is learning the features. The output layer is usually relatively inexpensive due to the small number of features provided as input to this layer after passing through several layers of pooling. When performing supervised training with gradient descent, every gradient step requires a complete run of forward propagation and backward propagation through the entire network. One way to reduce the cost of convolutional network training is to use features that are not trained in a supervised fashion.

There are three basic strategies for obtaining convolution kernels without supervised training. One is to simply initialize them randomly. Another is to design them by hand, for example by setting each kernel to detect edges at a certain orientation or scale. Finally, one can learn the kernels with an unsupervised criterion. For example, Coates *et al.* (2011) apply k-means clustering to small image patches, then use each learned centroid as a convolution kernel. Part III describes many more unsupervised learning approaches. Learning the features with an unsupervised criterion allows them to be determined separately from the classifier layer at the top of the architecture. One can then extract the features for the entire training set just once, essentially constructing a new training set for the last layer. Learning the last layer is then typically a convex optimization problem, assuming the last layer is something like logistic regression or an SVM.

Random filters often work surprisingly well in convolutional networks (Jarrett *et al.*, 2009; Saxe *et al.*, 2011; Pinto *et al.*, 2011; Cox and Pinto, 2011). Saxe *et al.* (2011) showed that layers consisting of convolution following by pooling naturally become frequency selective and translation invariant when assigned random weights. They argue that this provides an inexpensive way to choose the architecture of a convolutional network: first evaluate the performance of several convolutional network architectures by training only the last layer, then take the best of these architectures and train the entire architecture using a more expensive approach.

An intermediate approach is to learn the features, but using methods that do not require full forward and back-propagation at every gradient step. As with multilayer perceptrons, we use greedy layer-wise pretraining, to train the first layer in isolation, then extract all features from the first layer only once, then train the second layer in isolation given those features, and so on. Chapter 8 has described how to perform supervised greedy layer-wise pretraining, and part III extends this to greedy layer-wise pretraining using an unsupervised criterion at each layer. The canonical example of greedy layer-wise pretraining of a convolutional model is the convolutional deep belief network (Lee *et al.*, 2009). Convolutional networks offer

us the opportunity to take the pretraining strategy one step further than is possible with multilayer perceptrons. Instead of training an entire convolutional layer at a time, we can train a model of a small patch, as Coates *et al.* (2011) do with k-means. We can then use the parameters from this patch-based model to define the kernels of a convolutional layer. This means that it is possible to use unsupervised learning to train a convolutional network *without ever using convolution during the training process*. Using this approach, we can train very large models and incur a high computational cost only at inference time (Ranzato *et al.*, 2007b; Jarrett *et al.*, 2009; Kavukcuoglu *et al.*, 2010; Coates *et al.*, 2013). This approach was popular from roughly 2007–2013, when labeled datasets were small and computational power was more limited. Today, most convolutional networks are trained in a purely supervised fashion, using full forward and back-propagation through the entire network on each training iteration.

As with other approaches to unsupervised pretraining, it remains difficult to tease apart the cause of some of the benefits seen with this approach. Unsupervised pretraining may offer some regularization relative to supervised training, or it may simply allow us to train much larger architectures due to the reduced computational cost of the learning rule.

9.10 The Neuroscientific Basis for Convolutional Networks

Convolutional networks are perhaps the greatest success story of biologically inspired artificial intelligence. Though convolutional networks have been guided by many other fields, some of the key design principles of neural networks were drawn from neuroscience.

The history of convolutional networks begins with neuroscientific experiments long before the relevant computational models were developed. Neurophysiologists David Hubel and Torsten Wiesel collaborated for several years to determine many of the most basic facts about how the mammalian vision system works (Hubel and Wiesel, 1959, 1962, 1968). Their accomplishments were eventually recognized with a Nobel prize. Their findings that have had the greatest influence on contemporary deep learning models were based on recording the activity of individual neurons in cats. They observed how neurons in the cat's brain responded to images projected in precise locations on a screen in front of the cat. Their great discovery was that neurons in the early visual system responded most strongly to very specific patterns of light, such as precisely oriented bars, but responded hardly at all to other patterns.

Their work helped to characterize many aspects of brain function that are beyond the scope of this book. From the point of view of deep learning, we can focus on a simplified, cartoon view of brain function.

In this simplified view, we focus on a part of the brain called V1, also known as the **primary visual cortex**. V1 is the first area of the brain that begins to perform significantly advanced processing of visual input. In this cartoon view, images are formed by light arriving in the eye and stimulating the retina, the light-sensitive tissue in the back of the eye. The neurons in the retina perform some simple preprocessing of the image but do not substantially alter the way it is represented. The image then passes through the optic nerve and a brain region called the lateral geniculate nucleus. The main role, as far as we are concerned here, of both of these anatomical regions is primarily just to carry the signal from the eye to V1, which is located at the back of the head.

A convolutional network layer is designed to capture three properties of V1:

1. V1 is arranged in a spatial map. It actually has a two-dimensional structure mirroring the structure of the image in the retina. For example, light arriving at the lower half of the retina affects only the corresponding half of V1. Convolutional networks capture this property by having their features defined in terms of two dimensional maps.

2. V1 contains many **simple cells**. A simple cell's activity can to some extent be characterized by a linear function of the image in a small, spatially localized receptive field. The detector units of a convolutional network are designed to emulate these properties of simple cells.

3. V1 also contains many **complex cells**. These cells respond to features that are similar to those detected by simple cells, but complex cells are invariant to small shifts in the position of the feature. This inspires the pooling units of convolutional networks. Complex cells are also invariant to some changes in lighting that cannot be captured simply by pooling over spatial locations. These invariances have inspired some of the cross-channel pooling strategies in convolutional networks, such as maxout units (Goodfellow *et al.*, 2013a).

Though we know the most about V1, it is generally believed that the same basic principles apply to other areas of the visual system. In our cartoon view of the visual system, the basic strategy of detection followed by pooling is repeatedly applied as we move deeper into the brain. As we pass through multiple anatomical layers of the brain, we eventually find cells that respond to some specific concept and are invariant to many transformations of the input. These cells have been

nicknamed "grandmother cells"—the idea is that a person could have a neuron that activates when seeing an image of their grandmother, regardless of whether she appears in the left or right side of the image, whether the image is a close-up of her face or zoomed out shot of her entire body, whether she is brightly lit, or in shadow, etc.

These grandmother cells have been shown to actually exist in the human brain, in a region called the medial temporal lobe (Quiroga *et al.*, 2005). Researchers tested whether individual neurons would respond to photos of famous individuals. They found what has come to be called the "Halle Berry neuron": an individual neuron that is activated by the concept of Halle Berry. This neuron fires when a person sees a photo of Halle Berry, a drawing of Halle Berry, or even text containing the words "Halle Berry." Of course, this has nothing to do with Halle Berry herself; other neurons responded to the presence of Bill Clinton, Jennifer Aniston, etc.

These medial temporal lobe neurons are somewhat more general than modern convolutional networks, which would not automatically generalize to identifying a person or object when reading its name. The closest analog to a convolutional network's last layer of features is a brain area called the inferotemporal cortex (IT). When viewing an object, information flows from the retina, through the LGN, to V1, then onward to V2, then V4, then IT. This happens within the first 100ms of glimpsing an object. If a person is allowed to continue looking at the object for more time, then information will begin to flow backwards as the brain uses top-down feedback to update the activations in the lower level brain areas. However, if we interrupt the person's gaze, and observe only the firing rates that result from the first 100ms of mostly feedforward activation, then IT proves to be very similar to a convolutional network. Convolutional networks can predict IT firing rates, and also perform very similarly to (time limited) humans on object recognition tasks (DiCarlo, 2013).

That being said, there are many differences between convolutional networks and the mammalian vision system. Some of these differences are well known to computational neuroscientists, but outside the scope of this book. Some of these differences are not yet known, because many basic questions about how the mammalian vision system works remain unanswered. As a brief list:

- The human eye is mostly very low resolution, except for a tiny patch called the **fovea**. The fovea only observes an area about the size of a thumbnail held at arms length. Though we feel as if we can see an entire scene in high resolution, this is an illusion created by the subconscious part of our brain, as it stitches together several glimpses of small areas. Most convolutional networks actually receive large full resolution photographs as input. The human brain makes

several eye movements called **saccades** to glimpse the most visually salient or task-relevant parts of a scene. Incorporating similar attention mechanisms into deep learning models is an active research direction. In the context of deep learning, attention mechanisms have been most successful for natural language processing, as described in section 12.4.5.1. Several visual models with foveation mechanisms have been developed but so far have not become the dominant approach (Larochelle and Hinton, 2010; Denil *et al.*, 2012).

- The human visual system is integrated with many other senses, such as hearing, and factors like our moods and thoughts. Convolutional networks so far are purely visual.

- The human visual system does much more than just recognize objects. It is able to understand entire scenes including many objects and relationships between objects, and processes rich 3-D geometric information needed for our bodies to interface with the world. Convolutional networks have been applied to some of these problems but these applications are in their infancy.

- Even simple brain areas like V1 are heavily impacted by feedback from higher levels. Feedback has been explored extensively in neural network models but has not yet been shown to offer a compelling improvement.

- While feedforward IT firing rates capture much of the same information as convolutional network features, it is not clear how similar the intermediate computations are. The brain probably uses very different activation and pooling functions. An individual neuron's activation probably is not well-characterized by a single linear filter response. A recent model of V1 involves multiple quadratic filters for each neuron (Rust *et al.*, 2005). Indeed our cartoon picture of "simple cells" and "complex cells" might create a non-existent distinction; simple cells and complex cells might both be the same kind of cell but with their "parameters" enabling a continuum of behaviors ranging from what we call "simple" to what we call "complex."

It is also worth mentioning that neuroscience has told us relatively little about how to *train* convolutional networks. Model structures with parameter sharing across multiple spatial locations date back to early connectionist models of vision (Marr and Poggio, 1976), but these models did not use the modern back-propagation algorithm and gradient descent. For example, the Neocognitron (Fukushima, 1980) incorporated most of the model architecture design elements of the modern convolutional network but relied on a layer-wise unsupervised clustering algorithm.

Lang and Hinton (1988) introduced the use of back-propagation to train **time-delay neural networks** (TDNNs). To use contemporary terminology, TDNNs are one-dimensional convolutional networks applied to time series. Back-propagation applied to these models was not inspired by any neuroscientific observation and is considered by some to be biologically implausible. Following the success of back-propagation-based training of TDNNs, (LeCun *et al.*, 1989) developed the modern convolutional network by applying the same training algorithm to 2-D convolution applied to images.

So far we have described how simple cells are roughly linear and selective for certain features, complex cells are more nonlinear and become invariant to some transformations of these simple cell features, and stacks of layers that alternate between selectivity and invariance can yield grandmother cells for very specific phenomena. We have not yet described precisely what these individual cells detect. In a deep, nonlinear network, it can be difficult to understand the function of individual cells. Simple cells in the first layer are easier to analyze, because their responses are driven by a linear function. In an artificial neural network, we can just display an image of the convolution kernel to see what the corresponding channel of a convolutional layer responds to. In a biological neural network, we do not have access to the weights themselves. Instead, we put an electrode in the neuron itself, display several samples of white noise images in front of the animal's retina, and record how each of these samples causes the neuron to activate. We can then fit a linear model to these responses in order to obtain an approximation of the neuron's weights. This approach is known as **reverse correlation** (Ringach and Shapley, 2004).

Reverse correlation shows us that most V1 cells have weights that are described by **Gabor functions**. The Gabor function describes the weight at a 2-D point in the image. We can think of an image as being a function of 2-D coordinates, $I(x, y)$. Likewise, we can think of a simple cell as sampling the image at a set of locations, defined by a set of x coordinates $\mathbb{X}$ and a set of y coordinates, $\mathbb{Y}$, and applying weights that are also a function of the location, $w(x, y)$. From this point of view, the response of a simple cell to an image is given by

$$s(I) = \sum_{x \in \mathbb{X}} \sum_{y \in \mathbb{Y}} w(x, y) I(x, y). \tag{9.15}$$

Specifically, $w(x, y)$ takes the form of a Gabor function:

$$w(x, y; \alpha, \beta_x, \beta_y, f, \phi, x_0, y_0, \tau) = \alpha \exp\left(-\beta_x x'^2 - \beta_y y'^2\right) \cos(f x' + \phi), \tag{9.16}$$

where

$$x' = (x - x_0) \cos(\tau) + (y - y_0) \sin(\tau) \tag{9.17}$$

and

$$y' = -(x - x_0)\sin(\tau) + (y - y_0)\cos(\tau). \tag{9.18}$$

Here, α, β_x, β_y, f, ϕ, x_0, y_0, and τ are parameters that control the properties of the Gabor function. Figure 9.18 shows some examples of Gabor functions with different settings of these parameters.

The parameters x_0, y_0, and τ define a coordinate system. We translate and rotate x and y to form x' and y'. Specifically, the simple cell will respond to image features centered at the point (x_0, y_0), and it will respond to changes in brightness as we move along a line rotated τ radians from the horizontal.

Viewed as a function of x' and y', the function w then responds to changes in brightness as we move along the x' axis. It has two important factors: one is a Gaussian function and the other is a cosine function.

The Gaussian factor $\alpha \exp\left(-\beta_x x'^2 - \beta_y y'^2\right)$ can be seen as a gating term that ensures the simple cell will only respond to values near where x' and y' are both zero, in other words, near the center of the cell's receptive field. The scaling factor α adjusts the total magnitude of the simple cell's response, while β_x and β_y control how quickly its receptive field falls off.

The cosine factor $\cos(fx' + \phi)$ controls how the simple cell responds to changing brightness along the x' axis. The parameter f controls the frequency of the cosine and ϕ controls its phase offset.

Altogether, this cartoon view of simple cells means that a simple cell responds to a specific spatial frequency of brightness in a specific direction at a specific location. Simple cells are most excited when the wave of brightness in the image has the same phase as the weights. This occurs when the image is bright where the weights are positive and dark where the weights are negative. Simple cells are most inhibited when the wave of brightness is fully out of phase with the weights—when the image is dark where the weights are positive and bright where the weights are negative.

The cartoon view of a complex cell is that it computes the L^2 norm of the 2-D vector containing two simple cells' responses: $c(I) = \sqrt{s_0(I)^2 + s_1(I)^2}$. An important special case occurs when s_1 has all of the same parameters as s_0 except for ϕ, and ϕ is set such that s_1 is one quarter cycle out of phase with s_0. In this case, s_0 and s_1 form a **quadrature pair**. A complex cell defined in this way responds when the Gaussian reweighted image $I(x, y)\exp\left(-\beta_x x'^2 - \beta_y y'^2\right)$ contains a high amplitude sinusoidal wave with frequency f in direction τ near (x_0, y_0), *regardless of the phase offset of this wave.* In other words, the complex cell is invariant to small translations of the image in direction τ, or to negating the image

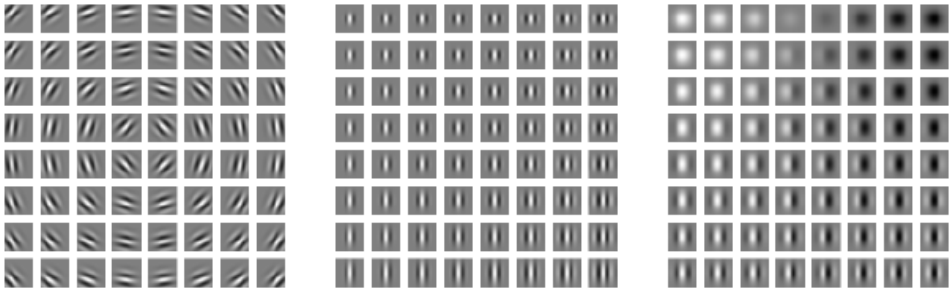

Figure 9.18: Gabor functions with a variety of parameter settings. White indicates large positive weight, black indicates large negative weight, and the background gray corresponds to zero weight. *(Left)*Gabor functions with different values of the parameters that control the coordinate system: x_0, y_0, and τ. Each Gabor function in this grid is assigned a value of x_0 and y_0 proportional to its position in its grid, and τ is chosen so that each Gabor filter is sensitive to the direction radiating out from the center of the grid. For the other two plots, x_0, y_0, and τ are fixed to zero. *(Center)*Gabor functions with different Gaussian scale parameters β_x and β_y. Gabor functions are arranged in increasing width (decreasing β_x) as we move left to right through the grid, and increasing height (decreasing β_y) as we move top to bottom. For the other two plots, the β values are fixed to 1.5× the image width. *(Right)*Gabor functions with different sinusoid parameters f and ϕ. As we move top to bottom, f increases, and as we move left to right, ϕ increases. For the other two plots, ϕ is fixed to 0 and f is fixed to 5× the image width.

(replacing black with white and vice versa).

Some of the most striking correspondences between neuroscience and machine learning come from visually comparing the features learned by machine learning models with those employed by V1. Olshausen and Field (1996) showed that a simple unsupervised learning algorithm, sparse coding, learns features with receptive fields similar to those of simple cells. Since then, we have found that an extremely wide variety of statistical learning algorithms learn features with Gabor-like functions when applied to natural images. This includes most deep learning algorithms, which learn these features in their first layer. Figure 9.19 shows some examples. Because so many different learning algorithms learn edge detectors, it is difficult to conclude that any specific learning algorithm is the "right" model of the brain just based on the features that it learns (though it can certainly be a bad sign if an algorithm does *not* learn some sort of edge detector when applied to natural images). These features are an important part of the statistical structure of natural images and can be recovered by many different approaches to statistical modeling. See Hyvärinen *et al.* (2009) for a review of the field of natural image statistics.

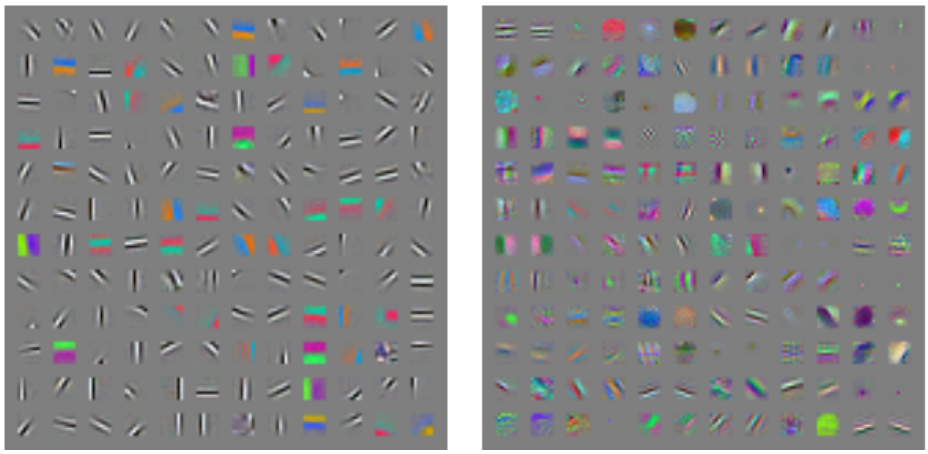

Figure 9.19: Many machine learning algorithms learn features that detect edges or specific colors of edges when applied to natural images. These feature detectors are reminiscent of the Gabor functions known to be present in primary visual cortex. *(Left)*Weights learned by an unsupervised learning algorithm (spike and slab sparse coding) applied to small image patches. *(Right)*Convolution kernels learned by the first layer of a fully supervised convolutional maxout network. Neighboring pairs of filters drive the same maxout unit.

9.11 Convolutional Networks and the History of Deep Learning

Convolutional networks have played an important role in the history of deep learning. They are a key example of a successful application of insights obtained by studying the brain to machine learning applications. They were also some of the first deep models to perform well, long before arbitrary deep models were considered viable. Convolutional networks were also some of the first neural networks to solve important commercial applications and remain at the forefront of commercial applications of deep learning today. For example, in the 1990s, the neural network research group at AT&T developed a convolutional network for reading checks (LeCun *et al.*, 1998b). By the end of the 1990s, this system deployed by NEC was reading over 10% of all the checks in the US. Later, several OCR and handwriting recognition systems based on convolutional nets were deployed by Microsoft (Simard *et al.*, 2003). See chapter 12 for more details on such applications and more modern applications of convolutional networks. See LeCun *et al.* (2010) for a more in-depth history of convolutional networks up to 2010.

Convolutional networks were also used to win many contests. The current intensity of commercial interest in deep learning began when Krizhevsky *et al.* (2012) won the ImageNet object recognition challenge, but convolutional networks

had been used to win other machine learning and computer vision contests with less impact for years earlier.

Convolutional nets were some of the first working deep networks trained with back-propagation. It is not entirely clear why convolutional networks succeeded when general back-propagation networks were considered to have failed. It may simply be that convolutional networks were more computationally efficient than fully connected networks, so it was easier to run multiple experiments with them and tune their implementation and hyperparameters. Larger networks also seem to be easier to train. With modern hardware, large fully connected networks appear to perform reasonably on many tasks, even when using datasets that were available and activation functions that were popular during the times when fully connected networks were believed not to work well. It may be that the primary barriers to the success of neural networks were psychological (practitioners did not expect neural networks to work, so they did not make a serious effort to use neural networks). Whatever the case, it is fortunate that convolutional networks performed well decades ago. In many ways, they carried the torch for the rest of deep learning and paved the way to the acceptance of neural networks in general.

Convolutional networks provide a way to specialize neural networks to work with data that has a clear grid-structured topology and to scale such models to very large size. This approach has been the most successful on a two-dimensional, image topology. To process one-dimensional, sequential data, we turn next to another powerful specialization of the neural networks framework: recurrent neural networks.

Chapter 10

Sequence Modeling: Recurrent and Recursive Nets

Recurrent neural networks or RNNs (Rumelhart *et al.*, 1986a) are a family of neural networks for processing sequential data. Much as a convolutional network is a neural network that is specialized for processing a grid of values $\mathbf{X}$ such as an image, a recurrent neural network is a neural network that is specialized for processing a sequence of values $\boldsymbol{x}^{(1)}, \ldots, \boldsymbol{x}^{(\tau)}$. Just as convolutional networks can readily scale to images with large width and height, and some convolutional networks can process images of variable size, recurrent networks can scale to much longer sequences than would be practical for networks without sequence-based specialization. Most recurrent networks can also process sequences of variable length.

To go from multi-layer networks to recurrent networks, we need to take advantage of one of the early ideas found in machine learning and statistical models of the 1980s: sharing parameters across different parts of a model. Parameter sharing makes it possible to extend and apply the model to examples of different forms (different lengths, here) and generalize across them. If we had separate parameters for each value of the time index, we could not generalize to sequence lengths not seen during training, nor share statistical strength across different sequence lengths and across different positions in time. Such sharing is particularly important when a specific piece of information can occur at multiple positions within the sequence. For example, consider the two sentences "I went to Nepal in 2009" and "In 2009, I went to Nepal." If we ask a machine learning model to read each sentence and extract the year in which the narrator went to Nepal, we would like it to recognize the year 2009 as the relevant piece of information, whether it appears in the sixth

word or the second word of the sentence. Suppose that we trained a feedforward network that processes sentences of fixed length. A traditional fully connected feedforward network would have separate parameters for each input feature, so it would need to learn all of the rules of the language separately at each position in the sentence. By comparison, a recurrent neural network shares the same weights across several time steps.

A related idea is the use of convolution across a 1-D temporal sequence. This convolutional approach is the basis for time-delay neural networks (Lang and Hinton, 1988; Waibel *et al.*, 1989; Lang *et al.*, 1990). The convolution operation allows a network to share parameters across time, but is shallow. The output of convolution is a sequence where each member of the output is a function of a small number of neighboring members of the input. The idea of parameter sharing manifests in the application of the same convolution kernel at each time step. Recurrent networks share parameters in a different way. Each member of the output is a function of the previous members of the output. Each member of the output is produced using the same update rule applied to the previous outputs. This recurrent formulation results in the sharing of parameters through a very deep computational graph.

For the simplicity of exposition, we refer to RNNs as operating on a sequence that contains vectors $\boldsymbol{x}^{(t)}$ with the time step index t ranging from 1 to τ. In practice, recurrent networks usually operate on minibatches of such sequences, with a different sequence length τ for each member of the minibatch. We have omitted the minibatch indices to simplify notation. Moreover, the time step index need not literally refer to the passage of time in the real world. Sometimes it refers only to the position in the sequence. RNNs may also be applied in two dimensions across spatial data such as images, and even when applied to data involving time, the network may have connections that go backwards in time, provided that the entire sequence is observed before it is provided to the network.

This chapter extends the idea of a computational graph to include cycles. These cycles represent the influence of the present value of a variable on its own value at a future time step. Such computational graphs allow us to define recurrent neural networks. We then describe many different ways to construct, train, and use recurrent neural networks.

For more information on recurrent neural networks than is available in this chapter, we refer the reader to the textbook of Graves (2012).

10.1 Unfolding Computational Graphs

A computational graph is a way to formalize the structure of a set of computations, such as those involved in mapping inputs and parameters to outputs and loss. Please refer to section 6.5.1 for a general introduction. In this section we explain the idea of **unfolding** a recursive or recurrent computation into a computational graph that has a repetitive structure, typically corresponding to a chain of events. Unfolding this graph results in the sharing of parameters across a deep network structure.

For example, consider the classical form of a dynamical system:

$$\boldsymbol{s}^{(t)} = f(\boldsymbol{s}^{(t-1)}; \boldsymbol{\theta}), \tag{10.1}$$

where $\boldsymbol{s}^{(t)}$ is called the state of the system.

Equation 10.1 is recurrent because the definition of $\boldsymbol{s}$ at time t refers back to the same definition at time $t-1$.

For a finite number of time steps τ, the graph can be unfolded by applying the definition $\tau - 1$ times. For example, if we unfold equation 10.1 for $\tau = 3$ time steps, we obtain

$$\begin{aligned} \boldsymbol{s}^{(3)} &= f(\boldsymbol{s}^{(2)}; \boldsymbol{\theta}) && (10.2) \\ &= f(f(\boldsymbol{s}^{(1)}; \boldsymbol{\theta}); \boldsymbol{\theta}) && (10.3) \end{aligned}$$

Unfolding the equation by repeatedly applying the definition in this way has yielded an expression that does not involve recurrence. Such an expression can now be represented by a traditional directed acyclic computational graph. The unfolded computational graph of equation 10.1 and equation 10.3 is illustrated in figure 10.1.

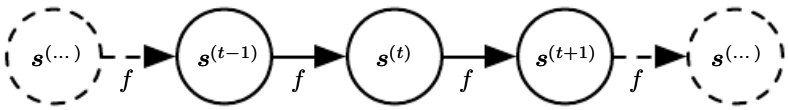

Figure 10.1: The classical dynamical system described by equation 10.1, illustrated as an unfolded computational graph. Each node represents the state at some time t and the function f maps the state at t to the state at $t+1$. The same parameters (the same value of $\boldsymbol{\theta}$ used to parametrize f) are used for all time steps.

As another example, let us consider a dynamical system driven by an external signal $\boldsymbol{x}^{(t)}$,

$$\boldsymbol{s}^{(t)} = f(\boldsymbol{s}^{(t-1)}, \boldsymbol{x}^{(t)}; \boldsymbol{\theta}), \tag{10.4}$$

where we see that the state now contains information about the whole past sequence.

Recurrent neural networks can be built in many different ways. Much as almost any function can be considered a feedforward neural network, essentially any function involving recurrence can be considered a recurrent neural network.

Many recurrent neural networks use equation 10.5 or a similar equation to define the values of their hidden units. To indicate that the state is the hidden units of the network, we now rewrite equation 10.4 using the variable $\boldsymbol{h}$ to represent the state:

$$\boldsymbol{h}^{(t)} = f(\boldsymbol{h}^{(t-1)}, \boldsymbol{x}^{(t)}; \boldsymbol{\theta}), \tag{10.5}$$

illustrated in figure 10.2, typical RNNs will add extra architectural features such as output layers that read information out of the state $\boldsymbol{h}$ to make predictions.

When the recurrent network is trained to perform a task that requires predicting the future from the past, the network typically learns to use $\boldsymbol{h}^{(t)}$ as a kind of lossy summary of the task-relevant aspects of the past sequence of inputs up to t. This summary is in general necessarily lossy, since it maps an arbitrary length sequence $(\boldsymbol{x}^{(t)}, \boldsymbol{x}^{(t-1)}, \boldsymbol{x}^{(t-2)}, \ldots, \boldsymbol{x}^{(2)}, \boldsymbol{x}^{(1)})$ to a fixed length vector $\boldsymbol{h}^{(t)}$. Depending on the training criterion, this summary might selectively keep some aspects of the past sequence with more precision than other aspects. For example, if the RNN is used in statistical language modeling, typically to predict the next word given previous words, it may not be necessary to store all of the information in the input sequence up to time t, but rather only enough information to predict the rest of the sentence. The most demanding situation is when we ask $\boldsymbol{h}^{(t)}$ to be rich enough to allow one to approximately recover the input sequence, as in autoencoder frameworks (chapter 14).

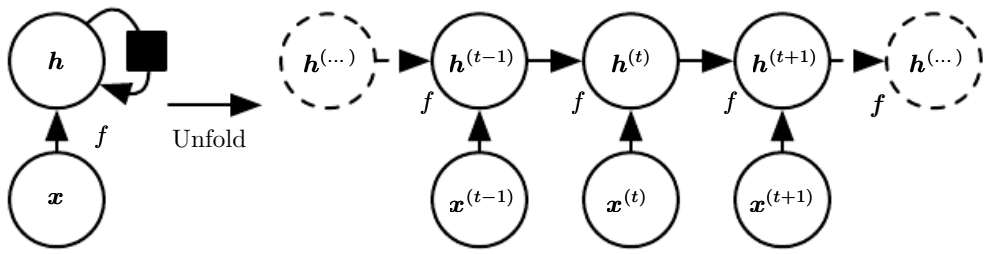

Figure 10.2: A recurrent network with no outputs. This recurrent network just processes information from the input $\boldsymbol{x}$ by incorporating it into the state $\boldsymbol{h}$ that is passed forward through time. *(Left)*Circuit diagram. The black square indicates a delay of a single time step. *(Right)*The same network seen as an unfolded computational graph, where each node is now associated with one particular time instance.

Equation 10.5 can be drawn in two different ways. One way to draw the RNN is with a diagram containing one node for every component that might exist in a

physical implementation of the model, such as a biological neural network. In this view, the network defines a circuit that operates in real time, with physical parts whose current state can influence their future state, as in the left of figure 10.2. Throughout this chapter, we use a black square in a circuit diagram to indicate that an interaction takes place with a delay of a single time step, from the state at time t to the state at time $t+1$. The other way to draw the RNN is as an unfolded computational graph, in which each component is represented by many different variables, with one variable per time step, representing the state of the component at that point in time. Each variable for each time step is drawn as a separate node of the computational graph, as in the right of figure 10.2. What we call unfolding is the operation that maps a circuit as in the left side of the figure to a computational graph with repeated pieces as in the right side. The unfolded graph now has a size that depends on the sequence length.

We can represent the unfolded recurrence after t steps with a function $g^{(t)}$:

$$\boldsymbol{h}^{(t)} = g^{(t)}(\boldsymbol{x}^{(t)}, \boldsymbol{x}^{(t-1)}, \boldsymbol{x}^{(t-2)}, \ldots, \boldsymbol{x}^{(2)}, \boldsymbol{x}^{(1)}) \tag{10.6}$$

$$= f(\boldsymbol{h}^{(t-1)}, \boldsymbol{x}^{(t)}; \boldsymbol{\theta}) \tag{10.7}$$

The function $g^{(t)}$ takes the whole past sequence $(\boldsymbol{x}^{(t)}, \boldsymbol{x}^{(t-1)}, \boldsymbol{x}^{(t-2)}, \ldots, \boldsymbol{x}^{(2)}, \boldsymbol{x}^{(1)})$ as input and produces the current state, but the unfolded recurrent structure allows us to factorize $g^{(t)}$ into repeated application of a function f. The unfolding process thus introduces two major advantages:

1. Regardless of the sequence length, the learned model always has the same input size, because it is specified in terms of transition from one state to another state, rather than specified in terms of a variable-length history of states.

2. It is possible to use the *same* transition function f with the same parameters at every time step.

These two factors make it possible to learn a single model f that operates on all time steps and all sequence lengths, rather than needing to learn a separate model $g^{(t)}$ for all possible time steps. Learning a single, shared model allows generalization to sequence lengths that did not appear in the training set, and allows the model to be estimated with far fewer training examples than would be required without parameter sharing.

Both the recurrent graph and the unrolled graph have their uses. The recurrent graph is succinct. The unfolded graph provides an explicit description of which computations to perform. The unfolded graph also helps to illustrate the idea of

information flow forward in time (computing outputs and losses) and backward in time (computing gradients) by explicitly showing the path along which this information flows.

10.2 Recurrent Neural Networks

Armed with the graph unrolling and parameter sharing ideas of section 10.1, we can design a wide variety of recurrent neural networks.

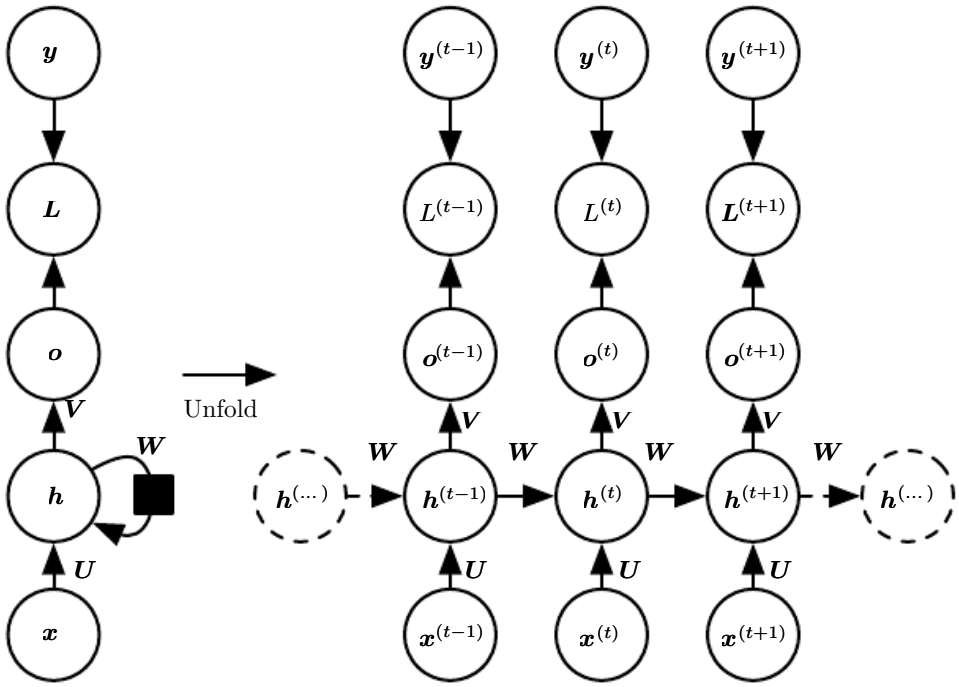

Figure 10.3: The computational graph to compute the training loss of a recurrent network that maps an input sequence of $\boldsymbol{x}$ values to a corresponding sequence of output $\boldsymbol{o}$ values. A loss L measures how far each $\boldsymbol{o}$ is from the corresponding training target $\boldsymbol{y}$. When using softmax outputs, we assume $\boldsymbol{o}$ is the unnormalized log probabilities. The loss L internally computes $\hat{\boldsymbol{y}} = \text{softmax}(\boldsymbol{o})$ and compares this to the target $\boldsymbol{y}$. The RNN has input to hidden connections parametrized by a weight matrix $\boldsymbol{U}$, hidden-to-hidden recurrent connections parametrized by a weight matrix $\boldsymbol{W}$, and hidden-to-output connections parametrized by a weight matrix $\boldsymbol{V}$. Equation 10.8 defines forward propagation in this model. *(Left)*The RNN and its loss drawn with recurrent connections. *(Right)*The same seen as an time-unfolded computational graph, where each node is now associated with one particular time instance.

Some examples of important design patterns for recurrent neural networks include the following:

- Recurrent networks that produce an output at each time step and have recurrent connections between hidden units, illustrated in figure 10.3.
- Recurrent networks that produce an output at each time step and have recurrent connections only from the output at one time step to the hidden units at the next time step, illustrated in figure 10.4
- Recurrent networks with recurrent connections between hidden units, that read an entire sequence and then produce a single output, illustrated in figure 10.5.

figure 10.3 is a reasonably representative example that we return to throughout most of the chapter.

The recurrent neural network of figure 10.3 and equation 10.8 is universal in the sense that any function computable by a Turing machine can be computed by such a recurrent network of a finite size. The output can be read from the RNN after a number of time steps that is asymptotically linear in the number of time steps used by the Turing machine and asymptotically linear in the length of the input (Siegelmann and Sontag, 1991; Siegelmann, 1995; Siegelmann and Sontag, 1995; Hyotyniemi, 1996). The functions computable by a Turing machine are discrete, so these results regard exact implementation of the function, not approximations. The RNN, when used as a Turing machine, takes a binary sequence as input and its outputs must be discretized to provide a binary output. It is possible to compute all functions in this setting using a single specific RNN of finite size (Siegelmann and Sontag (1995) use 886 units). The "input" of the Turing machine is a specification of the function to be computed, so the same network that simulates this Turing machine is sufficient for all problems. The theoretical RNN used for the proof can simulate an unbounded stack by representing its activations and weights with rational numbers of unbounded precision.

We now develop the forward propagation equations for the RNN depicted in figure 10.3. The figure does not specify the choice of activation function for the hidden units. Here we assume the hyperbolic tangent activation function. Also, the figure does not specify exactly what form the output and loss function take. Here we assume that the output is discrete, as if the RNN is used to predict words or characters. A natural way to represent discrete variables is to regard the output $\boldsymbol{o}$ as giving the unnormalized log probabilities of each possible value of the discrete variable. We can then apply the softmax operation as a post-processing step to obtain a vector $\hat{\boldsymbol{y}}$ of normalized probabilities over the output. Forward propagation begins with a specification of the initial state $\boldsymbol{h}^{(0)}$. Then, for each time step from

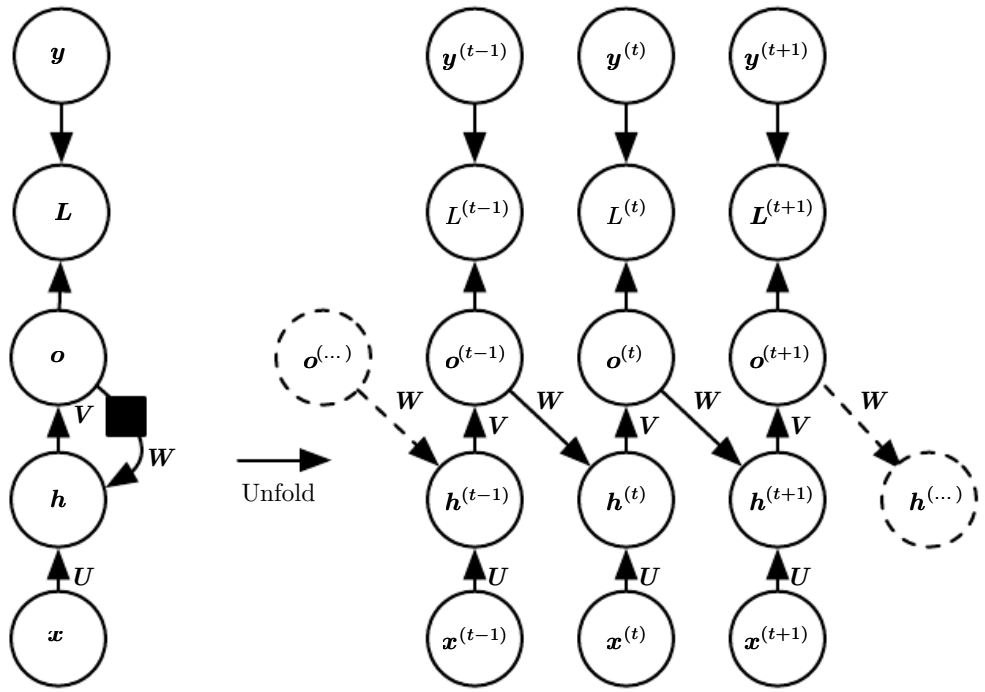

Figure 10.4: An RNN whose only recurrence is the feedback connection from the output to the hidden layer. At each time step t, the input is $\boldsymbol{x}_t$, the hidden layer activations are $\boldsymbol{h}^{(t)}$, the outputs are $\boldsymbol{o}^{(t)}$, the targets are $\boldsymbol{y}^{(t)}$ and the loss is $L^{(t)}$. *(Left)*Circuit diagram. *(Right)*Unfolded computational graph. Such an RNN is less powerful (can express a smaller set of functions) than those in the family represented by figure 10.3. The RNN in figure 10.3 can choose to put any information it wants about the past into its hidden representation $\boldsymbol{h}$ and transmit $\boldsymbol{h}$ to the future. The RNN in this figure is trained to put a specific output value into $\boldsymbol{o}$, and $\boldsymbol{o}$ is the only information it is allowed to send to the future. There are no direct connections from $\boldsymbol{h}$ going forward. The previous $\boldsymbol{h}$ is connected to the present only indirectly, via the predictions it was used to produce. Unless $\boldsymbol{o}$ is very high-dimensional and rich, it will usually lack important information from the past. This makes the RNN in this figure less powerful, but it may be easier to train because each time step can be trained in isolation from the others, allowing greater parallelization during training, as described in section 10.2.1.

$t = 1$ to $t = \tau$, we apply the following update equations:

$$\boldsymbol{a}^{(t)} = \boldsymbol{b} + \boldsymbol{W}\boldsymbol{h}^{(t-1)} + \boldsymbol{U}\boldsymbol{x}^{(t)} \tag{10.8}$$

$$\boldsymbol{h}^{(t)} = \tanh(\boldsymbol{a}^{(t)}) \tag{10.9}$$

$$\boldsymbol{o}^{(t)} = \boldsymbol{c} + \boldsymbol{V}\boldsymbol{h}^{(t)} \tag{10.10}$$

$$\hat{\boldsymbol{y}}^{(t)} = \text{softmax}(\boldsymbol{o}^{(t)}) \tag{10.11}$$

where the parameters are the bias vectors $\boldsymbol{b}$ and $\boldsymbol{c}$ along with the weight matrices $\boldsymbol{U}$, $\boldsymbol{V}$ and $\boldsymbol{W}$, respectively for input-to-hidden, hidden-to-output and hidden-to-hidden connections. This is an example of a recurrent network that maps an input sequence to an output sequence of the same length. The total loss for a given sequence of $\boldsymbol{x}$ values paired with a sequence of $\boldsymbol{y}$ values would then be just the sum of the losses over all the time steps. For example, if $L^{(t)}$ is the negative log-likelihood of $y^{(t)}$ given $\boldsymbol{x}^{(1)}, \dots, \boldsymbol{x}^{(t)}$, then

$$L\left(\{\boldsymbol{x}^{(1)}, \dots, \boldsymbol{x}^{(\tau)}\}, \{\boldsymbol{y}^{(1)}, \dots, \boldsymbol{y}^{(\tau)}\}\right) \tag{10.12}$$

$$= \sum_t L^{(t)} \tag{10.13}$$

$$= -\sum_t \log p_{\text{model}}\left(y^{(t)} \mid \{\boldsymbol{x}^{(1)}, \dots, \boldsymbol{x}^{(t)}\}\right), \tag{10.14}$$

where $p_{\text{model}}\left(y^{(t)} \mid \{\boldsymbol{x}^{(1)}, \dots, \boldsymbol{x}^{(t)}\}\right)$ is given by reading the entry for $y^{(t)}$ from the model's output vector $\hat{\boldsymbol{y}}^{(t)}$. Computing the gradient of this loss function with respect to the parameters is an expensive operation. The gradient computation involves performing a forward propagation pass moving left to right through our illustration of the unrolled graph in figure 10.3, followed by a backward propagation pass moving right to left through the graph. The runtime is $O(\tau)$ and cannot be reduced by parallelization because the forward propagation graph is inherently sequential; each time step may only be computed after the previous one. States computed in the forward pass must be stored until they are reused during the backward pass, so the memory cost is also $O(\tau)$. The back-propagation algorithm applied to the unrolled graph with $O(\tau)$ cost is called **back-propagation through time** or BPTT and is discussed further in section 10.2.2. The network with recurrence between hidden units is thus very powerful but also expensive to train. Is there an alternative?

10.2.1 Teacher Forcing and Networks with Output Recurrence

The network with recurrent connections only from the output at one time step to the hidden units at the next time step (shown in figure 10.4) is strictly less powerful

because it lacks hidden-to-hidden recurrent connections. For example, it cannot simulate a universal Turing machine. Because this network lacks hidden-to-hidden recurrence, it requires that the output units capture all of the information about the past that the network will use to predict the future. Because the output units are explicitly trained to match the training set targets, they are unlikely to capture the necessary information about the past history of the input, unless the user knows how to describe the full state of the system and provides it as part of the training set targets. The advantage of eliminating hidden-to-hidden recurrence is that, for any loss function based on comparing the prediction at time t to the training target at time t, all the time steps are decoupled. Training can thus be parallelized, with the gradient for each step t computed in isolation. There is no need to compute the output for the previous time step first, because the training set provides the ideal value of that output.

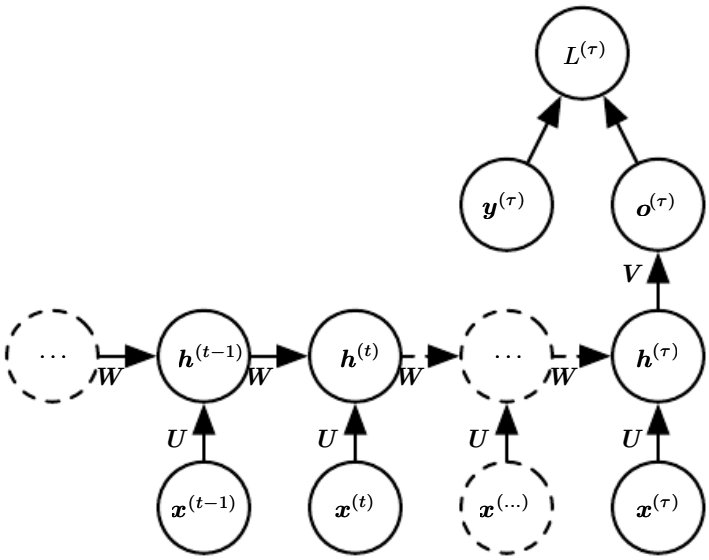

Figure 10.5: Time-unfolded recurrent neural network with a single output at the end of the sequence. Such a network can be used to summarize a sequence and produce a fixed-size representation used as input for further processing. There might be a target right at the end (as depicted here) or the gradient on the output $\boldsymbol{o}^{(t)}$ can be obtained by back-propagating from further downstream modules.

Models that have recurrent connections from their outputs leading back into the model may be trained with **teacher forcing**. Teacher forcing is a procedure that emerges from the maximum likelihood criterion, in which during training the model receives the ground truth output $y^{(t)}$ as input at time $t+1$. We can see this by examining a sequence with two time steps. The conditional maximum

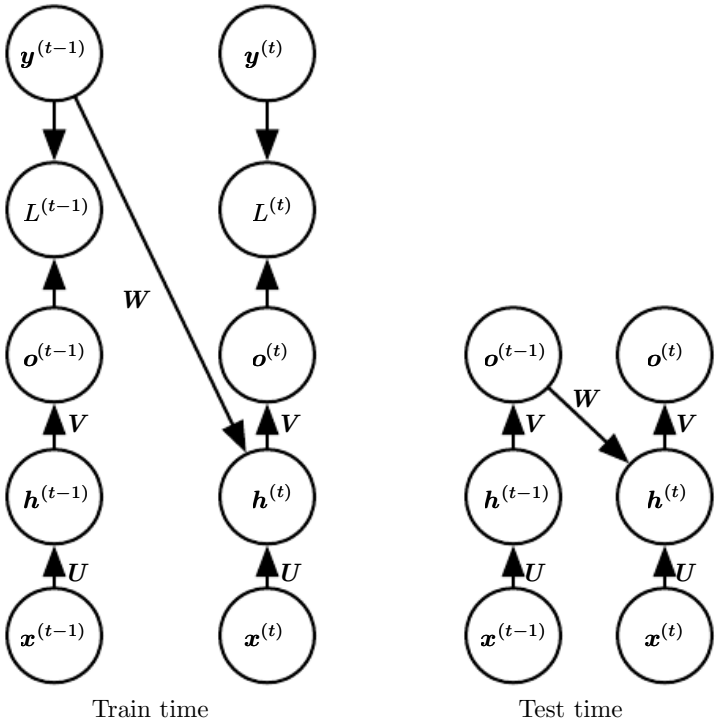

Figure 10.6: Illustration of teacher forcing. Teacher forcing is a training technique that is applicable to RNNs that have connections from their output to their hidden states at the next time step. *(Left)*At train time, we feed the *correct output* $\boldsymbol{y}^{(t)}$ drawn from the train set as input to $\boldsymbol{h}^{(t+1)}$. *(Right)*When the model is deployed, the true output is generally not known. In this case, we approximate the correct output $\boldsymbol{y}^{(t)}$ with the model's output $\boldsymbol{o}^{(t)}$, and feed the output back into the model.

likelihood criterion is

$$\log p\left(\boldsymbol{y}^{(1)}, \boldsymbol{y}^{(2)} \mid \boldsymbol{x}^{(1)}, \boldsymbol{x}^{(2)}\right) \tag{10.15}$$

$$= \log p\left(\boldsymbol{y}^{(2)} \mid \boldsymbol{y}^{(1)}, \boldsymbol{x}^{(1)}, \boldsymbol{x}^{(2)}\right) + \log p\left(\boldsymbol{y}^{(1)} \mid \boldsymbol{x}^{(1)}, \boldsymbol{x}^{(2)}\right) \tag{10.16}$$

In this example, we see that at time $t = 2$, the model is trained to maximize the conditional probability of $\boldsymbol{y}^{(2)}$ given *both* the $\boldsymbol{x}$ sequence so far and the previous $\boldsymbol{y}$ value from the training set. Maximum likelihood thus specifies that during training, rather than feeding the model's own output back into itself, these connections should be fed with the target values specifying what the correct output should be. This is illustrated in figure 10.6.

We originally motivated teacher forcing as allowing us to avoid back-propagation through time in models that lack hidden-to-hidden connections. Teacher forcing may still be applied to models that have hidden-to-hidden connections so long as they have connections from the output at one time step to values computed in the next time step. However, as soon as the hidden units become a function of earlier time steps, the BPTT algorithm is necessary. Some models may thus be trained with both teacher forcing and BPTT.

The disadvantage of strict teacher forcing arises if the network is going to be later used in an **open-loop** mode, with the network outputs (or samples from the output distribution) fed back as input. In this case, the kind of inputs that the network sees during training could be quite different from the kind of inputs that it will see at test time. One way to mitigate this problem is to train with both teacher-forced inputs and with free-running inputs, for example by predicting the correct target a number of steps in the future through the unfolded recurrent output-to-input paths. In this way, the network can learn to take into account input conditions (such as those it generates itself in the free-running mode) not seen during training and how to map the state back towards one that will make the network generate proper outputs after a few steps. Another approach (Bengio *et al.*, 2015b) to mitigate the gap between the inputs seen at train time and the inputs seen at test time randomly chooses to use generated values or actual data values as input. This approach exploits a curriculum learning strategy to gradually use more of the generated values as input.

10.2.2 Computing the Gradient in a Recurrent Neural Network

Computing the gradient through a recurrent neural network is straightforward. One simply applies the generalized back-propagation algorithm of section 6.5.6

to the unrolled computational graph. No specialized algorithms are necessary. Gradients obtained by back-propagation may then be used with any general-purpose gradient-based techniques to train an RNN.

To gain some intuition for how the BPTT algorithm behaves, we provide an example of how to compute gradients by BPTT for the RNN equations above (equation 10.8 and equation 10.12). The nodes of our computational graph include the parameters $\boldsymbol{U}$, $\boldsymbol{V}$, $\boldsymbol{W}$, $\boldsymbol{b}$ and $\boldsymbol{c}$ as well as the sequence of nodes indexed by t for $\boldsymbol{x}^{(t)}$, $\boldsymbol{h}^{(t)}$, $\boldsymbol{o}^{(t)}$ and $L^{(t)}$. For each node N we need to compute the gradient $\nabla_{\mathsf{N}} L$ recursively, based on the gradient computed at nodes that follow it in the graph. We start the recursion with the nodes immediately preceding the final loss

$$\frac{\partial L}{\partial L^{(t)}} = 1. \tag{10.17}$$

In this derivation we assume that the outputs $\boldsymbol{o}^{(t)}$ are used as the argument to the softmax function to obtain the vector $\hat{\boldsymbol{y}}$ of probabilities over the output. We also assume that the loss is the negative log-likelihood of the true target $y^{(t)}$ given the input so far. The gradient $\nabla_{\boldsymbol{o}^{(t)}} L$ on the outputs at time step t, for all i, t, is as follows:

$$\left(\nabla_{\boldsymbol{o}^{(t)}} L\right)_i = \frac{\partial L}{\partial o_i^{(t)}} = \frac{\partial L}{\partial L^{(t)}} \frac{\partial L^{(t)}}{\partial o_i^{(t)}} = \hat{y}_i^{(t)} - \mathbf{1}_{i, y^{(t)}}. \tag{10.18}$$

We work our way backwards, starting from the end of the sequence. At the final time step τ, $\boldsymbol{h}^{(\tau)}$ only has $\boldsymbol{o}^{(\tau)}$ as a descendent, so its gradient is simple:

$$\nabla_{\boldsymbol{h}^{(\tau)}} L = \boldsymbol{V}^\top \nabla_{\boldsymbol{o}^{(\tau)}} L. \tag{10.19}$$

We can then iterate backwards in time to back-propagate gradients through time, from $t = \tau - 1$ down to $t = 1$, noting that $\boldsymbol{h}^{(t)}$ (for $t < \tau$) has as descendents both $\boldsymbol{o}^{(t)}$ and $\boldsymbol{h}^{(t+1)}$. Its gradient is thus given by

$$\nabla_{\boldsymbol{h}^{(t)}} L = \left(\frac{\partial \boldsymbol{h}^{(t+1)}}{\partial \boldsymbol{h}^{(t)}}\right)^\top \left(\nabla_{\boldsymbol{h}^{(t+1)}} L\right) + \left(\frac{\partial \boldsymbol{o}^{(t)}}{\partial \boldsymbol{h}^{(t)}}\right)^\top \left(\nabla_{\boldsymbol{o}^{(t)}} L\right) \tag{10.20}$$

$$= \boldsymbol{W}^\top \left(\nabla_{\boldsymbol{h}^{(t+1)}} L\right) \operatorname{diag}\left(1 - \left(\boldsymbol{h}^{(t+1)}\right)^2\right) + \boldsymbol{V}^\top \left(\nabla_{\boldsymbol{o}^{(t)}} L\right) \tag{10.21}$$

where $\operatorname{diag}\left(1 - \left(\boldsymbol{h}^{(t+1)}\right)^2\right)$ indicates the diagonal matrix containing the elements $1 - (h_i^{(t+1)})^2$. This is the Jacobian of the hyperbolic tangent associated with the hidden unit i at time $t + 1$.